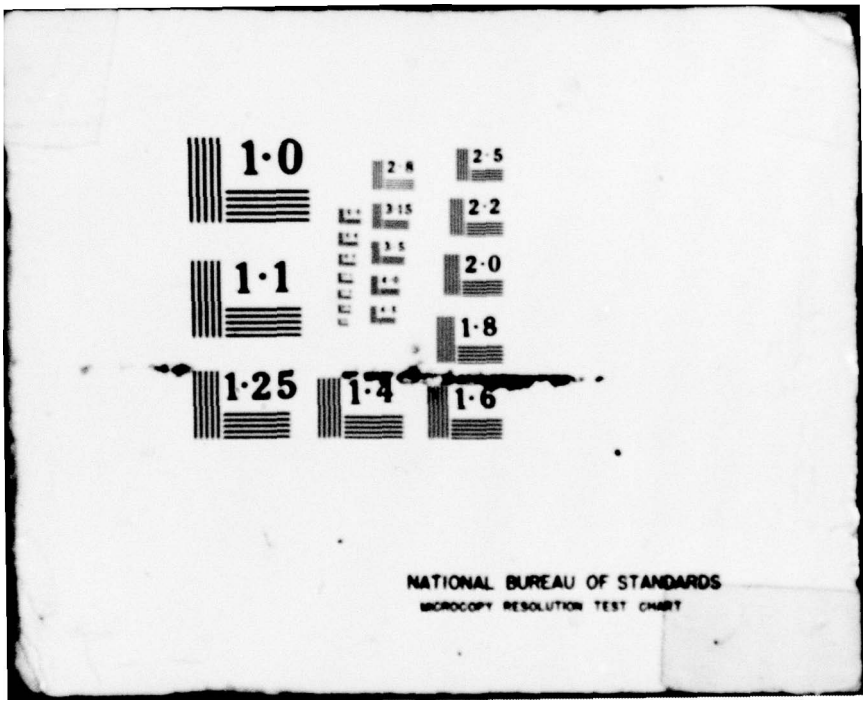
AD-A078 519 SOUTHERN METHODIST UNIV DALLAS TEX F/G 20/9
DESIGN OF INJECTION LASERS FOR IMPROVED RADIATION PERFORMANCE.(U)
NOV 79 J K BUTLER DAAG29-76-G-0146
UNCLASSIFIED ARO-13568.9-EL NL

1 OF 2
AD-
A078519




1·0
1·1
1·25
1·4
1·6
1·8
2·0
2·2
2·5
NATIONAL BUREAU OF STANDARDS
MICROCOPY RESOLUTION TEST CHART

ARO 13568.9-EL

LEVEL II

12

ADA078519

DESIGN OF INJECTION LASERS FOR IMPROVED RADIATION PERFORMANCE

FINAL REPORT

BY

JEROME K. BUTLER

See 1473

DDC
RECEIVED
DEC 18 1979
E

NOVEMBER 14, 1979

U. S. ARMY RESEARCH OFFICE

GRANT DAAG29-76-G-0146

SOUTHERN METHODIST UNIVERSITY

APPROVED FOR PUBLIC RELEASE:
DISTRIBUTION UNLIMITED

DDC FILE COPY

79 12 17 063

THE VIEW, OPINIONS, AND/OR FINDINGS CONTAINED IN THIS REPORT ARE THOSE OF THE AUTHOR(S) AND SHOULD NOT BE CONSTRUED AS AN OFFICIAL DEPARTMENT OF THE ARMY POSITION, POLICY, OR DICISION, UNLESS SO DESIGNATED BY OTHER DOCUMENTATION.

FOREWORD

This final report was prepared by Southern Methodist University, Dallas, Texas 75275, under U. S. Army Research Office Grant DAAG 29-76-G-0146. The work performed in the grant covered a period beginning February 23, 1976 to August 3., 1979. The work was carried out in the Electrical Engineering Department of the School of Engineering and Applied Science of Southern Methodist University, and was directed by the Principal Investigator, Dr. Jerome K. Butler.

Accession For
NTIS GRA&I
DDC TAB
Unannounced
Justification
By
Distribution/
Availability Codes
Dist | Avail and/or special
A

TABLE OF CONTENTS

Foreword

1. Statement of Problem

2. Summary of Results

3. References

4. Supported Personnel Involvment

5. Research Project Publications

6. Appendix A - Progress Reports

   Appendix B - Project Publications

   Appendix C - Dissertation Abstracts

1. STATEMENT OF PROBLEM

The research supported by this contract was concerned primarily with (1) the electromagnetic modes and (2) the radiation pattern characteristics of contemporary injection laser structures. The objective of this work was to investigate laser structures which can produce stable-beam radiation patterns. Because the radiation pattern in the plane of the p/n junction of many injection devices is influenced by the cavity geometry, stable-beam patterns can be obtained only from devices with proper and efficient control of the resonant cavity modes.

The control of lateral fields in lasers has been accomplished with many novel devices such as the channeled-substrate-planar, buried heterostructure and strip-loaded waveguide. These devices tend to be extremely complicated technologically so that it is advantageous to produce structures such as the simple stripe geometry device. The present drawback to the stripe laser is that it is laterally unstable. Much of our work has been aimed at rigorously modeling the electromagnetic modes of stripe lasers. We have also applied our analysis to other lasers such as the channeled-substrate-planar device.

2. SUMMARY OF RESULTS

The rapid development of semiconductor laser technology since the mid 1960's has pushed the field of optical communications to high levels of promise. Early modeling of the electromagnetic modes character in the plane perpendicular to the p/n junction was successful because the optical fields were confined due to the incorporation of optical barriers at heterojunctions.[1] Original cavity thicknesses (distance between heterojunctions) were d ~ 1 μm (Fig. 1).

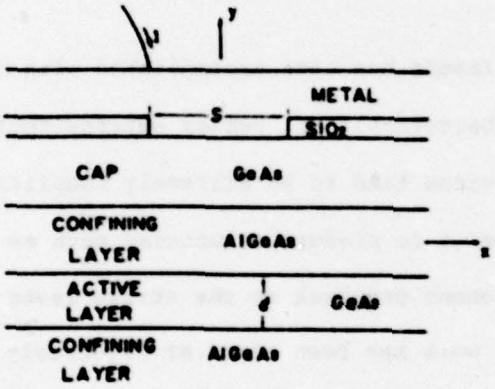


Fig. 1 Cross section of a stripe geometry laser structure. The active layer is bounded by the two AlGaAs layers.

In an effort to reduce the current density at threshold, the cavity thickness was reduced to values $d \lesssim 0.2\,\mu m$. These small thicknesses play a major role in the influence of the lateral mode behavior. The intense electric field in the cavity tends to stimulate recombination of electron/hole pairs and thus depletes the carrier density at the peak points of the optical field. To put this phenomena in perspective we must understand the mechanisms producing lateral confinement of the optical fields. Optical mode guiding along the lateral direction occurs because of changes in the real and imaginary parts of the dielectric constant. In stripe lasers, the optical mode is confined

to regions directly below the stripe. Thus the dielectric constant below the stripe differs from its value in lateral adjacent regions bordering the stripe region. For example, in Fig. 2 we show a cross section of a specific laser;

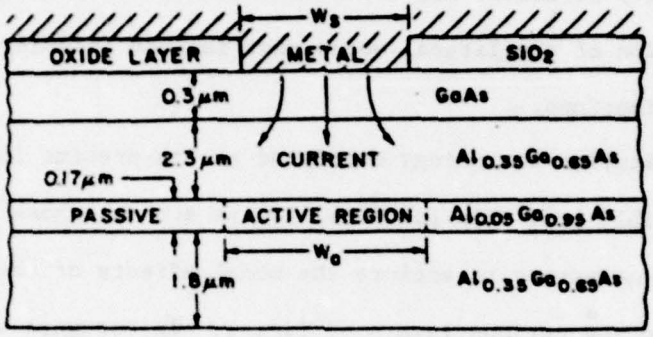


Fig. 2 Stripe contact laser with active region width W_a. Mode gain occurs in the active region while losses take place in the passive regions.

the active region is below the stripe while the passive regions are below the oxide layer. Factors affecting the dielectric distribution are:

1) Gain in the active and loss in the passive regions,

2) Lateral temperature variations,

3) Carrier density variations.

When the peak optical field depletes carriers under the stripe, the gain changes accordingly. Thus the refractive index changes according to (1) and (2) above.

In our work we have shown how asymmetric modes can be excited when the dielectric distribution becomes distorted.[2] These asymmetric modes cause extreme distortions in the radiation pattern. Furthermore, the amount of distortion is current dependent which reflects perturbation in the dielectric profile.

Another major accomplishment of our work is the first rigorous modeling of the cavity modes.[3,4] All previous analyses of the electromagnetic modes of stripe lasers have been approximate. We have shown that the vertical and lateral modes of cavity structure are interconnected and that a complete boundary value solution of the lateral modes must include interaction with vertical field distributions.

With laser fabrication technology developed at its present level, it is possible to reproducibly grow thin epitaxial layers such as those in Fig. 1. Consequently, it was necessary to explore the modal effects of the lasing field extentions into the various layers of Fig. 1. In our work we have accomplished an extensive analysis of the effects of device geometry on lateral mode behavior in stripe contact and channeled-substrate-planar lasers.[5,6]

As mentioned previously, the problems of lateral mode instabilities in stripe contact lasers have been paramount because there is a lack of lateral index guiding. Optical stripline structures have a "built-in" lateral index step.[7] Consequently, we have modeled the stripline in an effort to evaluate its mode behavior as an injection laser.[8]

Finally, we have devised an experimental technique for estimating refractive index steps of passive waveguides.[9] The intent of this effort was aimed at evaluating mode behavior of a laser structure in its wafer form. After the laser wafer is processed, slivers are cleaved (the width of the cleave actually forms the laser length). The slivers are then sawed to form the actual devices for mounting. Using our technique the waveguiding properties of the lasers in sliver form can be evaluated before final processing.

3. REFERENCES

1. H. Kressel and J. K. Butler, Semiconductor Lasers and Heterojunction LED's, Academic Press, New York, 1977.

2. J. K. Butler and H. S. Sommers, Jr., "Asymmetric Modes in Oxide Stripe Heterojunction Lasers," IEEE J. Quan. Electron., Vol. QE-14, pp. 413-417, June 1978.

3. J. K. Butler and J. B. Delaney, "A Rigorous Boundary Value Solution for the Lateral Modes of Stripe Geometry Injection Lasers," IEEE J. Quan. Electron., Vol. QE-14, pp. 507-513, July 1978.

4. J. B. Delaney and J. K. Butler, "Field Solutions for the lateral Modes of Stripe Geometry Injection lasers," IEEE J. Quan. Electron. (Submitted for publication)

5. J. K. Butler and J. B. Delaney, "Lateral Mode Control in Stripe Contact Injection Lasers," 1978 International Electron Devices Meeting, Washington, D.C., December 1978.

6. J. B. Delaney and J. K. Butler, "The Effect of Device Geometry on Lateral Mode Content of Stripe Geometry Lasers," IEEE J. Quan. Electron., Vol. QE-15, pp. 750-755, August 1979.

7. J. K. Butler, C. S. Wang and J. C Campbell, "Modal Characteristics of Optical Stripline Waveguides," J. Appl. Phys., Vol. 47, pp. 4033-4043, September 1976.

8. M. W. Scott and J. K. Butler, "Radiation Fields of Optical Stripline Waveguides," IEEE Trans. Microwave Th. and Tech. (To be published)

9. M. W. Scott and J. K. Butler, "Evaluation of Dielectric Optical Waveguides from Their Far Field Radiation Patterns," IEEE J. Quan. Electron. (To be published)

4. SUPPORTED PERSONNEL INVOLVEMENT

Dr. Jerome K. Butler, Principal Investigator

Dr. Chung S. Wang, Doctoral student, received a Ph. D. in May 1977. Dissertation: "Electromagnetic Modes of Heterojunction Injection Lasers." Abstract appended.

Mr. Joseph B. Delaney, Near completion of his research for the Ph. D.

Mr. Brent Sennette, Master degree student assisted in computer modeling.

Dr. Marion W. Scott, Doctoral student received a Ph. D. in August 1979. Dissertation: "Radiation Fields of Dielectric Optical Waveguides." Abstract appended.

5. RESEARCH PROJECT PUBLICATIONS

1. J. K. Butler, C. S. Wang and J. C. Campbell, "Optical Stripline Waveguides," 1976 Device Research Conference, Salt Lake City, Utah, June 21-23, 1976.

2. J. K. Butler and H. S. Sommers, Jr., "Asymmetric Modes in Oxide Stripe Heterojunction Lasers," IEEE J. Quantum Electronics, Vol. QE-14, pp 413-417, June 1978.

3. J. K. Butler and J. B. Delaney, "A Rigorous Boundary Value Solution for the Lateral Modes of Stripe Geometry Injection Lasers," IEEE J. Quantum Electronics, Vol. QE-14, pp. 507-513, July 1978.

4. J. K. Butler and J. B. Delaney, "Lateral Mode Control in Stripe Contact Injection Lasers," 1978 International Electron Devices Meeting, Tech. Dig., pp 634-637, December 1978.

5. J. B. Delaney and J. K. Butler, "The Effect of Device Geometry on Lateral Mode Content of Stripe Geometry Lasers," IEEE J. Quantum Electronics, Vol. QE-15, pp 750-755, August 1979.

6. M. W. Scott and J. K. Butler, "Radiation Fields of Optical Stripline Waveguides," IEEE Trans. Microwave Theory and Techniques, (Accepted for publication).

7. M. W. Scott and J. K. Butler, "Evaluation of Dielectric Optical Waveguides from thier Farfield Radiation Patterns," IEEE J. Quantum Electronics, (To be published January 1980).

8. J. B. Delaney and J. K. Butler, "Field Solutions for the Lateral Modes of Stripe Geometry Injection Lasers," IEEE J. Quantum Electronics, (Submitted for publication).

APPENDIX A

PROGRESS REPORTS

PROGRESS REPORT

20 COPIES REQUIRED

1. ARO PROPOSAL NUMBER: AMXRO-PRI-13568-EL

2. PERIOD COVERED BY REPORT: February 23, 1976 to June 30, 1976

3. TITLE OF PROPOSAL: Design of Injection Lasers for Improved Radiation Performance

4. CONTRACT OR GRANT NUMBER: DAAG29-76-G-0146

5. NAME OF INSTITUTION: Southern Methodist University

6. AUTHOR(S) OF REPORT: Jerome K. Butler

7. LIST OF MANUSCRIPTS SUBMITTED OR PUBLISHED UNDER ARO SPONSORSHIP DURING THIS PERIOD, INCLUDING JOURNAL REFERENCES:

"Optical Stripline Waveguides," The 1976 Device Research Conference, June 21-23, 1976, Salt Lake City, Utah.

8. SCIENTIFIC PERSONNEL SUPPORTED BY THIS PROJECT AND DEGREES AWARDED DURING THIS REPORTING PERIOD:

J. K. Butler
C. S. Wang

13568EL

PROFESSOR JEROME K. BUTLER
DEPT. OF ELECTRICAL ENGINEERING
SOUTHERN METHODIST UNIVERSITY
DALLAS, TX 75275

Introduction

The research carried out by this project is aimed at understanding the two-dimensional radiation characteristics of semiconductor injection lasers. Basically, the radiation pattern characteristics of injection lasers can be divided into two catagories: (1) the pattern in a plane perpendicular to the junction plane and (2) the pattern in the plane parallel to the junction. Much of the previous work in the literature is concerned with the pattern characteristics in the plane perpendicular to the junction. This is, of course, related to the fact that the mode structure perpendicular to the junction (the x-direction in Fig. 1) can be easily modeled using multilayer waveguides. On the other hand, very little modeling of the transverse W modes (y-direction of Fig. 1) has been made. This is primarily due to the fact that the optical field confinement along the y-direction is not well understood for some laser devices. In addition, the W mode selection characteristics are not well understood. For example, some stripe geometry lasers operate in high-order transverse W modes, yet the high-order modes have less optical feedback than some of the low orders.

In an effort to understand the waveguide characteristics of the transverse W-modes, we are modeling the radiation pattern in the y-z plane.

Research Direction

The simple Fourier transform formula [1-4] to connect the far-field radiation pattern and the near field has been used to analyze the transverse direction radiation phenomena. In most cases, the measured pattern is somewhat sharper than the theoretical one and at $\theta = \pm 90°$ (along the x-axis of Fig. 1), the simple Fourier transform formula does not lead to a null point at the facet. From ray optics, Snell's law indicates there will be a null at $\theta = \pm 90°$ due to the total internal reflection. Butler et al.[5] represented a mode by a spectrum of plane waves and determined the transmission characteristic of each plane wave. They compared calculated values with experimental patterns to determine the device geometry and dielectric parameters of various layers. Hockham[6] used a rather complicated procedure to obtain a formula which added a new factor to the Fourier transform formula. Lewin [7] interpreted this term as "Huygens obliquity factor". Both Butler's and Hockham's formula applied the saddle-point asymptotic technique to evaluate integrals and a cos θ term was obtained to satisfy the Snell's law at $\theta = \pm 90°$. Recently, Lewin[8] included a a multiplier into the radiation equation by using a weighted average resulting from the mode-conversion effects occurring on the laser-air interface. This method is relatively accurate and also can be used to calculate modal reflectivity which compares well with Ikegami's[9] numerical calculation. Reinhart et al.[10] proposed a method for calculating the modal reflectivity by decomposing the modal fields into an infinite number of plane waves; the plane wave reflection coefficient was used to obtain the modal reflection coefficient.

The above considerations are based on a one dimensional model. It is assumed that the facet fields are uniform along the junction (lateral direction). The research in this project is concerned with the model structure in the lateral direction which relates also to the radiation pattern in the plane parallel to the junction. Consequently, a model of the laser cavity is being developed to model the lateral cavity dimensions. This model will be applicable to presently fabricated devices such as stripe-geometry lasers[11], buried heterostructure lasers[12], and internally striped planar lasers.[13]

Gordon[14] extended Reinhart's[10] model from one to two dimensions which covers the finite waveguide width in junction plane, however, no explicit relation between the reflectivity and the stripe width has been explored. Nash[15] assumed that the gain under the stripe contract and the loss outside the stripe will produce a complex dielectric constant and gain with parabolic shape along the junction plane due to the current spreading under the stripe. Experimental evidence was reported by Cook and Nash[16] for gain-induced guiding and refractive-index antiguiding along the junction plane of the stripe-geometry DH lasers.

In the direction normal to the junction plane (transverse direction), the fields are confined by the index steps between the active region and the surrounding passive medium and have the sinusiodal shape. The modes can be restricted to the lowest order by making the active region very thin or index step very small. However, along the junction plane, the mode structure remains somewhat uncontrollable despite the introduction of the stripe contact. We have investigated the two dimensional radiation pattern and mode reflectivity. The active region under the stripe is

treated as an antenna aperture and a rectangular waveguide model is applied to study the radiation and modal reflectivity. Although, the change of index along the lateral direction is continuously varying instead of abruptly changing, the gradient of the refractive index can be neglected when the index variation is slow. The transmitted field can be obtained by matching appropriate fields at the laser-air interface. The half-power beamwidth in the transverse direction compares well with experiments while the lateral half-power beamwidth has a narrower value than the measured one. This may be due to our neglecting the loss outside the stripe in the active region.

The two dimensional modal reflectivity has been obtained by weighted average of the electric field with a specific multiplier to include the effect of mode conversion. The relation between the reflectivity and the stripe width is shown. The fundamental lateral mode has the largest reflectivity for typical stripe widths except near the cut-off width of the higher lateral modes. For large stripe widths, all modes approach the asymptotic value which can be obtained from the one dimensional model.

References

1. G. E. Fenner and J. D. Kingsley, J. Appl. Phys. 43, 3204 (1963).
2. R. F. Kazarino, V. O. Konstinov, V. J. Perel and A. L. Efros, Sov. Phys.-Solid State 7, 1210 (1965).
3. N. E. Byer and J. K. Butler, IEEE J. Quan. Electron. QE-6, 291 (1969).
4. M. J. Adams and M. Cross, Solid-State Electron. 14, 865 (1971).
5. J. K. Butler and J. Zorootchi, IEEE J. Quan. Electron. QE-10, 809 (1974).
6. G. A. Hockham, Electron. Letters 9, 389 (1973).
7. L. Lewin, Electron. Letters 10, 134 (1974).
8. L. Lewin, IEEE Trans. Microwave Theory and Tech. MTT-23, 576 (1975).
9. T. I. Ikegami, IEEE J. Quan. Electron. EQ-8, 470 (1972).
10. F. K. Reinhart, I. Hayashi, and M. B. Panish, J. Appl. Phys. 43, 4466, (1971).
11. J. E. Ripper, J. C. Dyment, L. A. D'Asaro, and T. L. Paoli, Appl. Phys. Lett. 18, 155 (1971).
12. T. Tsukada, J. Appl. Phys. 45, 4899 (1974).
13. M. Takusagawa, Proc. IEEE, 61, 1758 (1973).
14. E. I. Gordon, IEEE J. Quan. Electron. EQ-9, 772 (1973).
15. F. R. Nash, J. Appl. Phys. 44, 4696 (1973).
16. D. D. Cook and F. R. Nash, J. Appl. Phys. 46, 1660 (1975).

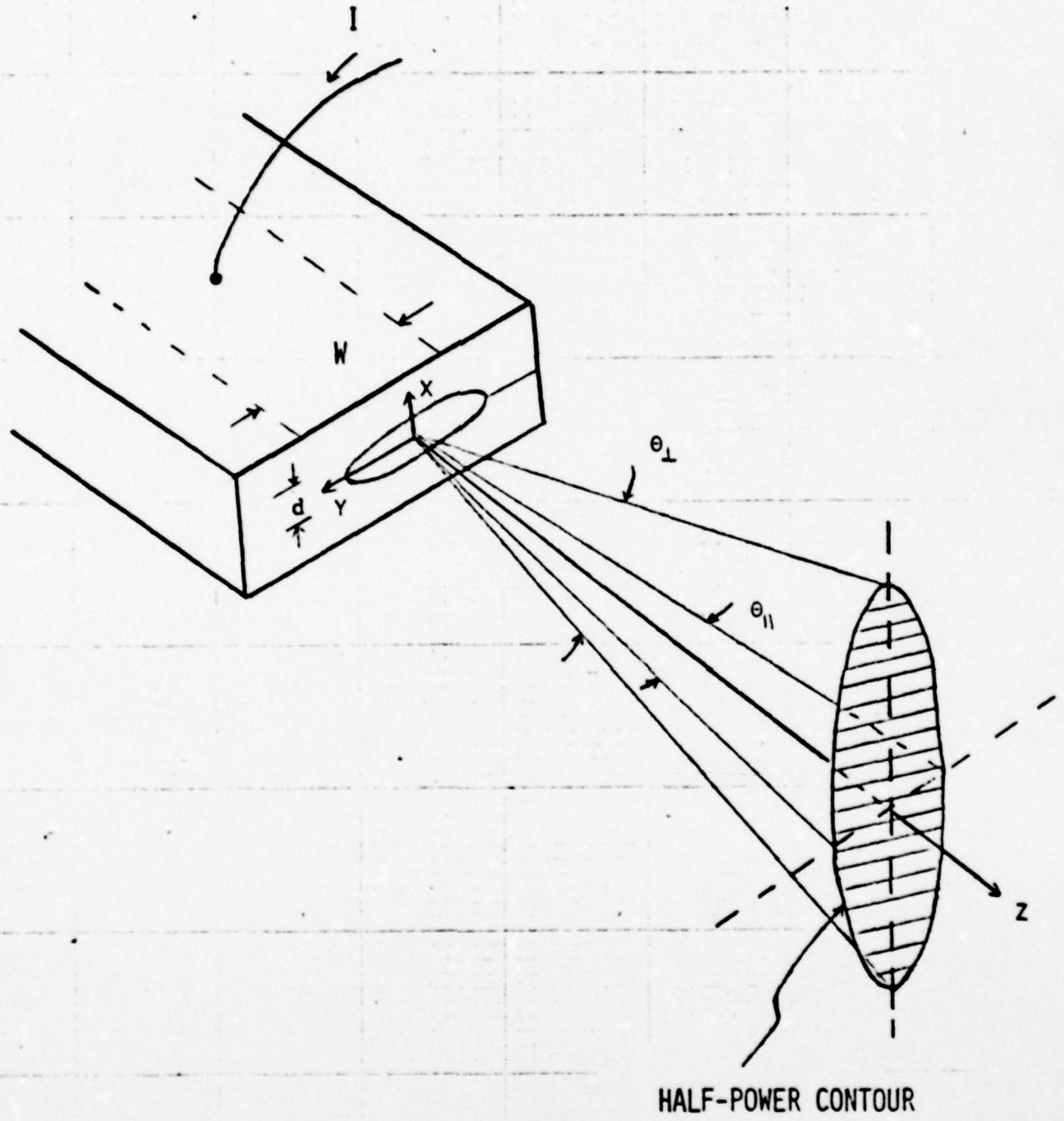


Fig. 1 Radiation from the end facet of an injection laser. The facet is located in the x-y plane with the z-axis normal to the facet. The half-power beam widths $\theta_\perp$ and $\theta_{||}$ are measured in the planes perpendicular and parallel to the junction plane.

PROGRESS REPORT

1. ARO PROPOSAL NUMBER: AMXRO-PRI-13568-EL

2. PERIOD COVERED BY REPORT: July 1, 1976 to December 31, 1976

3. TITLE OF PROPOSAL: Design of Injection Lasers for Improved Radiation Performance

4. CONTRACT OR GRANT NUMBER: DAAG29-76-G-0146

5. NAME OF INSTITUTION: Southern Methodist University

6. AUTHOR(S) OF REPORT: Jerome K. Butler

7. LIST OF MANUSCRIPTS SUBMITTED OR PUBLISHED UNDER ARO SPONSORSHIP DURING THIS PERIOD, INCLUDING JOURNAL REFERENCES:

8. SCIENTIFIC PERSONNEL SUPPORTED BY THIS PROJECT AND DEGREES AWARDED DURING THIS REPORTING PERIOD:

J. K. Butler
C. S. Wang
J. L. Delaney

13568EL

PROFESSOR JEROME K. BUTLER
DEPT. OF ELECTRICAL ENGINEERING
SOUTHERN METHODIST UNIVERSITY
DALLAS, TX 75275

Introduction

The research performed on this project has been directed toward the analysis of semiconductor laser modes in the plane of the junction. (Mode confinement perpendicular to the active region is due to the grown heterojunctions while confinement along the junction plane is associated with the device geometry. In the case of the stripe-geometry laser, confinement is due to the stripe contact as shown in Fig. 1.)

More specifically, we give brief results of our work concerned with: (1) a new waveguide model developed for stripe geometry lasers, (2) a comparison of theoretical and experimental radiation patterns in the plane of the junction (this pattern is tied to the lateral waveguide geometry), and (3) two dimensional mode reflectivity data.

Research Direction

In Fig. 1(a) we show a cross section of the laser geometry while in (b) we show the detailed geometry of the active region. In the direction normal to the junction plane (transverse direction), the fields are confined by the index steps between the active region and the surrounding passive media and have the sinusoidal shape. The mode can be restricted to the lowest order by making the active region very thin or the index step very small. However, along the junction plane, the mode structure remains somewhat uncontrollable despite the introduction of the stripe contact. The active region under the stripe is treated as an antenna aperture and a rectangular waveguide model is applied to study the radiation pattern and mode reflectivity.

Figure 2 shows the far-field radiation pattern in both the transverse (vertical) and lateral (horizontal) directions. The structure has $n_2 = 3.6$, $n_1 = n_3 = 3.46$, $n_4 = n_5 = 3.595$, $d = 0.25$ μm, and $2w = 13$ μm. The vertical direction radiation pattern is shown in Fig. 2 (a) where the half power beamwidth is 40.5° and is roughly the same as the one obtained from one dimensional model. The lateral direction radiation pattern has $\theta_{\parallel} \approx 3.6°$. This is somewhat narrow than the measured result which is shown in Fig. 2 (b). This discrepancy may be due to the uncertain estimation of n_4 and n_5 outside the active region in lateral direction. Also, the difference may be due to the fact that losses in regions 4 and 5, outside the active region, were neglected.

To more accurately model the radiation pattern in the horizontal direction, a waveguide geometry different from that shown in Fig. 1 must be explored. Current spreading under the stripe contact primarily determines the field distribution in lateral direction. A descrepancy between measured and calculated results may be due to the fact that current spreading was neglected. The refractive index does not change abruptly. Recently, Cook and Nash[1] claimed they found experimental evidence to show that lateral field confinement is due to: (1) gain-guiding, and (2) index anti-guiding. Overall, the gain induced guidance is predominant. In order to approximate the gradual change of the index, we apply the five-layer model[2] to represent the lateral direction change. For simplicity, only three-layer structure is considered in vertical direction. The model of the waveguide structure is shown in Fig. 3. We assume that the center region 3 has strong gains 50 cm^{-1} with large thickness; regions 2 and 4 have less gains 20 cm^{-1} with narrow widths. However, the outer regions 1 and 5, outside the stripe contact, have losses -10 cm^{-1}. In order to include the anti-guiding effect, we assume that the center layer has the lowest index 3.599 in lateral direction; two surrounding regions 2 and 4 have indices 3.5995; and two outer regions 1 and 5 have indices 3.6. The vertical confinement comes from the heterojunction index steps in which we have $n_6 = n_7 = 3.46$, $n_3 = 3.599$.

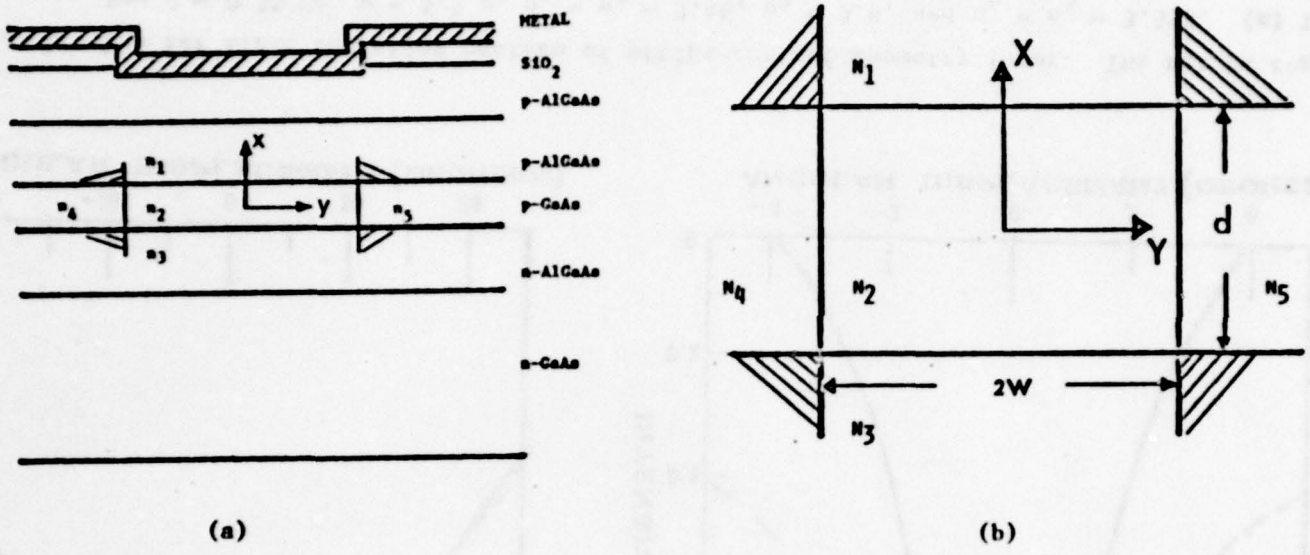
By suitable width adjustment of various regions and choosing gain-loss values, we can fit the calculated lateral radiation pattern to a measured one very accurately. For example, we choose $d_1 = d_3 = 2.625$ μm, $d_2 = 8.75$ μm and the index and gain/loss values of various regions as above in which the gain guiding and index anti-guiding effects are considered. The result is shown in Fig. 4. The calculated half power beamwidth is 7.2° which is about the same as the measured one.

Finally, the modal reflectivity of various two-dimensional modes has been obtained as a function of the stripe width. The results are shown in Fig. 5. (The parameters are listed in the figure.) We notice that the fundamental lateral mode has the largest reflectivity except near the cut-off width of the higher lateral modes. This means that the lower order lateral modes have a better chance to oscillate than the higher order ones. Also, there are minimal values near the cut-off stripe width of the various

lateral modes. As the stripe width is reduced further, the reflectivity of higher orders increases very sharply and may have a value larger than the fundamental mode. Generally, the lateral fundamental mode has the highest reflectivity. On the other hand, at large stripe widths $R_{1n} \rightarrow R_1$, the one dimensional reflectivity.

References

1. D. D. Cook and F. R. Nash, J. Appl. Phys. 46, 1660 (1975).
2. J. K. Butler, J. Appl. Phys. 42, 4447 (1971).



(a) (b)

Fig. 1 (a) The geometrical structure of GaAs-AlGaAs stripe-geometry lasers. (b) The rectangular model used to calculate the two dimensional radiation pattern and mode reflectivity. The shaded areas are assumed to be metallic with no field penetration.

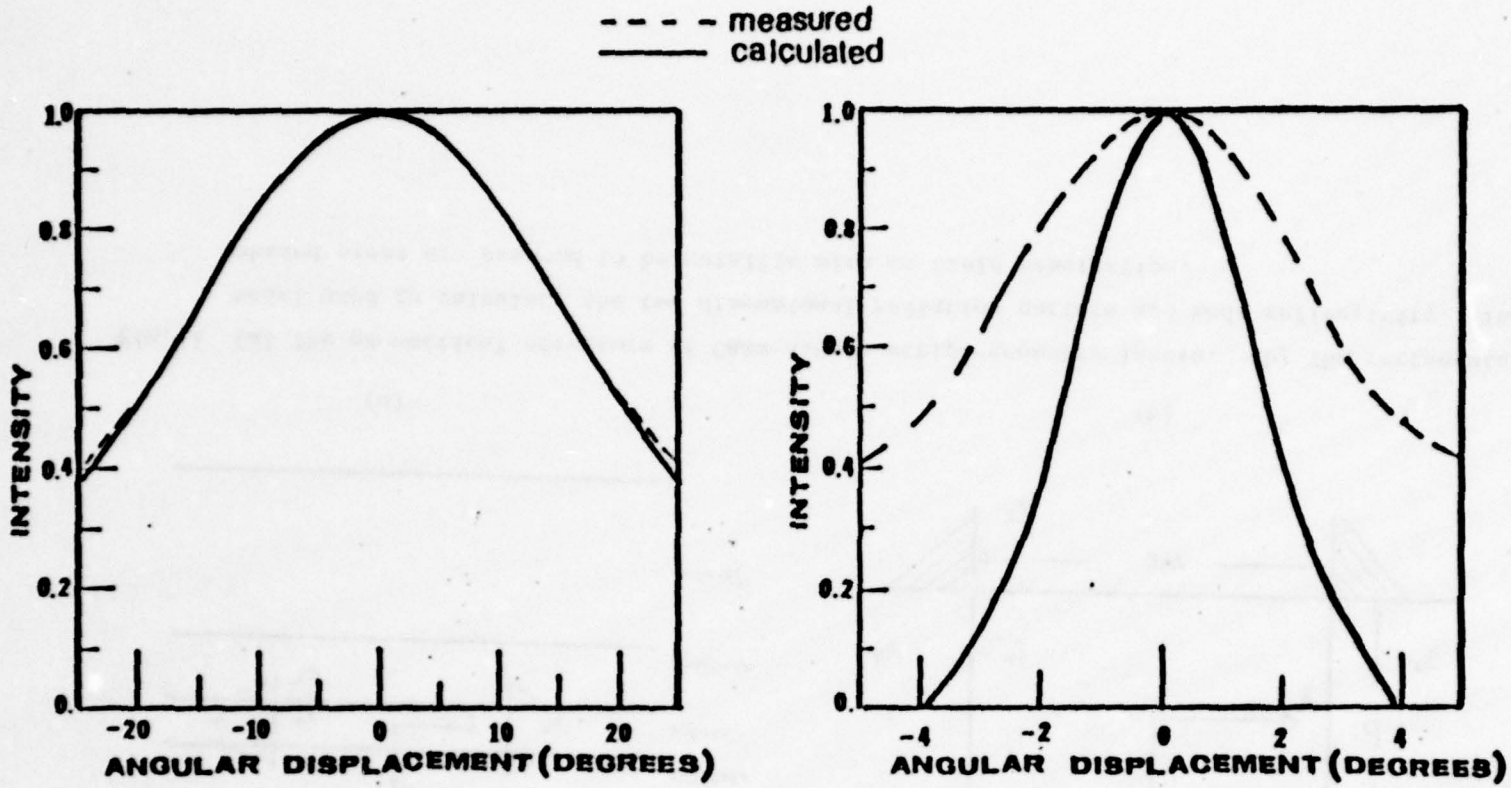


Fig. 2 The far field radiation pattern of stripe-contact geometry laser. The active region has d = 0.25 μm, w = 6.5 μ, $n_1 = n_3 = 3.46$, $n_2 = 3.6$, and $n_4 = n_5 = 3.595$. (a) The transverse direction (perpendicular to the junction) pattern E_ϕ, with $\phi = 0$. (b) The lateral direction (parallel to the junction) pattern E_θ with $\phi = \pi/2$. (The measured data were supplied by Dr. H. Kressel, RCA Laboratories.)

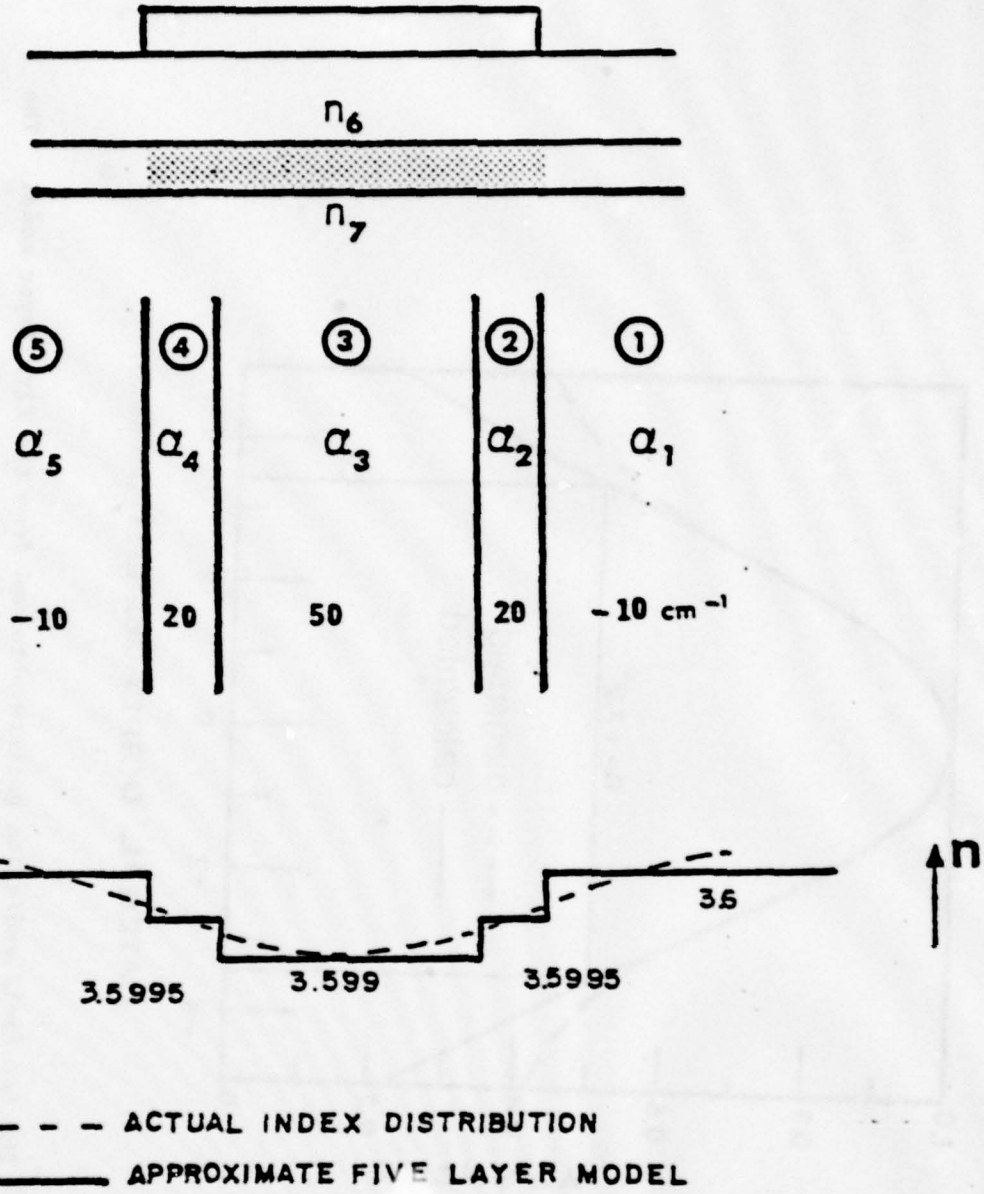


Fig. 3. Five layer model is used to approximate the lateral direction field distribution. The gain-guiding and index-antiguiding are shown.

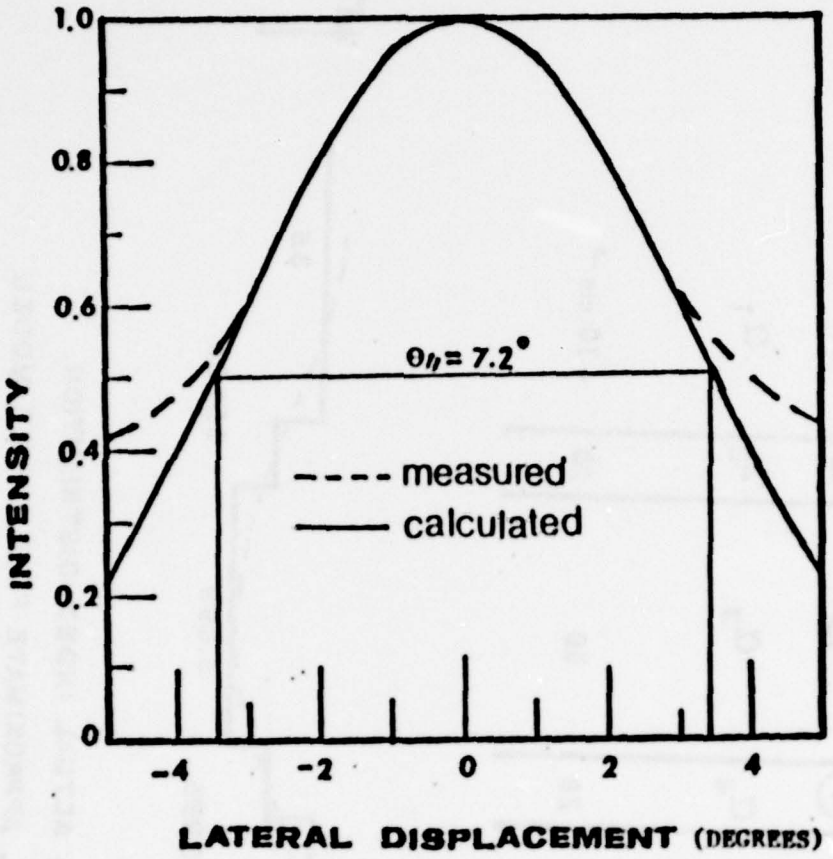


Fig. 4. The far field radiation pattern obtained from the five layer model. The calculated and measured results are in good agreement.

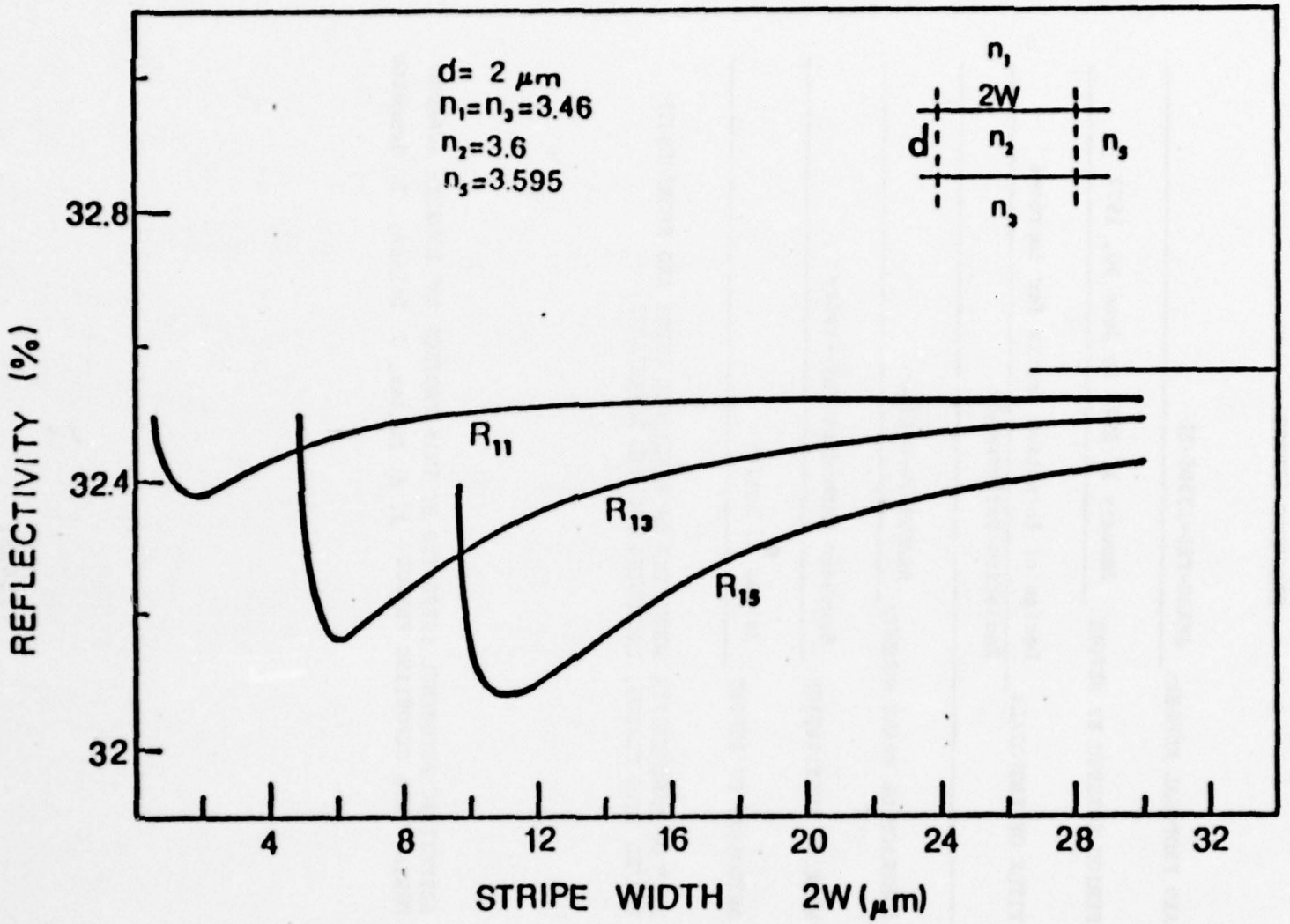


Fig. 5. The two dimensional reflectivity as a function of the stripe width. The fundamental mode has the lowest value in most range of stripe width.

PROGRESS REPORT

1. ARO PROPOSAL NUMBER: AMXRO-PRI-13568-EL

2. PERIOD COVERED BY REPORT: January 1, 1977 to June 30, 1977

3. TITLE OF PROPOSAL: Design of Injection Lasers for Improved Radiation Performance

4. CONTRACT OR GRANT NUMBER: DAAG29-76-G-0146

5. NAME OF INSTITUTION: Southern Methodist University

6. AUTHOR(S) OF REPORT: Jerome K. Butler

7. LIST OF MANUSCRIPTS SUBMITTED OR PUBLISHED UNDER ARO SPONSORSHIP DURING THIS PERIOD, INCLUDING JOURNAL REFERENCES:

8. SCIENTIFIC PERSONNEL SUPPORTED BY THIS PROJECT AND DEGREES AWARDED DURING THIS REPORTING PERIOD: J. K. Butler, J. Delaney, B. Sennette

13568EL

PROFESSOR JEROME K. BUTLER
DEPT. OF ELECTRICAL ENGINEERING
SOUTHERN METHODIST UNIVERSITY
DALLAS, TX 75275

BRIEF OUTLINE OF RESEARCH FINDINGS

The work during this previous period has been aimed at developing a comprehensive model of the stripe geometry laser structure. Typical laser wafers are fabricated by growing multiple layers of (Al Ga)As with varying percentages of Al and a final layer of GaAs. Contemporary structures have very narrow active layers ($\sim$ 0.1 - 0.2 μm) with small amounts of Al ($\sim$ 10%). The active layer is generally sandwiched between two (Al Ga)As layers containing approximately 30% Al. The final LPE growth layer is GaAs which is used to facilitate the forming of metallic contacts. However, first SiO_2 is deposited over the grown GaAs layer. Narrow stripes of SiO_2 are removed to form the light propagation axis. Finally, the metal layer is deposited over the SiO_2 and GaAs stripes.

The stripe metallic contact to the GaAs cap thus forms a path of current flow through the grown layers. The object of the stripe is to limit the lateral current spreading and to laterally confine the recombination region in the thin active layer.

The mathematical model which we are presently developing will allow for a complete analysis of mode characteristics in stripe lasers. This model takes in to account the complete details of the active region, the grown confining layers, the GaAs cap, and finally the SiO_2 - metallic layer formed over the GaAs. We have developed design curves which correlate the number of lateral waveguide modes with the stripe width and the level of pumping of the active region. The calculations show that lateral mode stability becomes a problem when lasers must be pumped at high levels. Lasers designed for single mode operation must be pumped at low levels. The complete details of our analysis are in preparation.

PROGRESS REPORT

(TWENTY COPIES REQUIRED)

1. ARO PROPOSAL NUMBER: AMXRO-PRI-13568-EL

2. PERIOD COVERED BY REPORT: July 1, 1977 to December 31, 1977

3. TITLE OF PROPOSAL: Design of Injection Lasers for Improved Radiation Performance

4. CONTRACT OR GRANT NUMBER: DAAG29-76-G-0146

5. NAME OF INSTITUTION: Southern Methodist University

6. AUTHOR(S) OF REPORT: Jerome K. Butler

7. LIST OF MANUSCRIPTS SUBMITTED OR PUBLISHED UNDER ARO SPONSORSHIP DURING THIS PERIOD, INCLUDING JOURNAL REFERENCES:

"Asymmetric Oxide Stripe Injection Lasers," J. K. Butler and H. S. Sommers, Jr. Submitted to IEEE J. Quan. Electron. (Part of this work is supported by a U. S. Army Research Office Grant to RCA Laboratories, Princeton, N.J.)

"Lateral Modes of Stripe Geometry Injection Lasers," J. K. Butler and J. B. Delaney, Submitted to IEEE J. Quan. Electron.

8. SCIENTIFIC PERSONNEL SUPPORTED BY THIS PROJECT AND DEGREES AWARDED DURING THIS REPORTING PERIOD:

J. K. Butler, J. B. Delaney, and B. Sennette

13568-EL

Dr. Jerome K. Butler
Southern Methodist University
Department of Electrical Engineering
Dallas, TX 75275

BRIEF OUTLINE OF RESEARCH FINDINGS

Much of the work over the previous period has been concerned with a study of modes in stripe geometry injection lasers. It has been found experimentally that oxide stripe lasers frequently produce radiation patterns with major lobes cocked at slight angles (0-10°) with respect to the normal of the end facet. In addition, the lobe direction is a function of drive current. (Obvious application considerations involve coupling laser output power to optical fibers. It is important to reduce beam jitter to obtain optimum coupling.) In an effort to understand the lateral patterns we have modelled stripe lasers with an asymmetric dielectric profile. The theoretical patterns of our model also produce asymmetric patterns. Consequently, we conclude that pattern instabilities are produced by laterally changing dielectric profiles.

Finally, most of the electromagnetic models of injection lasers with stripe contacts are insufficient in their descriptions of lateral modes. We have developed a new mathematical model useful for analyzing the field structure. For example, assuming a lateral parabolic dielectric profile the waveguide modes are written as linear combinations of Hermite-Gaussian functions. Previous analyses have assumed that lateral modes are described by single Hermite-Gaussian functions. For a given parabolic profile, the new model shows that the lateral field distribution of the fundamental mode spreads more than that obtained using previous models. Consequently, the radiation beamwidth will decrease. With the more accurate description of the lateral modes we can then obtain accurate dielectric profiles which are governed by the device geometry.

ASYMMETRIC MODES IN OXIDE STRIPE HETEROJUNCTION LASERS*

J. K. Butler+ and H. S. Sommers, Jr.
RCA Laboratories
Princeton, N. J. 08540

ABSTRACT

The region between the pair of heterojunctions of an oxide-stripe laser is modelled by a step profile in the lateral distribution (parallel to the heterojunctions) of the gain and of the refractive index, in an attempt to gain insight about the interpretation of the asymmetric radiation patterns frequently observed. A region of width W_a concentric with the stripe contact is subdivided into three sections, in each of which the gain and index are uniform. The step heights for the gain distribution and for the index distribution are given complementary symmetry, with the gain maximum superimposed on the index minimum. Asymmetry is introduced by lateral shift of the extrema at fixed W_a. With values of gain, index step, and W_a that seem reasonable for the laser studied, the near and far fields reproduce the measured profiles of a representative 10 μm stripe laser. The offset of the spontaneous profile is about 3 μm from the center of the stripe, and the beam has a single lobe for all low order modes with offset of order 5° from the facet normal. Because of the near cancellation of gain guiding by index antiguiding which is required to give the observed asymmetries, the propagation constant becomes very sensitive to injection level; this may explain the observed non-monotonic change of modal power and the very rapid shift of modal wavelength with current.

*Work supported in part by the U.S. Army Research Office.
+Permanent address, Southern Methodist University, Dallas, TX 75275

ABSTRACT

LATERAL MODES OF STRIPE GEOMETRY INJECTION LASERS*

by

J. K. Butler and J. B. Delaney
Southern Methodist University
Dallas, TX 75275

A new mathematical model useful for analyzing lateral modes of stripe geometry lasers is presented. The oxide stripe laser is modeled as a three layer waveguide in which the dielectric constant of the active layer varies only along the lateral direction; the dielectric constant of the surrounding passive layers is assumed to be position independent. The solution technique affords a rigorous matching of the fields of the active layer with those of the surrounding passive layers. To illustrate the model, the modes of a waveguide with parabolic dielectric variation along the lateral direction are investigated. The fields are written as a linear combination of Hermite-Gaussian (H-G) functions; heretofore, fields have been described with a single H-G function. The lateral field distribution of the fundamental mode spreads more than the one obtained using single H-G functions. Fundamental mode spread (spot size at halfpower) is calculated and related to the gain distribution. In addition, the peak gain fields are determined at threshold for various waveguide geometries.

*Supported by the U. S. Army Research Office.

PROGRESS REPORT

(TWENTY COPIES REQUIRED)

1. ARO PROPOSAL NUMBER: AMXRO-PRI-13568-EL

2. PERIOD COVERED BY REPORT: January 1, 1978 - June 30, 1978

3. TITLE OF PROPOSAL: Design of Injection Lasers for Improved Radiation Performance

4. CONTRACT OR GRANT NUMBER: DAAG29-76-G-0146

5. NAME OF INSTITUTION: Southern Methodist University

6. AUTHOR(S) OF REPORT: Jerome K. Butler

7. LIST OF MANUSCRIPTS SUBMITTED OR PUBLISHED UNDER ARO SPONSORSHIP DURING THIS PERIOD, INCLUDING JOURNAL REFERENCES:

"A Rigorus Boundary Value Solution for the Lateral Modes of Stripe Geometry Injection Lasers," To Be Published in IEEE J. Quan. El.

"Lateral Mode Content of Stripe Geometry Laser Structures," Submitted to IEEE J. Quan. El.

8. SCIENTIFIC PERSONNEL SUPPORTED BY THIS PROJECT AND DEGREES AWARDED DURING THIS REPORTING PERIOD:

J. K. Butler
J. B. Delaney

13568-EL

Dr. Jerome K. Butler
Southern Methodist University
Department of Electrical Engineering
Dallas, TX 75275

BRIEF OUTLINE OF RESEARCH FINDINGS

Over this last period we have developed for the first time a mathematical model for analyzing the optical fields of stripe geometry injection lasers. The aim here has been to develop such a model so that an accurate description of the lateral dielectric profile can be used for analyzing the lateral modes. Previous work on this grant has shown the important result: asymmetric dielectric profiles (asymmetric about the center of the stripe contact) lead to a distortion of the mode radiation pattern. With our new rigorous model complete radiation pattern behavior can be understood.

In this previous period we have developed a model which describes the number of lateral modes which may propagate in stripe geometry lasers and related devices. This study also addresses the problems of "kinks" or the high nonlinearities in the P-I diode characteristics. These kinks are primarily caused by the drive sensitive dielectric profile which of course governs the mode pattern and the mode content.

In conclusion, we have greatly increased our understanding of the performance characteristics of various laser devices. It is clear that the classical stripe-geometry devices will have to a certain degree mode stability and pattern distortion problems.

ABSTRACT

LATERAL MODE CONTENT OF STRIPE GEOMETRY LASER STRUCTURES*

by

J.B. Delaney and J.K. Butler
Southern Methodist University
Dallas, Texas 75275

and

H. Kressel
RCA Laboratories
Princeton, N.J. 08540

A model is presented describing the lateral mode content of stripe geometry laser structures. A dielectric discontinuity in the lateral junction plane, determined from the gain/loss profile of the active layer and from the total geometrical structure of stripe geometry devices, is calculated and related to the cutoff conditions of the various lateral modes. In our model, characterized by a step in the lateral complex dielectric constant of the active layer, the cutoff conditions are dependent upon the gain region width defined by injection under the stripe. The model also provides a comparative analysis of the standard oxide stripe and the channeled-substrate lasers. We examine conditions under which the fundamental mode is unstable and in fact may not propagate.

*This work was supported by U.S. Army Research Office.

ABSTRACT

A RIGOROUS BOUNDARY VALUE SOLUTION FOR THE LATERAL MODES OF STRIPE GEOMETRY INJECTION LASERS*

by

J. K. Butler and J. B. Delaney
Southern Methodist University
Dallas, TX 75275

A new mathematical model useful for analyzing lateral modes of stripe geometry lasers is presented. The oxide stripe laser is modeled as a three layer waveguide in which the dielectric constant of the active layer varies only along the lateral direction; the dielectric constant of the surrounding passive layers is assumed to be position independent. The solution technique affords a rigorous matching of the fields of the active layer with those of the surrounding passive layers. To illustrate the model, the modes of a waveguide with parabolic dielectric variation along the lateral direction are investigated. The fields are written as a linear combination of Hermite-Gaussian (H-G) functions; heretofore, fields have been described with a single H-G function. Fundamental mode spread (spot size at halfpower) is calculated and related to the gain distribution. (Previous estimates of the lateral field spread of the fundamental mode using a single H-G function not rigorously matched at the boundaries can yield spot sizes as much as 30% different from results calculated from linear combinations of H-G functions.) In addition, the peak gain fields are determined at threshold for various waveguide geometries.

*Supported by the U.S. Army Research Office.

PROGRESS REPORT

(TWENTY COPIES REQUIRED)

1. ARO PROPOSAL NUMBER: AMXRO-PRI-13568-EL

2. PERIOD COVERED BY REPORT: July 1, 1978 to December 31, 1978

3. TITLE OF PROPOSAL: Design of Injection Lasers for Improved Radiation Performance

4. CONTRACT OR GRANT NUMBER: DAAG29-76-G-0146

5. NAME OF INSTITUTION: Southern Methodist University

6. AUTHOR(S) OF REPORT: Jerome K. Butler

7. LIST OF MANUSCRIPTS SUBMITTED OR PUBLISHED UNDER ARO SPONSORSHIP DURING THIS PERIOD, INCLUDING JOURNAL REFERENCES:

"Lateral Mode Control in Stripe Contact Injection Lasers, " IEEE International Electron Devices Meeting, Dec. 4-6, 1978, Washington, D.C.

"The Effect of Device Geometry on Lateral Mode Content of Stripe Geometry Lasers," To Be Published IEEE J. Quan. El.

8. SCIENTIFIC PERSONNEL SUPPORTED BY THIS PROJECT AND DEGREES AWARDED DURING THIS REPORTING PERIOD:

Jerome K. Butler
Joseph B. Delaney
Marion W. Scott

13568-EL

Dr. Jerome K. Butler
Southern Methodist University
Department of Electrical Engineering
Dallas, TX 75275

BRIEF OUTLINE OF RESEARCH FINDINGS

The work over this past period has progressed along two lines: (1) Theoretical investigation of lateral waveguide modes and (2) Experimental investigation of wave propagation in laser structures.

J. B. Delaney has worked primarily in theoretical aspects of lateral mode characteristics. One of the primary research topics in injection laser studies concerns the development of devices which support stable oscillating modes. Instabilities produce "kinks" in the power-current characteristics and radiation patterns with lobe directions that are sensitive to drive. Stripe geometry lasers have instabilities which are attributed to the index antiguiding nature of the waveguide modes. Index antiguiding is primarily due to carrier injection in the active region and thus depresses the refractive index there. We have shown that the overall device geometry of stripe lasers can contribute to antiguiding effects.

M. W. Scott has been working on the experimental investigations. (He has also made a study of radiation patterns from optical stripline waveguides. These waveguides are constructed similar to stripe geometry lasers. He is in the final stages of his manuscript preparation "Radiation from Optical Stripline Waveguide.") The experimental measurements being conducted concern the focusing of 1.15 micron radiation from a He-Ne laser on the facet of a stripe geometry laser and observing the mode structure on the opposite facet. The lasers were prepared at RCA Laboratories, Princeton, N. J. and were mounted on special headers so that observations of front and rear facets could be made. Our basic objective for this study is to develop an understanding of waveguiding in lasers by probing the waveguide with light at 1.15 microns which is insensitive to the waveguide gain which guides the light at the 0.83 micron wavelength.

PROGRESS REPORT

(TWENTY COPIES REQUIRED)

1. ARO PROPOSAL NUMBER: AMXRO-PRI-13568-EL

2. PERIOD COVERED BY REPORT: January 1, 1979 to June 30, 1979

3. TITLE OF PROPOSAL: Design of Injection Lasers for Improved Radiation Performance

4. CONTRACT OR GRANT NUMBER: DAAG29-76-G-0146

5. NAME OF INSTITUTION: Southern Methodist University

6. AUTHOR(S) OF REPORT: Jerome K. Butler

7. LIST OF MANUSCRIPTS SUBMITTED OR PUBLISHED UNDER ARO SPONSORSHIP DURING THIS PERIOD, INCLUDING JOURNAL REFERENCES:

"Radiation Fields of Optical Stripline Waveguides," (Submitted to IEEE Trans. Microwave Th. and Tech)

"Evaluation of Dielectric Optical Waveguides from their Far Field Radiation Patterns," (Submitted to IEEE J. Quan. Electron.)

8. SCIENTIFIC PERSONNEL SUPPORTED BY THIS PROJECT AND DEGREES AWARDED DURING THIS REPORTING PERIOD:

Jerome K. Butler
Joseph B. Delaney
Marion W. Scott

13568-EL

Dr. Jerome K. Butler
Department of Electrical Engineering
Southern Methodist University
Dallas, TX 75275

BRIEF OUTLINE OF RESEARCH FINDINGS

The work over this past period has progressed along: (1) theoretical investigations of lateral waveguide modes and (2) experimental investigations of wave propagation in laser structures. Our aim is directed toward the development of stable, single mode lasers important for many system applications.

J. B. Delaney's work in the analysis of laser modes is proving to be extremely valuable for characterizing contemporary laser structures. His work discussed in the last progress report (Details to be published in IEEE J. Quan. Electron., Aug. 1978) concerned the development of a waveguide model for stripe lasers with proper attention focused on the overall geometry, including the metallic stripe contact and isolating SiO_2 layers. The analysis was also applied to channel-substrate-planar (CSP) lasers which are relatively mode stable. Our calculations indicated that CSP devices are more mode stable than the stripe lasers. The analysis is being further developed in order to explore its full implementation on new devices.

J. B. Delaney's recent work which is being prepared for publication concerns the far field radiation of stripe lasers with small stripe widths S (<5 μm). Present literature indicates the lateral field beam (parallel to the junction plane) decreases as the active layer thickness d decreases (below 0.2 μm). Our new work shows that the lateral beam broadens as d drops. Further, the required gain at threshold, g_{th}, is developed in terms of S and d. Our results show that for a given d, an optimum S can be determined; this correlates to the determination of a minimum value of current at threshold.

Much of the analysis mentioned above require knowledge of the optical properties (the dielectric constant) of the device material (epitaxial SiO_2 and metallic layers). The epitaxial and SiO_2 layers have published optical properties, whereas, those of the metal contact are relatively unknown. (Contemporary devices have active regions near the contact with optical fields penetrating the metal.) Also, the mechanism producing lateral mode confinement in stripe lasers is still an unknown. Hence, we have been developing experimental methods to explore the various unknown parameters. M. Scott has continued to develop this important area of our program. His recent work submitted for publication concerned the pattern measurement of a laser cavity which was excited with an external source. From the far field measurement we estimated the properties of the epitaxial grown layers.

Evaluation of Dielectric Optical Waveguides From Their Far Field Radiation Patterns*

by M. W. Scott and J. K. Butler
Southern Methodist University
Dallas, Texas 75205

ABSTRACT

An experimental technique for determining the characteristics of dielectric optical waveguides is presented. The far field pattern of the waveguide is measured and compared with a theoretical pattern. The presence of spurious light in the far field complicates the measurement, but this difficulty can be minimized for many structures. Application to semiconductor laser structures is discussed. Determining the waveguiding properties of laser structures prior to processing can result in the early detection of faults for increased yield.

*Supported by U. S. Army Research Office

APPENDIX B

PROJECT PUBLICATIONS

1976 Device Research Conference, Salt Lake City, Utah

IIA-2 Optical Stripline Waveguides -
J. K. Butler and C. S. Wang, Southern Methodist University, Dallas, Texas 75275 and J. C. Campbell, Texas Instruments, Dallas, Texas 75222

One class of channel waveguides frequently proposed as elements in integrated optical circuits are optical striplines.[1] The structure consists of an underlying substrate with an index n_3, a slab of thickness, d, having a refractive index n_2, and an overlayed stripe of width 2w and an index n_1; the index $n_2 > n_1, n_3$. Optical confinement of the fields is restricted to the slab in the region below the stripe. Previous theoretical investigations[1,2] of these waveguides have used an artificial index discontinuity to explain the lateral optical confinement. The approach described here is to assume the waveguide modes are composed of a continuum of plane waves. Confinement to the region below the stripe is obtained by spatial interference. The propagation constants are calculated as a function of waveguide geometries. Model cutoff conditions are determined as a function of the slab thickness (d) and stripe width (2w) for a range of index steps. The observed modes reported by Blum et al.[3] agree with our calculations. We have measured the lateral field profiles of several GaAs optical striplines; experimental-theoretical comparisons are made.

We have fabricated several directional couplers consisting of parallel optical stripline waveguides. The coupling lengths of these devices have been measured for different waveguide widths and separations. Using our theoretical model we have calculated the coupling lengths; the experimental and theoretical coupling lengths are in agreement.

[1] E. Furuta, E. Noda and A. Ibaya, Appl. Opt. 13, 322 (1974).
[2] V. Ramaswamy, Bell Syst. Tech. J. 53, 697 (1974).
[3] F. A. Blum, D. W. Shaw and W. C. Holton, Appl. Phys. Lett. 25, 116 (1974).

Asymmetric Modes in Oxide Stripe Heterojunction Lasers

JEROME K. BUTLER, MEMBER, IEEE, AND HENRY S. SOMMERS, JR.

Abstract—The region between the pair of heterojunctions of an oxide stripe laser is modeled by a step profile in the lateral distribution (parallel to the heterojunctions) of the gain and of the refractive index, in an attempt to gain insight about the interpretation of the asymmetric radiation patterns frequently observed. A region of width b'_g concentric with the stripe contact is subdivided into three sections, in each of which the gain and index are uniform. The step heights for the gain distribution and for the index distribution are given complementary symmetry, with the gain maximum superimposed on the index minimum. Asymmetry is introduced by lateral shift of the extrema at fixed b'_g. With values of gain, index step, and b'_g that seem reasonable for the laser studied, the near and far fields reproduce the measured profiles of a representative 10 μm stripe laser. The offset of the spontaneous profile is about 3 μm from the center of the stripe, and the beam has a single lobe for all low-order modes with offset of order 5° from the facet normal. Because of the near cancellation of gain guiding by index antiguiding which is required to give the observed asymmetries, the propagation constant becomes very sensitive to injection level; this may explain the observed nonmonotonic change of modal power and the very rapid shift of modal wavelength with current.

Manuscript received October 17, 1977; revised December 16, 1977 and January 23, 1978. This work was supported in part by the U.S. Army Research Office.

J. K. Butler is with the Institute of Technology, Southern Methodist University, Dallas, TX 75275.

H. S. Sommers, Jr. is with RCA Laboratories, Princeton, NJ 08540.

I. Introduction

THIS paper presents a theoretical model of the lateral modes (modes in the junction plane) of the narrow oxide stripe injection laser which encompasses several experimental features that are not produced by the popular Hermite-Gaussian (H-G) model [1]. The investigation was prompted by our experimental studies of a large number of oxide stripe

0018-9197/78/0600-0413$00.75 © 1978 IEEE

lasers prepared from a variety of double-heterojunction wafers with thin cavities. In particular, the H-G model fails to account for the following observed properties. 1) In a sizeable fraction of individual lasers, the facet illumination (near-field) and the lateral (far-field) profile are markedly asymmetrical in respect to the gain profile and the normal to the facet, respectively [2]. This characteristic has also been noted in other laboratories [3]. 2) While the spatial patterns are often quite complex, with much resolved structure, they show little variation with current or output power [2]. This suggests that the mode profile depends but weakly on mode order.

II. Theoretical Model

The new theoretical model introduces an ad hoc dielectric profile which permits a machine study to find the *sizes* of the spatial asymmetries in the real and imaginary parts of the dielectric constant to produce the observed asymmetries of modal patterns. For pedagogical reasons, the treatment is cast in the customary terms of index antiguiding and gain guiding associated with the free carrier distribution, but does not imply that the carrier distribution is the complete explanation of the dielectric profile. It is found that a near-cancellation of the two types of guiding together with a suitable asymmetry common to both produces the kinds of patterns observed. While the adjusted sizes of the spatial asymmetries are found to be consistent with the present sketchy ideas used to connect the free carrier density and dielectric constant, the contribution of the paper is not support or nonsupport of their utility, but rather knowledge of both a profile which can yield such asymmetric modes and of its dispersion relations [4].

The effect of the concave refractive index and convex gain profiles is to produce modes confined laterally due to the gain. The modes are "gain guided" [5]-[7] as opposed to "index guided." Now for a specific complex dielectric profile related to the gain and index profiles, modal complex propagation constants and field profiles come from a solution of Maxwell's equations. Thus, each lateral mode propagates as $\exp(g_r z)$ where g_r, the gain of the rth mode, is determined from the complex propagation constant. The value of g_r is in a sense prorated over the lateral gain profile for each mode. It should also be noted that field profiles of index-guided modes are rather insensitive to gain profiles, whereas, field profiles of gain-guided modes are tightly coupled to the gain profile.

The electromagnetic field equations of two-dimensional waveguides can be approximated as discussed by Marcatili [8], and the field equations developed by assuming only one transverse component of the electric field. The cross section of the laser structure shown in Fig. 1 has optical fields concentrated in the vicinity of the active region with electric fields polarized parallel to the active layer. Current flowing through the active region produces optical gain spread over a width W_a. To approximate the effect of the nonuniform lateral distribution of carrier density, the active region is partitioned into three regions, which are supported on either side by passive regions (Fig. 2). Detail (a) shows the passive regions 1, 5 and the regions 2, 3, and 4 of the active section; detail (b) shows the corresponding gains, which represent regeneration in the active section and dissipation in the passive wings; and detail (c)

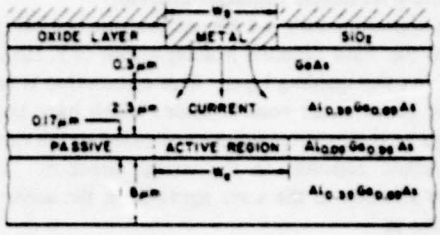


Fig. 1. Cross section of wafer 536 DH-CW with oxide stripe contact.

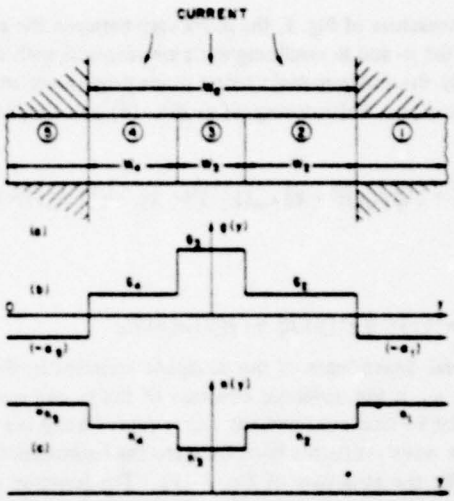


Fig. 2. Step waveguide model of laser in Fig. 1. (a) Partition of layer between heterojunctions into three active regions 2, 3, 4, and two passive regions 1, 5. (b) Gain profile. (c) Index profile.

shows the index of refraction, which increases from the minimum in the high gain central region. The guiding by the gain maximum is sufficient to overcome the defocusing effect of the index minimum.

For wave propagation in the z direction of the form $\exp(i\omega t - \gamma z)$ where $\gamma = \alpha/2 + i\beta$, the transverse dependence of the field quantities becomes:

$$E_x = 0$$

$$E_y = \psi(x, y) \tag{1}$$

$$E_z = \frac{1}{\gamma}\frac{\partial \psi}{\partial y} \tag{2}$$

$$H_x = -\frac{i}{k_0 \eta_0 \gamma}\left[k_0^2 \kappa(x, y) + \frac{\partial^2}{\partial y^2}\right]\psi \tag{3}$$

$$H_y = \frac{-i}{\gamma k_0 \eta_0}\frac{\partial^2 \psi}{\partial x \partial y} \tag{4}$$

$$H_z = \frac{i}{k_0 \eta_0}\frac{\partial \psi}{\partial x} \tag{5}$$

where k_0 is the free space wave number, $\eta_0 = 120\pi\ \Omega$, and $\kappa(x, y)$ is the relative dielectric constant. The transverse wave function ψ satisfies

$$\nabla_t^2 \psi + (k_0^2 \kappa + \gamma^2)\psi = 0, \tag{6}$$

where ∇_t^2 is the transverse Laplacian operator.

As a first approximation, we assume that the vertical (x) dependence of the wave function is independent of y, the lateral position in the waveguiding layer. This assumption is reasonable for the lasers under consideration, which have large dielectric steps at the heterojunctions compared to the variation in the dielectric constant in the lateral direction. Consequently, the solution to the wave equation in the active layer can be written as

$$\psi(x, y) = \psi(x)\,\psi(y). \tag{7}$$

For the structure of Fig. 1, the index step between the active layer and the p- and n- confining walls are identical with $\Delta n \simeq 0.19$. Only the fundamental vertical mode propagates, so that $\psi(x) = \cos k_x x$. Substituting $\psi(y)$ into (6) and simplifying [7]

$$\frac{d^2\psi(y)}{dy^2} + \{k_0^2\kappa(y)\Gamma + k_0^2\kappa_w(1-\Gamma) - k_x^2 + \gamma^2\}\,\psi(y) = 0 \tag{8}$$

where

$$\kappa(y) = n^2(y) - \tfrac{1}{2}g^2(y)/k_0^2 + i\,g(y)\,n(y)/k_0$$

is the lateral dependence of the dielectric constant in the active layer, κ_w is the dielectric constant of the p- and n-walls, and Γ is the vertical confinement factor representing the fraction of the wave inside the layer between the heterojunctions. $\Gamma \simeq 0.6$ for the structure of Fig. 1 [9]. The function $\psi(y)$ found from (8) determines predominantly the near-field behavior along y and the corresponding lateral radiation pattern.

The modal far-field patterns in the lateral direction can be shaped by varying both the index and gain profiles [Fig. 2(b) and (c)]. Of course when both $g(y)$ and $n(y)$ are symmetric, the modal patterns are symmetric about the facet normal, whether $n(y)$ sags below or rises above the outside values n_1, n_5 ($n_1 = n_5$). As a first approximation for modeling stripe contact lasers, we take $\alpha_1 = \alpha_5$, $g_2 = g_4$, $n_1 = n_5$, and $n_2 = n_4$. Also we choose g_2 and n_2 as average between their outside and inside values i.e., $g_2 = (g_3 - \alpha_1)/2$ and $n_2 = (n_3 + n_1)/2$. Thus the step models of $g(y)$ and $n(y)$ approximate the smooth continuous distributions.

When the high-gain region is centered in W_a, the modal patterns are similar to the H-G functions. However, as region 3 is shifted gradually to either the right or left of center, the far-field patterns become asymmetric about the facet normal. The major lobe of the fundamental mode shifts off the facet normal. For example when $n_3 - n_1 \sim 10^{-3}$ and when region 3 is shifted off center by 1 μm, the major lobe can shift almost 10° off the axis normal, and the higher modes have lost the characteristic H-G shapes [10].

III. Comparison with Experimental Patterns

We studied a conventional oxide stripe laser 7/77-9#4 whose patterns illustrate the asymmetry typical of many of our stripe contact lasers. Fig. 1 is the cross section of the starting wafer 536DH-CW, which was grown by liquid-phase epitaxy. The carrier concentrations of the semiconducting layers, reading from top to bottom, are 10^{18}/cm^3 p type, 3×10^{17} p, a low concentration in the active region from a trace of Si, and 2×10^{17} n type. The laser had an oxide stripe metallic contact [11] about 10 μm wide and cleaved facets separated 100 μm. One facet had a dielectric reflecting coating. According to the theory of current spreading in a two-layer cap [2], the effective width of the recombination region is 10 μm greater than the width of the contact.

All studies used a low duty cycle pulsed current (20 ns nominal width, 5000/s) to avoid significant heating. Measurements were made with a box car integrator with 10 ns nominal gate width as a peak detector. The spontaneous emission was transmitted through a tandem pair of 100 Å bandpass filters with centers 600 Å less than the coherent band. This short wave emission gives an account of the junction voltage at the output facet [2]. Further details of the technique are given in [2].

The PI (polarization index) characteristic was nearly linear with soft turn-on. No marked structure was present in it beyond a slight waviness. We have observed all the effects discussed in lasers with very linear characteristic curves as well as those with sharp kinks in PI, but have been unable to correlate any of the reported properties with kinks or structure. The patterns here presented were in the soft turn-on region close to threshold.

The model parameters and widths of regions 2, 3, and 4 were adjusted so that the theoretical pattern of a pure mode approximated both the monochromatic far-field pattern and the coherent near-field. The listed index steps are consistent with our limited knowledge of the carrier concentration beneath the stripe contact and of the dependence of refractive index on carrier density [7]. With the gain parameters of Table I, the modal gain $g = -\alpha = -2$ Real (γ) is about 100 cm^{-1} for each of the three lowest modes. At threshold, $g = (1/\Gamma)\alpha_{end}$, a condition satisfied by $\Gamma = 0.6$ and $\alpha_{end} = 60$ cm^{-1}.

Fig. 3 compares the experimental near-field patterns with the calculated *second*-order ($S = 2$) lateral mode. The shape of the spontaneous emission at 50 mA (threshold = 40 mA) is symmetrical with half width (full width at half power) of 14 μm; it is assumed to be concentric with W_a of Fig. 2 to enable comparison with the calculations. The coherent pattern at 50 mA, $P \approx 4$ mW, (B-experimental) is a single lobe with faint structure, half width of 8 μm, and offset of -2 μm from the spontaneous. The calculated pattern (B-theory) has a half width of 3.8 μm and displacement of -3.6 μm. The detail at the bottom of the figure locates the positions of the gain steps.

The corresponding beam profiles are shown in Fig. 4. The solid curve is measured at 52 mA and wavelength of 8192 Å with resolution of 0.4 Å. It is a single lobe with weak minor structure, half width of 7°, and peak at -6° from the normal to the facet. The theoretical curve (broken line) is similar but with slightly less structure, and has the same half width and offset.

The agreement between model calculation and observation (in particular of the beam profiles, where the instrumentation has selected a pure mode rather than the average over all S modes in the entire spectrum which is recorded for the near field) gives enough credence to the model to warrant analysis

TABLE I
PARAMETERS USED FOR MODES OF FIG. 2 $\lambda_0 = 0.82\ \mu m$

Region	1	2	3	4	5
widths (μm)	∞	6	5	4	∞
Refractive (a) index	3.6	3.598	3.596	3.598	3.6
Gain (cm^{-1}) (b)	~60	130	300	130	~60

(a) $n(y)$.
(b) $g(y)$.

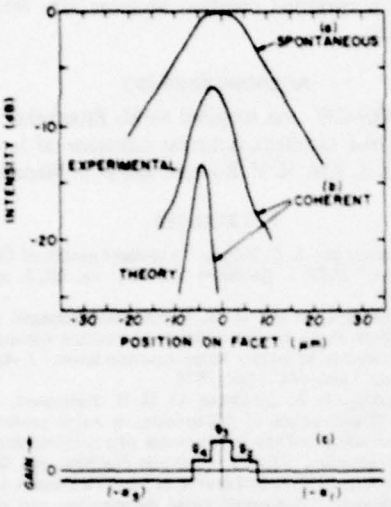


Fig. 3. Near Field. (a) Spontaneous intensity measured at short wavelength. (b) Coherent pattern—measured and calculated for second-order mode. (c) Positions of steps used in calculation. Center of active region W_a' of Fig. 2 assumed to lie on center of spontaneous profile. Note that the theoretical and experimental patterns in (b) are both shifted in same direction. Patterns of laser 7/77-9#4 10 mA above threshold, $P \approx 4$ mW.

of the theoretical patterns of different S modes. Fig. 5 shows the three lowest, with detail (a) the facet illumination and (b) the beam profiles. One striking feature is the similarity of the shapes, especially in the beam profiles; all the profiles are dominated by a single lobe, with half width varying from 6.5° for the lowest mode to 4° for $S = 3$. Also the near fields of $S = 1$ and 2 are nearly identical, and only by $S = 3$ is pronounced structure appearing. Another interesting feature of both sets of patterns is the direction of the displacement, which changes sign between successive modes; in the figure, odd modes are displaced to the right, even to the left. The calculated modal dispersions are $\Delta\lambda_{12} \approx -0.9$ Å and $\Delta\lambda_{23} \approx -2.5$ Å. For a box mode in a waveguide of width 14 μm (the value of W_a in Table I) the corresponding values would be -0.75 and -1.3 Å [12].

In our model we find that the wavelength and the near- and far-field patterns of each mode are functions of the dielectric profile. It has been found experimentally that the gain profile above threshold is a function of drive current [2], [3]. Hence, the parameters of Table I will change with current and so the frequencies and patterns will change with output power. Such a power dependence experimentally found is illustrated in Fig. 6. Detail (a) shows a high resolution (0.15 Å) spectrum

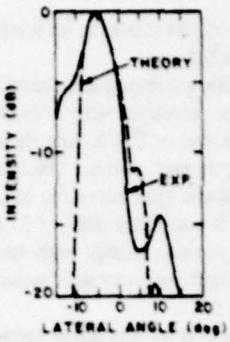


Fig. 4. Beam profiles, conditions of Fig. 3. Both patterns have a single lobe, shift above -5°.

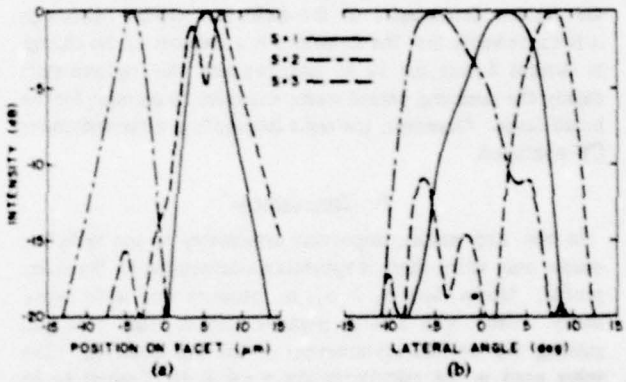


Fig. 5. Near- and far-field calculations, three lowest modes. Note that beam profiles have only a single lobe. (a) Facet illumination. (b) Beam profile.

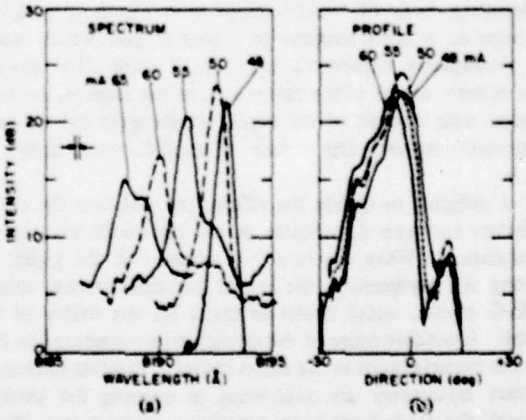


Fig. 6. Section of spectrum and beam profile at different currents. Note the steady shift with current of position of peak. Detail (a) has one normalization, detail (b) another. Power under 50 mA trace ≈ 0.2 mA. Laser 7/77-9#4.

of the beam collected by a large aperture aspheric lens for total power ranging from 3 to 6 mW (the power under the dashed line for 50 mA is about 0.2 mW). Notice the shift with current of the wavelength of the mode with no evidence of excitation of other lateral modes until 65 mA. A curious fea-

ture not predicted by the model in its present sophistication is the wide line, about 0.5 Å.

Fig. 6(b) gives the corresponding lateral profiles. The aspheric lens has been replaced with a cylindrical one, the slit widened to a resolution of 0.4 Å, and the spectrometer tuned to maximum signal at each current. Notice the nearly perfect repetition of the shape (the curve for 65 mA duplicates that for 60 mA except for an extra shift of 2° and slight change in power). The one obvious change with current is in the position of the peak, which seems to shift monotonically from -2° at 48 mA to -9° at 65.

Experimental features of the many stripe lasers with asymmetrical beams that we have studied are the shift of wavelength and field profiles with current and the broad spectral lines. Beam and spectral shifts with current can be tied to the current dependence of the dielectric profile. Although it is conceivable that the linewidth is a measure of the change in current during the 10 ns sampling gate, the required shift during the sampling period seems excessive to account for the broad lines. Moreover, the same linewidth is observed under CW operation.

IV. Discussion

In our step model, important asymmetry in the radiation occurs only when there is appreciable defocusing by the index profile. Modes with $n_3 > n_1, n_4$ produce very little asymmetry. Only with a large negative step in index plus gain guiding did we find asymmetries of the size observed. The value used in the calculation $\Delta n = -4 \times 10^{-3}$ seems to be compatible with our present understanding of the perturbation to the index accompanying injection of enough free carriers to give the required local gain of 300 cm^{-1}.

Because of the near cancellation of gain guiding by index antiguiding, both of which change with injection level, the propagation is quite sensitive to change in gain, which makes the propagation constant a function of current (or power). This rubbery nature of the cavity may be the cause of the large changes with current of the modal wavelengths and the nonmonotonic current dependence of modal power shown in Fig. 6.

It is difficult to decide the efficacy of replacing the actual dielectric and gain distribution in the laser with the step approximation. When the step 3 is centered in the guide, removing the asymmetry, the modal patterns become similar to H-G modes, which seems to speak for the utility of the model. A possible cause of the asymmetries introduced in Fig. 2 is the imperfections in the stripe contact. Possible sources of contact asymmetry are shadowing in opening the window through the oxide layer or in deposition of the metal. While we have modeled the distortion as a fixed displacement of the extrema of both gain and index, it seems probable that displacement of one relative to the other would serve as well. The latter has the attractive feature that the distortion need not affect the current distribution, agreeing with our observation of a quite symmetric spontaneous pattern on the facet accompanying strongly distorted coherent patterns.

In conclusion we have shown with a specific example that an asymmetric step waveguide can produce the type of distorted patterns observed in many stripe lasers; that for it the dependence of pattern shape on mode number is so weak that the modal content cannot be readily estimated from the beam profile; and that when index defocusing is comparable with gain guiding, the propagation constant becomes very sensitive to changes in gain.

Acknowledgment

Wafer 536DH-C.W. was supplied by M. Ettenberg. We also acknowledge the excellent technical assistance of L. Elbaum, M. G. Harvey, A. Kan, H. V. Kowger, and D. P. Marinelli.

References

[1] T. H. Zachos and J. E. Ripper, "Resonant modes of GaAs junction lasers," *IEEE J. Quantum Electron.*, vol. QE-5, pp. 29-37, Jan. 1969.

[2] H. S. Sommers, Jr. and D. O. North, "Experimental and theoretical study of the spatial variation of junction voltage and current distribution in narrow stripe injection lasers," *J. Appl. Phys.* vol. 48, pp. 4460-4467, Oct. 1977.

[3] P. A. Kirkby, A. R. Goodman, G. H. B. Thompson, and P. R. Selway, "Observations of self-focusing in stripe geometry semiconductor lasers and the development of a comprehensive model of their operation," *IEEE J. Quantum Electron.*, vol. QE-13, pp. 705-719, Aug. 1977; K. Kobayashi, R. Lang, H. Yonezu, I. Sakuma, and I. Hayashi, "Horizontal mode deformation and anomalous lasing properties of stripe geometry injection lasers-experimental," *Japan J. Appl. Phys.*, vol. 16, pp. 207-208, Jan. 1977.

[4] N. Chinone, "Nonlinearity in power-output-current characteristics of stripe-geometry injection lasers," *J. Appl. Phys.*, vol. 48, pp. 3237-3243, Aug. 1977, introduces an asymmetry in gain profile as perturbation to the H-G treatment, and examines the effect on the fundamental mode. We are concerned with the distorted *high-order* modes which are excited in our narrow stripe lasers.

[5] D. D. Cook and F. R. Nash, "Gain-induced guiding and astigmatic output beams of GaAs lasers," *J. Appl. Phys.*, vol. 46, pp. 1660-1672, Apr. 1975.

[6] B. W. Hakki, "Striped GaAs lasers: Mode size and efficiency," *J. Appl. Phys.*, vol. 46, pp. 2723-2730, June 1975.

[7] T. L. Paoli, "Waveguiding in a stripe-geometry junction laser," *IEEE J. Quantum Electron.*, vol. QE-13, pp. 662-668, Aug. 1977.

[8] E. A. J. Marcatili, "Dielectric rectangular waveguide and directional coupler for integrated optics," *Bell Syst. Tech. J.*, vol. 48, pp. 2071-2102, Sept. 1969.

[9] J. K. Butler and H. Kressel, "Design curves for double heterojunction laser diodes," *RCA Rev.*, vol. 38, pp. 542-558, Dec. 1977.

[10] L. I. Schiff, *Quantum Mechanics*. New York: McGraw-Hill, 1955, p. 60.

[11] I. Ladany and H. Kressel, "The influence of device fabrication parameters on the gradual degradation of (AlGa)As CW laser diodes," *Appl. Phys. Lett.*, vol. 25, pp. 708-710, Dec. 15, 1974.

[12] H. S. Sommers, Jr. and D. O. North, "The power spectrum of injection lasers: The theory and experiment on a nonlinear model of lasing," *Solid-State Electron.*, vol. 19, pp. 675-699, 1976.

A Rigorous Boundary Value Solution for the Lateral Modes of Stripe Geometry Injection Lasers

JEROME K. BUTLER, MEMBER, IEEE, AND JOSEPH B. DELANEY

Abstract—A new mathematical model useful for analyzing lateral modes of stripe geometry lasers is presented. The oxide stripe laser is modeled as a three-layer waveguide in which the dielectric constant of the active layer varies only along the lateral direction; the dielectric constant of the surrounding passive layers is assumed to be position independent. The solution technique affords a rigorous matching of the fields of the active layer with those of the surrounding passive layers. To illustrate the model, the modes of a waveguide with parabolic dielectric variation along the lateral direction are investigated. The fields are written as a linear combination of Hermite-Gaussian (H-G) functions; heretofore, fields have been described with a single H-G function. Fundamental mode spread (spot size at halfpower) is calculated and related to the gain distribution. (Previous estimates of the lateral field spread of the fundamental mode using a single H-G function not rigorously matched at the boundaries can yield spot sizes as much as 30 percent different from results calculated from linear combinations of H-G functions.) In addition, the peak gain fields are determined at threshold for various waveguide geometries.

Introduction

THE modal characteristics of stripe geometry injection lasers are presented here. The theoretical model developed allows for a rigorous treatment of both lateral (along the junction plane) and vertical modes of the oxide stripe injection lasers. Early work focused on a model which treated the active region as a light guiding structure with a smooth continuous dielectric variation along the transverse directions as opposed to abrupt index steps. In particular, the assumed dielectric variation along the lateral (x direction) and the vertical (y direction) was parabolic of the form $\epsilon(x, y) = \epsilon_0(ax^2 + by^2)$ [1]. The accuracy of this description is not unreasonable since it was applied to modeling homojunction lasers. However, the model is not applicable to heterojunction devices where the grown active layer, generally very thin for contemporary CW lasers, is sandwiched between two passive layers with smaller dielectric constants [2]. A more accurate description of the active layer is one with a refractive index which is constant along the vertical direction but varies parabolically along the lateral dimension [3], [4]. This dielectric description is reasonable since carrier inversion is uniform along the vertical dimension, whereas the inversion is not uniform along the lateral dimension due to current spreading from the stripe contact.

Manuscript received January 9, 1978; revised March 15, 1978. This work was supported by the U.S. Army Research Office.

The authors are with the Institute of Technology, Southern Methodist University, Dallas, TX 75275.

Standard techniques for solving boundary value problems do not readily apply to the geometry of the regions in the vicinity of the active layer. Consequently, previous analyses of the lateral mode structure of contemporary CW stripe geometry devices have been approximate. In particular, the dielectric constant of the active layer varies along the lateral dimension while the dielectric constant of the bounding p- and n-AlGaAs layers is homogeneous. For parabolic index variations in the active layer, the solution of the wave equation yields Hermite-Gaussian (H-G) functions. On the other hand, solutions of the wave equation in the layers bounding the active regions are not H-G functions. Appropriate field quantities cannot be matched at the boundaries. The method used here incorporates a technique developed previously [5]. The solution of the wave equation in the active layer is written as a linear combination of H-G functions whereas, in the bounding passive regions, the solution of the wave equation is written as a linear combination of plane waves. Using boundary conditions at the heterojunctions, an eigenequation is developed whose solution gives the appropriate modal propagation constants. The normal modes of the laser structure are linear combinations of H-G functions with weighting coefficients dependent upon the specifics of the geometry. The theory is developed to the extent that complex dielectric constants can be used in the model. This means that structures which have either lateral index or gain guiding properties can be analyzed.

An understanding of lateral mode stability of stripe geometry lasers has led to interest in accurate modeling of the lateral index profile and of lateral mode characteristics. Lateral mode perturbation due to nonparabolicity of the gain profile was also treated by expanding the fundamental mode in a series of H-G functions [6]. A complete model for the lateral mode characteristics would then include these perturbed solutions due to aberrations of the parabolic gain profile properly matched at the boundaries as we have discussed. However, in this paper we address ourselves solely to the effects on lateral modes of matching solutions at the boundaries and illustrate these effects using a parabolic dielectric model.

Theory

Due to the nature of the geometrical structure of stripe geometry injection lasers, it is difficult to formulate a simple eigenvalue problem accurately characterizing the modes. As mentioned previously, the eigenmodes of stripe geometry lasers can be described as linear combinations of H-G func-

0018-9197/78/0700-0507$00.75 © 1978 IEEE

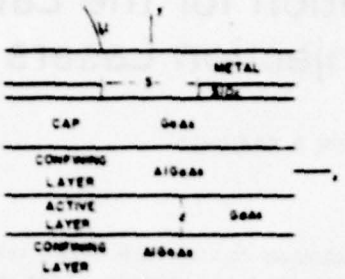


Fig. 1. Cross section of contemporary stripe geometry injection lasers.

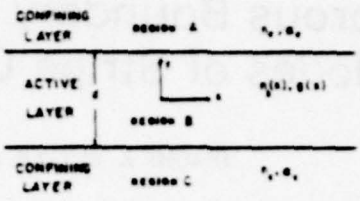


Fig. 2. The simplified waveguide geometry associated with the oxide stripe laser. The active layer B is sandwiched by two passive layers A and C which confine the vertical field. The lateral field is limited by the gain distribution.

tions obtained from a solution of Maxwell's equations. The field equations are reduced to an approximate form which describes the waveguide modes having electric fields polarized either along x or y as shown in Fig. 1. The fields with x and y polarizations are defined by the sets of modes $\{E^x_{pm}\}$ and $\{E^y_{pm}\}$, respectively [7]. Since most injection lasers have fields polarized predominantly along x [8], we limit our discussion to the E^x modes. Assuming mode propagation has the form $\exp(i\omega t - \gamma z)$ where $\gamma = -G/2 + i\beta$, the field equations become (the superscript x is dropped)

$$E_x = \Psi(x, y) \tag{1}$$

$$E_y = 0 \tag{2}$$

$$E_z = \frac{1}{\gamma} \frac{\partial \Psi}{\partial x} \tag{3}$$

$$H_x = \frac{i}{\gamma k_0 \eta_0} \frac{\partial^2 \Psi}{\partial x \partial y} \tag{4}$$

$$H_y = \frac{i}{\gamma k_0 \eta_0} \left(k_0^2 \kappa + \frac{\partial^2}{\partial y^2} \right) \Psi \tag{5}$$

$$H_z = -\frac{i}{k_0 \eta_0} \frac{\partial \Psi}{\partial y} \tag{6}$$

where k_0 is the free space wavenumber, $\eta_0 = 120\pi\ \Omega$, and $\kappa(x, y)$ is the relative dielectric constant. The transverse wavefunction Ψ satisfies

$$\nabla_t^2 \Psi + (k_0^2 \kappa + \gamma^2) \Psi = 0. \tag{7}$$

In the vicinity of the active region, the waveguide geometry has a form illustrated by Fig. 2. In the active layer, lateral field confinement is due to the following:

1) the nonuniform distribution of the index of refraction: and

2) the nonuniform distribution of the gain/losses [9], [10].

A reason that makes determination of the main source of lateral confinement difficult is the fact that the optical gain/loss coefficient and the index of refraction are inextricably related. On the other hand, the source of optical confinement along the vertical y direction can be easily determined. The large refractive index discontinuities at the heterojunctions which bound the active layer are almost solely responsible for both optical and carrier confinement to the active layer.

To formulate the laser modes the waveguide will be characterized as follows. The two horizontal passive layers A and C have complex dielectric constants which are position independent. The refractive index of these layers is determined by the lasing wavelength and aluminum concentration; the bulk absorption coefficient is positive. The active layer B is assumed to have a complex dielectric constant which is dependent only on the lateral x direction.

In the following mathematical formulation we assume that the dielectric constant is symmetrical about $x = 0$. In the active layer the wave equation has the form

$$\nabla_t^2 \Psi_b + [k_0^2 \kappa(x) + \gamma^2] \Psi_b = 0 \tag{8}$$

and $\kappa(x)$ is the complex dielectric constant of the active layer which has only lateral variations. In the active layer, the solution to (8) can be obtained by separation of variables; we write a typical solution of the form

$$\Psi_b(x, y) = \psi_b(x)\, \phi_b(y) \tag{9}$$

where the vertical function ϕ_b is

$$\phi_b(y) = \cos qy. \tag{10}$$

The lateral field function satisfies

$$\frac{d^2 \psi_b}{dx^2} + [k_0^2 \kappa(x) - q^2 + \gamma^2] \psi_b = 0. \tag{11}$$

As is well known, there exist two sets of vertical modes $\phi_b(y)$ where (10) is the solution of even modes about $y = 0$. The modes can have discrete q values representing trapped modes or it can take on a range of continuous q values, radiation modes along the y direction. The number of trapped vertical modes is dependent upon the cavity width d and the index steps between the active region and neighboring regions A and C [8]. Contemporary CW injection lasers have narrow active layers, $d \sim 0.1$-0.3 μm, and moderate index steps. These structures generally support only the fundamental trapped mode. Consequently, we limit our discussion here to only the fundamental vertical mode.

We now consider the solutions of (11) which give the lateral mode character. It should be noted that (11) has a one-dimensional form similar to typical slab waveguides. For example, the quantity $\gamma^2 - q^2$ can be interpreted as a one-dimensional eigenvalue.

The solution for $\psi_b(x)$ can be effected once the value of $\kappa(x)$ is specified. In terms of the bulk parameters, $n(x)$ the local refractive index and $\alpha(x)/g(x)$ the local absorption/gain coefficient, the dielectric constant can be approximated as

$$\kappa(x) \simeq n^2(x) - i\alpha(x) n(x)/k_0. \tag{12}$$

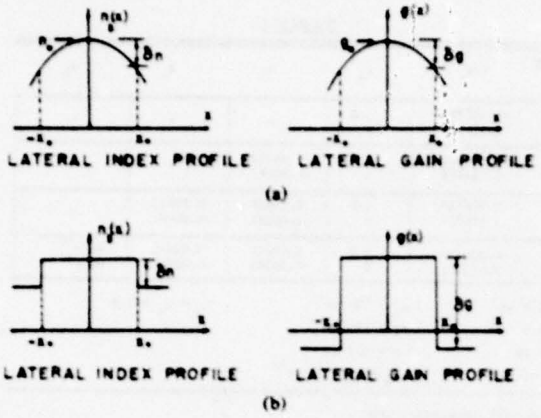


Fig. 3. The index and gain profiles of the active layer B. (a) Parabolic index and gain profiles and (b) step profiles.

In the case of negative absorption or gain, we write simply $\alpha(x) = -g(x)$. In Fig. 3 we illustrate two index, absorption/gain profiles. In Fig. 3(a), the index/gain has a parabolic profile while in (b) the optical parameters are shown to have step changes. Before we discuss the details of a specific structure, we note that the lateral modes obtained from the parabolic index model are only discrete, trapped modes whereas the step index model has a set of trapped as well as radiation modes. In our discussion, only the trapped modes will be used, and for the sake of convenience we consider the parabolic index profile. Therefore, the dielectric constant in the active layer is

$$\kappa(x) = \kappa_0 - k_0^2 a^2 x^2 \tag{13}$$

where κ_0 is the complex dielectric at $x = 0$. From (12), one gets

$$\kappa_0 = n^2(0) + ig(0)n(0)/(k_0 \cdot 10^4).$$

Using the parameters $n_0 = n(0)$, $g_0 = g(0)$, δn, δg, and x_0 we have

$$a^2 \simeq (2n_0\delta n + in_0\delta g/k_0 \cdot 10^4)/(k_0x_0)^2$$

where x_0 is in μm, k_0 has dimensions μm^{-1}, g, δg are in cm^{-1}. The wave equation becomes

$$\frac{d^2\psi_b}{dx^2} + [k_0^2\kappa_0 + \gamma^2 - q^2 - a^2k_0^2x^2]\psi_b = 0. \tag{14}$$

The solution of (14) yields the standard H-G wavefunctions. However, if we take a single H-G function, then the boundary conditions at the heterojunction interfaces cannot be met. It is therefore necessary to define a mode as one being a linear combination of H-G functions. The solution has the form (the b subscript on $\psi(x)$ and $\phi(x)$ is temporarily dropped for notational convenience)

$$\Psi_b(x, y) = \sum_{l=0}^{\infty} A_l\phi_l(y)\psi_l(x) \tag{15}$$

where

$$\phi_l(y) = \cos q_l y \tag{16a}$$

$$\psi_l(x) = H_l(\sqrt{a}k_0x)\exp\left(-\frac{a}{2}k_0^2x^2\right). \tag{16b}$$

In (16b) H_l is the Hermite polynomial, and q_l satisfies

$$k_0^2\kappa_0 + \gamma^2 = q_l^2 + k_0^2a(2l + 1). \tag{17}$$

The lateral modes can be divided into two sets depending upon whether the fields are even or odd about $x = 0$. For even fields the index $l = 0, 2, 4 \cdots$ whereas the odd fields have $l = 1, 3, 5, \cdots$. We limit our discussion here only to the even fields since primary interest will be focused on the fundamental waveguide mode.

A transverse mode is of course defined by a given propagation constant γ. Therefore $\Psi_b(x, y)$ in (15) gives the transverse modal field distribution with the total field solution being

$$\Psi_b(x, y)e^{-\gamma z} = e^{-\gamma z}\sum_{l=0}^{\infty} A_l\phi_l(y)\psi_l(x). \tag{18}$$

We see that the right-hand side of (17) must be independent of the index l. Even though q_l the vertical "wavenumber" varies with l, the vertical y dependence in (15) defines a specific waveguide mode which in our case is the fundamental vertical mode. This particular aspect of the problem will be better understood as we develop the total transverse mode eigenvalue solutions.

For the sake of simplicity, we consider a symmetric waveguide structure along the vertical so that $\Psi_a(x, y) = \Psi_c(x, -y)$ (double heterostructure GaAs-AlGaAs lasers are generally fabricated with equal amounts of aluminum in the p- and n-walls sandwiching the active layer). Outside the active layer, the wavefunction

$$\Psi_a(x, y) = \int_0^{\infty} B(\chi)\cos\chi x \exp\left[\left(\frac{d}{2} - y\right)(\chi^2 - k_a^2 - \gamma^2)^{1/2}\right]d\chi \tag{19}$$

which is symmetric about $x = 0$.

To determine $B(\chi)$ and the propagation constant γ, it is necessary to apply the appropriate boundary conditions at the heterojunctions. Therefore at $y = d/2$

$$\sum_{l=0,2,\cdots}^{\infty} A_l\phi_l\left(\frac{d}{2}\right)\psi_l(x) = \int_0^{\infty} B(\chi)\cos\chi x\, d\chi. \tag{20}$$

From the inverse Fourier transform $B(\chi)$ is

$$B(\chi) = \frac{2}{\pi}\sum_l A_l\phi_l\left(\frac{d}{2}\right)\bar{\psi}_l(\chi) \tag{21}$$

where we have defined the transform pair

$$\bar{\psi}_l(\chi) = \int_0^{\infty}\psi_l(x)\cos\chi x\, dx \tag{22a}$$

$$\psi_l(x) = \frac{2}{\pi}\int_0^{\infty}\bar{\psi}_l(\chi)\cos\chi x\, d\chi. \tag{22b}$$

Matching the field derivatives gives

$$\sum_l A_l \phi_l'\left(\frac{d}{2}\right) \psi_l(x) = -\int_0^\infty B(\chi)\,(\chi^2 - k_a^2 - \gamma^2)^{1/2} \cdot \cos \chi x \, d\chi. \tag{23}$$

The term

$$\phi'\left(\frac{d}{2}\right) = (d\phi/dy)_{y=d/2}.$$

Using the orthogonality relation

$$k_0 \int_0^\infty \psi_l(x)\,\psi_{l'}(x)\,dx = N_l \delta_{ll'} \tag{24}$$

where $\delta_{ll'}$ is the Kronecker delta and

$$N_l = \left(\frac{\pi}{a}\right)^{1/2} 2^{l-1} l! \tag{25}$$

we get the following relation

$$A_{l'} = \sum_l \Omega_{l'l} A_l. \tag{26}$$

The matrix elements

$$\Omega_{l'l} = -\frac{2}{\pi} \frac{\phi_l\left(\frac{d}{2}\right)}{N_{l'}\phi_{l'}'\left(\frac{d}{2}\right)} \int_0^\infty \bar{\psi}_{l'}(\chi) \cdot (\chi^2 - k_a^2 - \gamma^2)^{1/2}\, \bar{\psi}_l(\chi)\, d\chi. \tag{27}$$

The propagation constant γ is now determined from (26). The nontrivial solution is given as roots of the equation

$$\det (E - \Omega) = 0 \tag{28}$$

where E is the unit matrix. Note that the matrices E and Ω have infinite order. Consequently, it is impossible to find the eigenvalues γ by standard techniques. One approach is to assume a 1×1 matrix and determine γ from the resulting transcendental equation. Next expand E and Ω to 2×2, etc. The resulting sequence of γ values thus forms a Cauchy sequence. If the sequence approaches a limiting value as the matrix orders increase then the sequence converges. In Table I we show the fundamental mode γ values for different matrix orders. Note also the expansion coefficients $A_0, A_2, A_4 \cdots$ can be calculated after the appropriate eigenvalues are found.

For the sake of completeness, at this point we reconsider the various modes involved in this formulation. Different lateral modes are found from solutions of (28). For example, for a 1×1 matrix there will be only one eigenvalue, the one approximating the fundamental mode, while for a 2×2 matrix, there exist two eigenvalues, those of the fundamental and first-order modes. As the matrix orders increase, the complete set of lateral modes is calculated. The vertical modes can be found from (28) by judicious choices of q. To understand this, consider first the simple 1×1 equation with H–G functions

TABLE I

MATRIX ORDER	γ/k_0 [1]	A_0	A_2	A_4	A_6
1x1	-0.000399 3.524209	1.0 0	-	-	-
2x2	-0.000415 3.524219	1.0 0	0.04971 -0.00117	-	-
3x3	-0.000415 3.524219	1.0 0	0.05229 -0.00185	0.00113 -0.00021	-
4x4	-0.000417 3.524219	1.0 0	0.05217 -0.00295	0.00112 -0.00023	-2×10^{-4} 4×10^{-5}

$\lambda = 0.9$ μm $\quad \beta_b = 100\ \text{cm}^{-1} \quad n_a = n_c = 3.5$
$n_b = 3.6 \quad \beta_0 = 100\ \text{cm}^{-1}$
$a_0 = 5$ μm $\quad a = 0.2$ μm
$\Delta n = -0.0005 \quad \beta_a = \beta_c = 20\ \text{cm}^{-1}$

[1] Real part, imaginary part

$$\bar{\psi}_l(\chi) = (-1)^{l/2} \left(\frac{\pi}{2a}\right)^{1/2} H_l\left(\frac{\chi}{a^{1/2}}\right) \exp\left(-\frac{\chi^2}{2a}\right) \tag{29}$$

so that

$$\Omega_{oo} = \frac{2}{(\pi a)^{1/2}} \frac{\cos\left(q_0 \frac{d}{2}\right)}{q_0 \sin\left(q_0 \frac{d}{2}\right)} \int_0^\infty (\chi^2 - k_a^2 - \gamma^2)^{1/2} \cdot \exp\left(-\frac{\chi^2}{a}\right) d\chi. \tag{30}$$

In the limiting case $a \to 0$ (no curvature),

$$\Omega_{oo} \longrightarrow \frac{(-\gamma^2 - k_a^2)^{1/2}}{q_0} \frac{\cos\left(q_0 \frac{d}{2}\right)}{\sin\left(q_0 \frac{d}{2}\right)}. \tag{31}$$

The resulting eigenequation $\Omega_{oo} = 1$ is identical to that of the three-layer slab waveguide where $p_0 = (-\gamma^2 - k_a^2)^{1/2}$ and $p_0^2 + q_0^2 = k_0^2(\kappa_b - \kappa_a)$. Consequently, vertical modes found from (31) can be characterized by different q_0 values found from $p_0 = q_0 \tan(q_0 d/2)$. The $q_l (l = 2, 4, \cdots)$ values used in (28) are very close to q_0 when a is small (typical stripe laser structures). From (17) we find $q_l^2 = q_0^2 + 2la$.

Numerical Solutions

Several numerical solutions pertaining to contemporary stripe geometry lasers will be presented now. In particular we will study the convergence of the eigenvalues pertaining to the fundamental waveguide mode and fundamental mode spot sizes as a function of device geometry.

As mentioned previously, the solution of the eigenvalue equation (28) cannot be obtained using matrices *of infinite* order. Therefore, to determine the trend of the fundamental mode field solutions we first assume that the matrix orders of E and Ω are 1×1 and increase their orders up to 4×4 and observe convergence of fields and their eigenvalues. The specific parameters used in our model defining the parabolic dielectric constant are given in Table I. In the table, we show the values of the normalized propagation constant for the

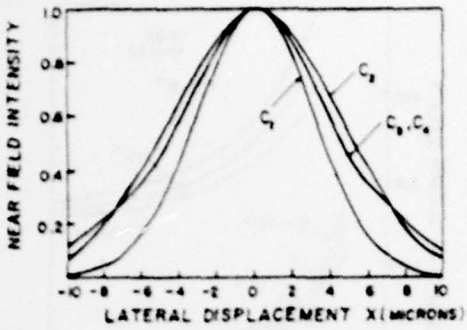


Fig. 4. The lateral field profiles of the fundamental waveguide mode for different expansion orders. C_1 pertains to the one component case while C_4 is for the four component case. Table I gives the expansion coefficients with the waveguide parameters.

various orders and the expansion coefficients A_i where it is arbitrarily assumed that $A_0 = 1 + i0$ for all cases. Note that for the four component case the magnitude of the coefficients decreases rapidly which means that the structure in region B has an x dependence of the form of a Gaussian function. These expansion coefficients are strongly dependent upon geometrical parameters such as the cavity width d and dielectric steps. The rate of convergence of the A_i's slows as d decreases. This means that for thin cavities, high percentages of high-order H-G functions are present in the fundamental cavity mode. It should be noted that the value of γ changes with matrix order; however, the difference between successive values decreases with order. In general, it is found that the single-component case is reasonably accurate for structures which have large d values or when the optical field energy is confined to the active region B.

The lateral field distribution of the fundamental waveguide mode is shown in Fig. 4. Curve C_1 represents the lateral field profile when the matrix order is 1 × 1 (one component) while C_4 pertains to the matrix of order 4 × 4 (four component). It is important to note that the curves C_3 and C_4 are almost identical which implies that the eigenvalues and fields are converging rapidly with respect to matrix order. It is seen that the effect of the high-order terms of the field expansion is to increase the lateral distribution of the field or to increase the field spot size. Physically, the spot size increase results from the optical field in region B leaking energy into the surrounding layers A and C. This lateral spreading effect is due to the fact that there is no mechanism to laterally confine the waveguide modes in regions A and C; lateral confinement is due solely to the graded dielectric constant in the active layer B.

We next turn our attention to calculations of the lateral spot sizes at halfpower as a function of the gain distribution parameter $2x_0$. In these calculations we define x_0 as the point where lateral gain is zero; i.e., $\delta g = g_0$. The value of g_0 will be appropriately adjusted so that the modal gain $G = 2\text{Real}(\gamma) = 50\ \text{cm}^{-1}$ which accounts for radiation end losses. This value approximates the end losses of a laser of length $L = 240\ \mu\text{m}$. In the various curves obtained from numerical calculations, we assume that the index of refraction at a given point along the lateral direction is a function of the gain or carrier inversion at that point. When the value δn is negative, the index of refraction provides an antiguiding effect, while if δn is positive, the refractive index provides a guiding effect. In these calculations we assume the relation

$$R = \delta n/\delta g\ \text{cm} \tag{32}$$

where the parameter R represents the effect of the gain on the index. When $R = 0$, the index has no curvature. Assume for example $\delta g = 100\ \text{cm}^{-1}$ and $R = 10^{-5}$ cm then $\delta n = 0.001$. In Figs. 5 and 6 we show the total width of the fundamental mode at halfpower as a function of the gain width $2x_0$ for index steps $n_0 - n_e = 0.1$ (Fig. 5) and 0.2 (Fig. 6); in (a), the total cavity thickness is 0.2 μm while in (b) the width is 0.1 μm.

Using the single H-G function to describe the fundamental mode, the spot size B is given by [3]

$$B = \frac{2(\ln 2)^{1/2}}{k_0 a_r^{1/2}\,\Gamma^{1/4}} \tag{33}$$

where Γ is the vertical field confinement factor and

$$a_r = \text{Real}(a) = \frac{(n_0 g_0)^{1/2}}{k_0 x_0}\ \text{Real}\,(2R + i\,10^{-4}/k_0)^{1/2}. \tag{34}$$

The peak gain g_0 is given by

$$g_0 = \frac{[1 + (1 + 8k_0 x_0^2 n_0 G\,10^{-4})^{1/2}]^2}{8k_0 x_0^2 n_0\,10^{-4}} + \frac{1-\Gamma}{\Gamma}\alpha_e. \tag{35}$$

The term $(1 - \Gamma)\alpha_e/\Gamma$ in (35) represents loss in the p- and n-regions adjacent to the active layer when $\alpha_e = \alpha_c$ [13].

As an example, take $d = 0.2\ \mu\text{m}$, $2x_0 = 10\ \mu\text{m}$, $\lambda = 0.9\ \mu\text{m}$, $G = 50\ \text{cm}^{-1}$, $\alpha_e = \alpha_c = 20\ \text{cm}^{-1}$, $n_0 = 3.6$, $n_e = n_c = 3.4$, and $R = 0$. The confinement factor $\Gamma = 0.6$ so that (33) gives $B = 7.36\ \mu\text{m}$. From our more exact model we find a spot size of 8.02 μm, an 8 percent difference. In general we find that the computed spot size using our model differs from the approximate B by as much as 30 percent. We show in Fig. 6 (dashed curves) the approximate beam size B found from (33). The relative comparisons between the approximate curves and the numerical ones are similar for other d values and index steps.

The active peak gain g_0 is shown in Figs. 7 and 8. We note again that g_0 is chosen such that the modal gain is 50 cm^{-1} to account for end losses. The two sets of curves are for $d = 0.1$ and 0.2 μm; the required gain for each set starts to increase for $2x_0$ values below $\sim 10\ \mu\text{m}$. Finally, we show in Fig. 9 the peak gain g_0 as a function of cavity thickness D for a given gain region thickness $2x_0$.

Conclusion

A new mathematical model describing the waveguide modes of the stripe geometry injection laser has been presented. Previous models used to describe these lasers have not given sufficient detail to the interaction between the vertical and lateral fields and to the nature of the boundary between the active layer and the passive p- and n-AlGaAs walls. The model presented here was applied to structures with dielectric step variations in the vertical direction and with parabolic varia-

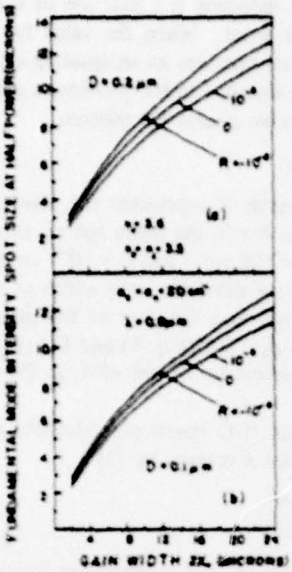


Fig. 5. Lateral field spot size as a function of the active region gain width. (a) $d = 0.2$ μm and (b) $d = 0.1$ μm. $a_0 = a_c = 20$ cm^{-1} and $n_0 = 3.6$, $n_s = n_c = 3.5$.

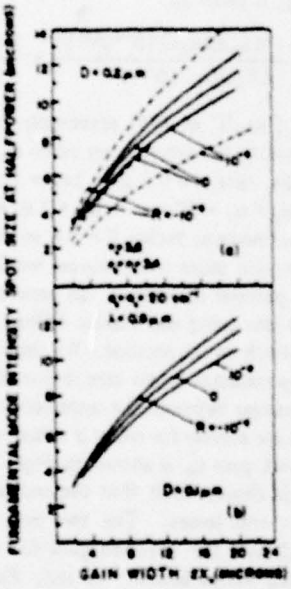


Fig. 6. Lateral field spot size as a function of the active region gain width. (a) $d = 0.2$ μm and (b) $d = 0.1$ μm. $a_0 = a_c = 20$ cm^{-1} and $n_0 = 3.6$, $n_s = n_c = 3.4$. The dashed curves in (a) are the approximate spot size found from (33).

tions of the dielectric constant along the lateral direction; lateral variations were limited to the active layer. Although we described the mode structure of the lateral parabolic varying dielectric, the model can be used to analyze arbitrary dielectric variations.

To understand the nature of the field solutions using an approximate technique with limited expansion coefficients, we have shown how the eigenvalues and fundamental mode field functions behave using a single component expansion and then increasing the number of expansion coefficients up to four.

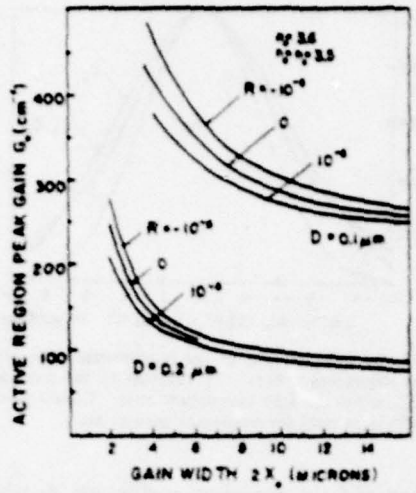


Fig. 7. Active region peak gain versus $2x_0$. Mode gain $G = 50$ cm^{-1} = end losses. Spot size and waveguide data are shown in Fig. 5.

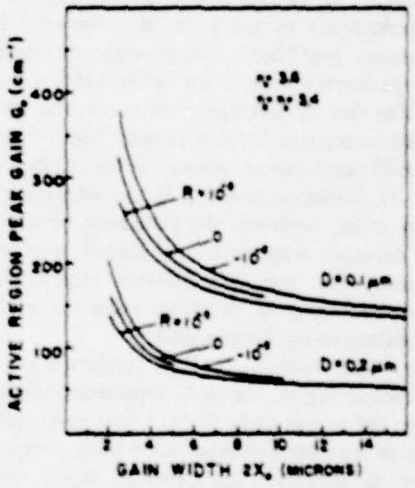


Fig. 8. Active region peak gain versus $2x_0$. Mode gain $G = 50$ cm^{-1}. Spot size and waveguide data are shown in Fig. 6.

Fundamental mode field intensity spot sizes were calculated for different cavity configurations. In particular we have focused our attention on the lateral field spot sizes as a function of the active region gain width. This width can of course be associated with current spreading from the stripe contact provided the complete geometrical picture, Fig. 1, is known [11], [12]. For example, current spreading from the metallic stripe contact is a function of the resistivities and thicknesses of the various layers below the contact. From Fig. 5, we see that the fundamental mode spot size is a function of the gain region width $2x_0$, the active layer thickness, and the parameter R

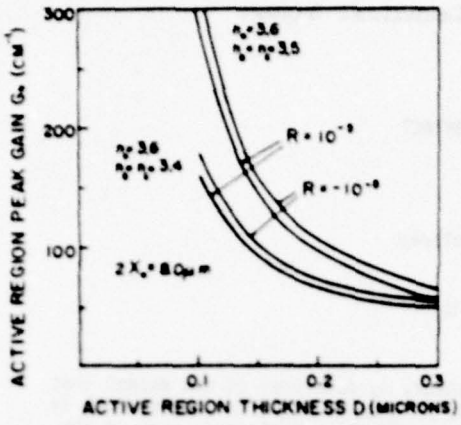


Fig. 9. Active region peak gain as a function of cavity thickness d. The mode gain $G = 50\ cm^{-1}$. The two sets of curves are for the index steps $n_0 - n_s = 0.1$ and 0.2.

which ties the index variations of the active region to the gain. We note that reasonable perturbations of the index with gain do not appreciably affect the fundamental mode spot size; however, we *do* note that the spot size will be larger for an anti-index guiding mode as opposed to an index guided one. Perhaps one peculiarity we found is the fact that the spot size becomes less sensitive with R as the active layer thickness decreases. The reason for this occurance is due to the fact that the gain becomes more sensitive with respect to R for the thin active layers. As the gain increases, the gain guiding effect on the fundamental mode becomes more pronounced and thus acts as a strong confining mechanism.

References

[1] T. H. Zachos and J. E. Ripper, "Resonant modes of GaAs junction lasers," *IEEE J. Quantum Electron.*, vol. QE-5, pp. 29-37, Jan. 1969.

[2] I. Ladany and H. Kressel, "The influence of device fabrication parameters on the gradual degradation of (AlGa)As CW laser diodes," *Appl. Phys. Lett.*, vol. 25, pp. 708-710, Dec. 15, 1974.

[3] T. L. Paoli, "Waveguiding in a stripe-geometry junction laser," *IEEE J. Quantum Electron.*, vol. QE-13, pp. 662-668, Aug. 1977.

[4] G. H. B. Thompson, "A theory for filamentation in semiconductor lasers including the dependence of dielectric constant on injected carrier density," *Opto-Electron.*, vol. 4, pp. 257-310, 1972.

[5] J. K. Butler, C. S. Wang, and J. C. Campbell, "Modal characteristics of optical stripline waveguides," *J. Appl. Phys.*, vol. 47, pp. 4033-4043, Sept. 1976.

[6] N. Chinone, "Nonlinearity in power-output-current characteristics of stripe-geometry injection lasers," *J. Appl. Phys.*, vol. 48, pp. 3237-3243, Aug. 1977.

[7] E. A. J. Marcatili, "Dielectric rectangular waveguide and directional coupler for integrated optics," *Bell Sys. Tech. J.*, vol. 49, pp. 2071-2102, Sept. 1969.

[8] H. S. Sommers, Jr., "Experimental properties of injection lasers. V. Strong polarization," *J. Appl. Phys.*, vol. 45, pp. 237-242, Jan. 1974.

[9] F. R. Nash, "Mode guidance parallel to the junction plane of double-heterostructure GaAs lasers," *J. Appl. Phys.*, vol. 44, pp. 4696-4707, Oct. 1973.

[10] D. D. Cook and F. R. Nash, "Gain-induced guiding and astigmatic output beams of GaAs lasers," *J. Appl. Phys.*, vol. 46, pp. 1660-1672, Apr. 1975.

[11] B. W. Hakki, "Striped GaAs lasers: Mode size and efficiency," *J. Appl. Phys.*, vol. 46, pp. 2723-2730, June 1975.

[12] H. S. Sommers, Jr. and D. O. North, "Experimental and theoretical study of the spatial variation of junction voltage and current distribution in narrow strip injection lasers," *J. Appl. Phys.*, vol. 48, pp. 4460-4467, Nov. 1977.

[13] H. Kressel and J. K. Butler, *Semiconductor Lasers and Heterojunction LEDs*. New York: Academic, 1977, p. 165.

1978 International Electron Devices Meeting, Technical Digest

LATERAL MODE CONTROL IN STRIPE CONTACT INJECTION LASERS*

Jerome K. Butler and Joseph B. Delaney

Southern Methodist University
Dallas, Texas

ABSTRACT

Injection lasers having nonlinearities or "kinks" in their P-I (power-current) curves are due primarily to lateral mode hopping and waveguide shifting with current. This paper is aimed at the fabrication of linear devices with due considerations of waveguide design for lateral mode stability. We model a heterostructure laser and calculate a lateral dielectric discontinuity based on the gain/loss profile of the active layer and the overall geometry. This discontinuity serves as a figure of merit for lateral mode stability. We compare two important double-heterostructure lasers: (1) the oxide-stripe geometry, and (2) the channeled substrate planar (CSP). Calculations show that CSP devices have strong lateral index confinement, whereas, the oxide-stripe lasers have a lateral gain confinement dependent upon drive.

INTRODUCTION

The analysis of the lateral modes of stripe geometry lasers is complicated by the frequently uncertain dielectric profile in the junction plane. Current interest centers on structures that produce fundamental lateral mode operation over as wide a power emission range as possible. We compare two types of planar stripe laser structures with the objective of determining the structural requirements for fundamental lateral mode operation. We analyze the oxide-defined stripe geometry configuration (1,2) and the channeled-substrate planar laser (3). In both cases, we deal with structures where the degree of radiation spread from the active region into the vertical regions of the device is controlled. Because there are regions of varying loss the propagation constants for the lateral modes differ. It is possible to produce substantial differences between the fundamental and the higher order lateral modes -- a condition favorable for maintaining fundamental mode operation under certain conditions discussed in this paper.

*Supported in part by the U. S. Army Research Office.

The theory is developed to the extent that sensitivity of lateral modes to stripe width is known once an effective dielectric step in the horizontal direction is calculated. This dielectric step is a consequence of basic five-layer waveguide considerations and is dependent upon device geometry and pertinent material parameters. Cutoff conditions for the fundamental and higher order modes are derived as a function of the lateral dielectric step and stripe width. Earlier work related fundamental mode operation to waveguide width only for the strip-loaded waveguide (4).

WAVEGUIDE CHARACTERISTICS

The detailed geometry of the oxide stripe structure is shown in Fig. 1(a); regions denoted by unprimed numbers lie beneath the metallic stripe while primed regions lie beneath the oxide. The fields are confined vertically to region 4 due to the refractive index barriers produced by the two heterojunctions at the 3-4 and 4-5 region boundaries. Lateral confinement to the region below the metallic contact is due to the variations in the complex dielectric constant, which is related to the gain and losses of the active layer. We assume current spreading under the stripe contact is negligible and as a first order approximation assume the gain in region 4 and the absorption coefficient in region 4' are constants. Since the index of the active region is complicated by anamalous dispersion, thermal and free carrier effects(5) the actual refractive index step may be positive or negative. The geometry of the CSP laser is shown in Fig. 1(b). Analysis of this device proceeds along lines similar to that of the oxide stripe laser.

In Fig. 1 the dashed lines represent boundaries in the lateral direction which separate regions having different complex dielectric constants. In some waveguiding structures (6) these lateral boundaries are not real but are referred to as pseudo because modes are confined when a pseudo-index step arising from different propagation constants on either side of the boundary becomes positive. The lateral boundaries here are not pseudo since there is a real gain/loss profile in the active layer that provides a guiding mechanism even if the lateral index step is negative and anti-index guiding occurs. Assuming a mode

form $\exp(i\omega t - \gamma z)$, where $\gamma = -G/2 + iB$, the even mode solutions are

$$w(x,y) = A_e \begin{cases} \cos(h_{x_4} x)\cos(h_{y_4} y) & \text{(region 4)} \\ \frac{\kappa_4}{\kappa_{4'}} \cos(h_{x_{4'}} x)\cos(h_{y_{4'}} \frac{s}{2})\exp[h_{y_{4'}}(\frac{s}{2} - y)] & \text{(region 4')} \end{cases} \quad (1)$$

where x and y directions are along the vertical and lateral directions respectively. The propagation constants are related to the complex dielectric by

$$h_{x_4}^2 + h_{y_4}^2 = k_0^2 \kappa_4 + \gamma^2 \quad (2)$$

$$h_{x_{4'}}^2 + h_{y_{4'}}^2 = k_0^2 \kappa_{4'} + \gamma^2 \quad (3)$$

where κ_4 and $\kappa_{4'}$ are the complex dielectric constants of regions 4 and 4'. Matching fields at the boundary yields

$$\tan(h_{y_4}\frac{s}{2}) = \frac{\kappa_4}{\kappa_{4'}} \frac{h_{y_{4'}}}{h_{y_4}} \quad (4)$$

$$h_{y_4}^2 + h_{y_{4'}}^2 = k_0^2 \Delta \quad (5)$$

where k_0 is the free space wave number. In Eq. (5) the complex dielectric step Δ is written as

$$\Delta = \Delta' + i\Delta'' = \kappa_4 - \kappa_{4'} \quad (6)$$

To facilitate machine calculations we normalize the lateral wave numbers and active region width,

$$H_i = h_i/k_0 \ , \ S = k_0 s \quad (7)$$

Cutoff for a particular lateral mode occurs when $\mathrm{Real}(H_{4'}) = 0$, i.e., the mode is not confined to the active region. With $H_i = H_i + iH_i$ and setting $H_{4'} = 0$ we obtain a set of equations involving S and the complex dielectric step. The solution of these generalized equations are shown in Fig. 2. The ordinate is $S\Delta'' 1/2$ and the abscissa is Δ'/Δ''. Δ' is related to the effective lateral index step; it is positive for index guiding and negative for anti-index guiding. Δ'' is proportional to the effective gain and losses of the active layer. The fact that the ordinate contains Δ'' implies that for a given S, the gain of the active region can be made large enough to make any mode propagate. Mode selection is solely due to the cavity Q; those modes requiring the smallest gain from the active region are excited.

DIELECTRIC STEPS

To determine the dielectric discontinuity we calculate the complex propagation constant γ using the five-layer slab model (7) with material identical to that of regions 1-5. Next, γ' is computed using regions 1'-5'. The <u>effective</u> complex refractive indices are

$$h_4 = \kappa_4^{1/2} = -i\gamma/k_0 \quad (8a)$$

$$h_{4'} = \kappa_{4'}^{1/2} = -i\gamma/k_0 \quad (8b)$$

and the dielectric step is

$$\Delta = (\gamma'^2 - \gamma^2)/k_0^2 \quad (9)$$

Figure 1(a) shows the five-layer slab model of the oxide stripe geometry device along with representative parameters. Fig. 1(b) adaps the model to a channeled substrate and the parameters therein are selected to closely resemble those used by Aiki et al.(8). The absorption coefficient α_i and index of refraction $n_i = \kappa_i^{1/2}$ are included for the ith regions. Only the roots of the lowest mode perpendicular to the junction plane are selected, and the gain in the unprimed region is adjusted until the wave travels with a modal gain G = 30 /cm which accounts for radiation cavity-end losses.

For stripe geometry lasers, Δ'/Δ'' is negative while it is positive for CSP lasers. Before discussing their actual values we first show the active region gain, g_{th}, required for the lasers as a function of s. Fig. 3 shows g_{th} for the stripe geometry. For d = 2.0 μm the gain of the fundamental mode increases rapidly for s < 5 μm whereas the gain for the second mode increases for s < 10 μm. This implies an optimum s value lies between 5 and 10 μm. When d = 0.5 μm, g_{th} values are higher because light leaks into the p-GaAs cap. Nevertheless, both sets of curves exhibit similar character. Fig. 4 shows g_{th} for the CSP laser. Note that g_{th} for the fundamental mode has soft dependence on t between 0.3 and 0.8 μm. However, for the second mode g_{th} rises radiply for s < 10μm and t = 0.8 μm. For favorable single mode operation we conclude that for t = 0.3 μm, s < 5 μm while for t = 0.8 μm, s < 8 μm.

For all structures the gain curves show that fundamental mode operation always occurs because its gain is smallest. However, actual devices with large s values operate in high-order modes. This occurs because gain profile deformations cause switchings of mode preference. These instabilities are frequently observed in stripe lasers and to a lesser degree in CSP devices. The prominant reason for instabilities is the fact that stripe geometry lasers have gain guided modes influenced by gain profile deformations. These anti-index guided modes have negative Δ'/Δ'' values. Even though the actual refractive index of the active layer is assumed constant, the effective index step is negative because of mode interactions with the metallic and oxide contacts.

In Fig. 2 we plot the locus of points on the cutoff curves. For a given s, the value of $S\Delta^{1/2}$ and Δ'/Δ'' are calculated. Stripe lasers have negative Δ'/Δ'' values while CSP lasers have positive ones; the amout of index guiding is proportional to Δ'/Δ''. When devices have large positive dielectric step ratios, their modes are insensitive to gain profile deformations while devices with negative ratios have unstable modes.

Contours representing the different structures were computed for the fundamental mode gain. High-order mode contours would follow those of the fundamental at large ordinate values but as $s \to 0$ the contours approach different limiting points; for example, the second mode terminates on $S\Delta^{1/2} = 3.75$ and $\Delta'/\Delta'' = 0$. Note that for the stripe geometry device with $d = 0.5$ μm, the fundamental mode contour crosses the second order mode cutoff at $s = 8$ μm, below this s value the second mode does not exist at fundamental mode gain values. On the other hand, the CSP with $t = 0.3$ μm crosses the second mode cutoff at $s = 2.5$ μm. At large s values, second order modes exist at fundamental mode threshold gains. The gain curves show that the fundamental mode should always be excited over the high-order ones. Mode hopping is a consequence of gain profile deformations and its effect on mode profiles; CSP lasers have lateral index guiding as reflected in positive Δ'/Δ''values, and are stable because they are rather insensitive to gain deformations.

ACKNOWLEDGEMENT

Discussions with H. Kressel and C. J. Nuese are gratefully acknowledged.

REFERENCES

1. T. H. Zachos and J. E. Ripper, "Resonant modes of GaAs junction lasers," IEEE J. Quan. Electron., vol. QE-5, pp. 29-37, Jan. 1969.

2. I. Ladany and H. Kressel, "The influence of device fabrication parameters on the gradual degradation of (AlGa)As cw laser diodes," Appl. Phys. Lett., vol. 25, pp. 708-710, Dec. 15, 1974

3. K. Aiki, M. Nakamura, T. Kuroda, J. Umeda, R. Ito, N. Chinone, and M. Maeda, "Transverse mode stabilized $Al_xGa_{1-x}As$ injection lasers with channeled-substrate-planar structure," IEEE J. Quan. Electron., vol. QE-14, pp. 89-94, Feb. 1978

4. H. Kawaguchi and T. Kawadami, "Transverse-mode control in an injection laser by a strip-loaded waveguide," IEEE J. Quan. Electron., vol. QE-13, pp. 556-560, August 1977.

5. F. R. Nash, "Mode guidance parallel to the junction plane of double-heterostructure GaAs lasers," J. Appl. Phys., vol. 44, pp. 4696-4707, October 1973.

6. J. K. Butler, C. S. Wang, and J. C. Campbell, "Modal characteristics of optical stripline waveguides," J. Appl. Phys., vol. 47, pp. 4033-4043, September 1976.

7. H. Kressel and J. K. Butler, Semiconductor Lasers and Heterojunction LED's (Academic Press, New York, 1977).

8. K. Aiki, M. Nakamura, T. Kuroda, and J. Umeda, "Channeled-substrate-planar structure (AlGa)As injection lasers," Appl. Phys. Lett., vol. 30, pp. 649-651, June 1977.

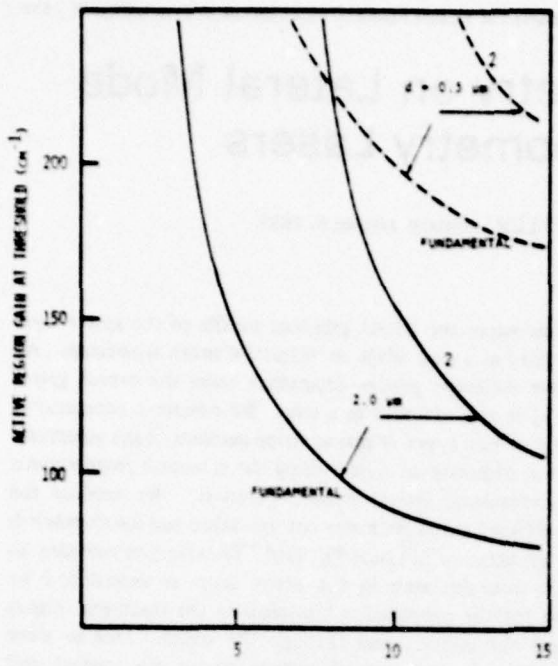


Fig. 3 Active region gain versus s for the stripe geometry laser. Mode gain G = 30 /cm.

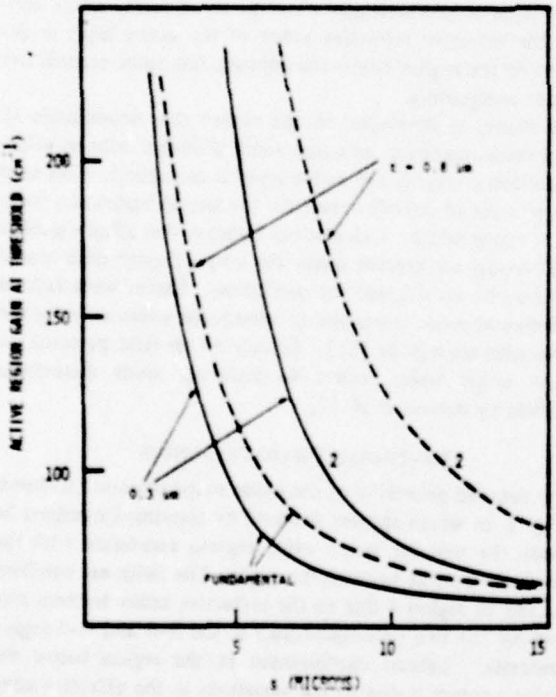
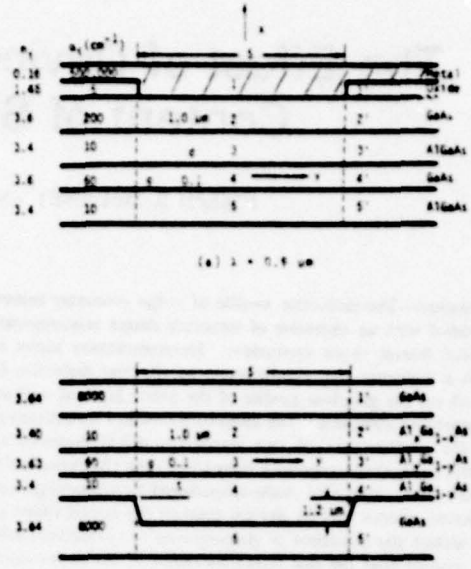
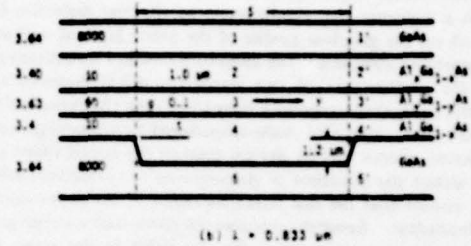


Fig. 4 Active region gain versus s for the CSP laser. Mode gain G = 30 /cm.



(a) s = 0.5 μm



(b) s = 0.833 μm

Fig. 1 The (a) oxide-stripe and (b) channeled-substrate planar (CSP) structures. The total stripe width is s. The gain of the active region g is adjusted to have a mode gain G = 30 /cm.

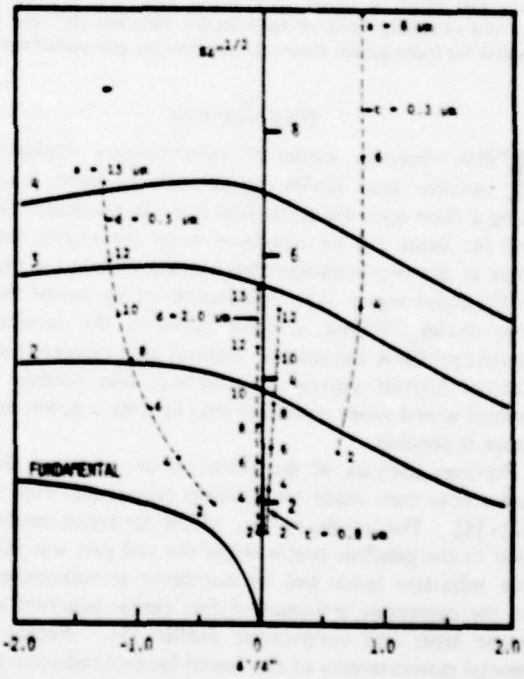


Fig. 2 Generalized lateral mode cutoff curves for modes 1 through 4 derived from the lateral eigenequation. The plot is valid for both oxide-stripe geometry and CSP structures. S is the normalized stripe width $S = s_{eff}$. The dashed contour curves apply to the fundamental mode; the two dashed curves for $\Delta'/\Delta''=0$ correspond to the CSP laser while those with $\Delta'/\Delta''<0$ are for the stripe geometry laser.

The Effect of Device Geometry on Lateral Mode Content of Stripe Geometry Lasers

JOSEPH B. DELANEY AND JEROME K. BUTLER, SENIOR MEMBER, IEEE

Abstract—The dielectric profile of stripe geometry injection lasers is modeled with an objective of structure design requirements for fundamental lateral mode operation. Heterostructure lasers are modeled with a dielectric step profile using an effective dielectric discontinuity based on the gain/loss profile of the active layer as well as the overall geometrical structure. The analysis provides a quantitative comparison of the performance of two important double-heterostructure lasers: 1) the oxide-stripe geometry laser and 2) the channeled-substrate planar (CSP) laser. Modes of oxide-stripe lasers have lateral gain confinement, whereas, modes of CSP devices have strong lateral index confinement. To isolate the influence of geometry on the effective dielectric profile we assume that the real refractive index of the active layer is position independent. Resulting calculations show that a stripe geometry laser inherently has a depressed effective index in the active region below the metallic contact. This phenomenon alone produces index antiguiding. In actual devices, both geometry and free carrier injection into the active region produce lateral index antiguiding.

Lateral mode cut-off conditions are calculated as functions of the effective complex dielectric step and the stripe width. The results show that cutoff is related in a unique fashion to the ratio of the real and imaginary parts of the complex dielectric step; the ratio is positive for index guided modes and negative for gain guided ones.

Introduction

THE transverse modes of contemporary double-heterojunction laser diodes can be analyzed rather accurately using a three-layer dielectric structure. In particular, the near and far fields can be calculated from the known dielectric steps at the two heterojunction boundaries and the thickness of the active region [1]. The analysis of the *lateral* modes of laser diodes, however, is complicated by the uncertain dielectric profile in the junction plane of stripe geometry devices. Current interest centers on structures that produce fundamental lateral mode operation over as wide a power emission range as possible.

Previous analyses of the lateral modes of stripe geometry lasers have been made by assuming various dielectric profiles [2]-[8]. The imaginary part of the dielectric constant was tied to the gain/loss profile while the real part was related to the refractive index and its associated perturbations owing to the competing influence of free carrier injection into the active layer and temperature profile [5]. Recent experimental measurements of the lateral far-field radiation patterns of stripe geometry devices indicate that the local refractive index of the active region is depressed which implies that the mode is strongly gain guided [7].

Manuscript received December 4, 1978; revised February 2, 1979. This work was supported by the United States Army Research Office.

The authors are with the Department of Electrical Engineering, Southern Methodist University, Dallas, TX 75275.

In this paper the lateral gain/loss profile of the active layer is modeled as a step while its refractive index is constant. An effective dielectric profile dependent upon the overall geometry [9] is also modeled as a step. We present a comparative analysis of two types of planar stripe geometry laser structures with the objective of determining the structure requirements for fundamental lateral mode operation. We analyze the oxide-defined stripe geometry configuration and the channeled-substrate planar (CSP) laser [9], [10]. The effective complex dielectric constant step in the active layer is determined by solving for the propagation constants in the transverse planes through the contact and through the oxide. Due to wave interactions in the vertical regions under the contact and oxide, the effective dielectric step is a strong function of the overall geometry as well as gain/losses in the active layer. By assuming a uniform index of refraction in the active layer, we isolate the influence of device structure on fundamental lateral mode operation. Calculations show that when the active layer is geometrically close to the metallic stripe contact, the effective refractive index of the active layer is depressed in the region below the contact; this alone contributes to index antiguiding.

The theory is developed to the extent that dependence of lateral mode operation on stripe width is known once an effective dielectric step in the active layer is calculated. This step leads to a set of cut-off curves for the lateral modes as a function of stripe width. Calculations indicate that all gain guided lateral modes are present under the stripe, though their modal gains may be insufficient for oscillation. Earlier work related fundamental mode operation to waveguide width only for the strip-loaded waveguide [11]. Calculated far-field patterns for narrow stripe lasers reflect fundamental mode distortions described by Asbeck *et al.* [7].

Waveguide Characteristics

The detailed geometry of the oxide stripe structure is shown in Fig. 1, in which regions denoted by unprimed numbers lie beneath the metallic stripe while regions associated with the primed numbers lie beneath the oxide. The fields are confined vertically to region 4 due to the refractive index barriers produced by the two heterojunctions at the 3-4 and 4-5 region boundaries. Lateral confinement to the region below the metallic contact is due to the variations in the effective complex dielectric constant. The mathematical model follows from that first developed by Marcatili [12] and focuses attention on the unshaded regions shown in Fig. 2(a). The width and thickness of region 4 are s and d_4, respectively. The

0018-9197/79/0800-0750$00.75 © 1979 IEEE

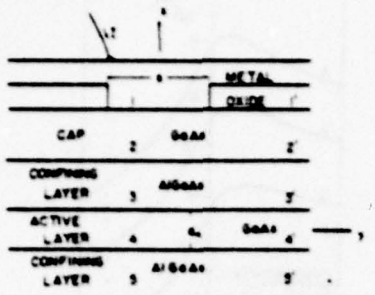


Fig. 1. Cross section of contemporary stripe geometry lasers.

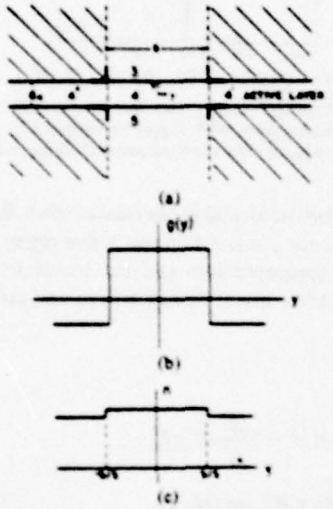


Fig. 2. Cross section of the active region of an injection laser. (a) Marcatili model. (b) step model of active layer lateral gain/loss profile, and (c) step model of refractive index in the active layer.

former is taken nominally as the stripe width. For well-guided modes, the field decays exponentially in regions 3, 5, and 4'. The power traveling in the shaded regions is negligible and no attempt is made to match the fields along the edges of the shaded areas.

Current flowing into the active layer from the contact spreads laterally with distance from the contact so that the actual "gain width" may be different from the stripe contact width s. The degree of current spread is determined by carrier diffusion and depends on the thicknesses and resistivities of the p-GaAs "cap" layer and the p-AlGaAs confining wall [13]-[16]. Fig. 2(b) indicates the step profile of the effective gain/absorption and the effective index profile is illustrated in Fig. 2(c). The actual refractive index of the active region is complicated by anomalous dispersion, thermal, and free-carrier effects [5]; these effects are not included in our analysis since we are isolating the influence of overall device geometry on laser performance. In our model the effective dielectric profile is modified only by wave interaction with the active region gain and the overall geometrical structure. For example, the dielectric profiles of the stripe contact and CSP lasers are affected by the metal/oxide layer and the etched channels, respectively.

The optical fields are divided into two sets of modes $E^x_{p,q}$ and $E^y_{p,q}$ [12]. Since contemporary heterostructure lasers have thin active regions ($d_3 \sim 0.1$ to 0.3 μm) and electric fields polarized predominantly along the lateral direction [17] [y direction in Fig. 2(a)], we need consider only the $E^y_{p,q}$ modes. Furthermore, we restrict discussion to even modes with respect to $x = 0$ and $y = 0$, and assume a mode of the form $\exp(i\omega t - \gamma z)$, where $\gamma = -G/2 + i\beta$ is the complex propagation constant. The $E^y_{p,q}$ modes are determined from the field equations (the superscript y is dropped).

$$E_x = 0 \tag{1a}$$

$$E_z = \frac{1}{\gamma}\frac{\partial E_y}{\partial y} \tag{1b}$$

$$H_x = \frac{-i}{k_0\eta_0\gamma}\left[k_0^2\kappa + \frac{\partial^2}{\partial y^2}\right]E_y \tag{1c}$$

$$H_y = \frac{-i}{k_0\eta_0\gamma}\frac{\partial^2 E_y}{\partial x \partial y} \tag{1d}$$

$$H_z = \frac{i}{k_0\eta_0}\frac{\partial E_y}{\partial x} \tag{1e}$$

wherein k_0 is the free-space wavenumber, η_0 is the free-space wave impedance, and κ is the relative dielectric constant. E_y satisfies the wave equation

$$\nabla_t^2\psi + (k_0^2\kappa + \gamma^2)\psi = 0 \tag{2}$$

where

$$\nabla_t^2 = \frac{\partial^2}{\partial x^2} + \frac{\partial^2}{\partial y^2}.$$

Referring again to Fig. 2(a), the 3-4 and 4-5 lines represent real vertical boundaries separating two distinct materials. These boundaries are of course heterojunctions, with built-in index steps, so that light guiding results from a positive index increment. The 4-4' dashed lines represent boundaries in the lateral direction which separate regions having different complex dielectric constants. In some waveguiding structures [18] these lateral boundaries are not real but are referred to as "pseudo" because modes are confined when the effective refractive index step, as derived from the imaginary parts of the complex propagation constants on either side of the boundary, becomes positive. The lateral boundaries of Fig. 2(a) separate gain and loss regions in the active layer so that a guiding mechanism is provided regardless of a positive or negative effective index step at the boundary.

The importance of the lateral 4-4' boundary becomes apparent after we develop the eigenequation pertaining to lateral confinement. In regions 4 and 4' the solutions of the wave equation become

$$\psi(x,y) = A_e \begin{cases} \cos(h_{x_4}x)\cos(h_{y_4}y) & \text{(region 4)} \\ \dfrac{\kappa_4}{\kappa_4}\cos(h_{x_4}x)\cos\left(h_{y_4}\dfrac{s}{2}\right) & \\ \quad \cdot \exp\left[h_{y_4}\left(\dfrac{s}{2} - y\right)\right] & \text{(region 4')} \end{cases} \tag{3}$$

The constant A_i is determined from normalization conditions. In the ith region, the propagation constants h_{x_i} and h_{y_i} are related to the complex dielectric constant κ_i by the equations

$$h_{x_4}^2 + h_{y_4}^2 = k_0^2 \kappa_4 + \gamma^2 \tag{4a}$$

$$h_{x_{4'}}^2 + h_{y_{4'}}^2 = k_0^2 \kappa_{4'} + \gamma^2. \tag{4b}$$

Matching fields at the 4-4' boundary are obtained by placing $h_{x_4} = h_{x_{4'}}$. This gives the lateral eigenequations

$$\tan\left(h_{y_4}\frac{s}{2}\right) = \frac{\kappa_4}{\kappa_{4'}}\frac{h_{y_{4'}}}{h_{y_4}} \tag{5}$$

$$h_{y_4}^2 + h_{y_{4'}}^2 = k_0^2 \Delta. \tag{6}$$

In (6) the complex dielectric step Δ is written as

$$\Delta = \Delta' + i\Delta'' = \kappa_4 - \kappa_{4'}. \tag{7}$$

The imaginary part of the dielectric constant of each region is determined from elementary considerations. For example, with harmonic time variation $\exp(i\omega t)$, the complex dielectric constant takes the form $\kappa_i = \kappa_i' - i(\sigma_i/\epsilon_0\omega) = \kappa_i' - i\kappa_i''$, where $n_i \simeq \kappa_i'^{1/2}$ is the index of refraction, σ_i is the optical conductivity in the ith region and ϵ_0 is the vacuum permittivity. In regions of optical absorption (region 4') σ is positive while in regions having population inversion (region 4), σ is negative. As a result, the imaginary part of Δ is positive.

It is important to note that the dielectric step in (7) is the difference between the dielectric constants of regions 4 and 4'. To include the effects of the light interaction of the active layer with all regions, it is necessary to define the effective dielectric step [10], [11], [18]. This lateral step is found by first calculating a complex propagation constant ζ for a transverse mode using a five-layer model [1] with material identical to that of regions 1-5. Another propagation constant ζ' is computed using regions 1'-5'. The effective complex refractive indexes of these modes are $\bar{n} = -i\zeta/k_0$ and $\bar{n}' = -i\zeta'/k_0$. The effective dielectric step becomes $\Delta = (\zeta'^2 - \zeta^2)/k_0^2$. The lateral mode character is governed by the effective step which includes the actual dielectric constants of the active layer as well as those of all vertical regions.

Cutoff Conditions

The basic conditions relating the waveguide stripe width to the dielectric step at cutoff for the various lateral modes is discussed in this section. For the structure shown in Fig. 2(a), the eigenvalues governing the field shapes of lateral modes are determined from solutions of (5) for even modes while the odd modes satisfy

$$h_{4'} = \frac{-\kappa_{4'}}{\kappa_4} h_4 \operatorname{ctn}\left(h_4\frac{s}{2}\right). \tag{8}$$

(For simplicity, the y subscripts have been dropped.)

In addition, h_4 and $h_{4'}$ satisfy (6) for both even and odd modes. The ratio $\kappa_4/\kappa_{4'} \simeq 1$ for contemporary laser structures. To facilitate machine calculations we normalize the lateral wavenumbers and active region width

$$H_i = h_i/k_0 \tag{9}$$

$$S = k_0 s. \tag{10}$$

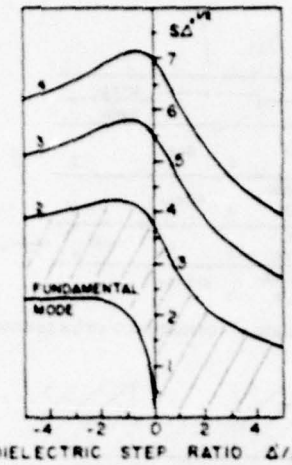


Fig. 3. Generalized cutoff curves for the lateral step model of an injection laser. Waveguides with values represented by points in the shaded region propogate only the fundamental lateral mode.

Cutoff for a particular lateral mode occurs when $\mathrm{Re}\,(H_{4'}) \to 0$, i.e., the mode is not confined to the active region. Equations (5) and (6) are separated into real and imaginary parts using $H_i = H_i' + iH_i''$. After minor manipulations and setting $H_{4'}' = 0$, we obtain

$$2H_4'H_4'' = \Delta'' \tag{11}$$

$$H_4'^2 - H_4''^2 - H_{4'}''^2 = 2\frac{\Delta'}{\Delta''}H_4'H_4'' \tag{12}$$

$$H_4'' \sinh(H_4''S) = H_4' \sin(H_4'S) \tag{13}$$

$$H_{4'}'' = H_4'' \tan\left(\frac{H_4'S}{2}\right) + H_4' \tanh\left(\frac{H_4''S}{2}\right). \tag{14}$$

Eliminating $H_{4'}''$, in the last three equations we have two simultaneous equations with the variables defined as $H_4'S$ and $H_4''S$ where the term Δ'/Δ'' is treated as a parameter. In the case of lossless waveguides, $\Delta'/\Delta'' = \infty$. For stripe geometry structures, the ratio Δ'/Δ'' may of course be either positive or negative. Therefore, for a given ratio Δ'/Δ'' the quantities $H_4'S$ and $H_4''S$ can be computed and substituted into (11) thus giving the value of S at cutoff. Fig. 3 shows $S\Delta''^{1/2}$ as a function of Δ'/Δ''. Waveguides with values represented by points in the shaded region propagate only the fundamental lateral mode and points above the curve labeled mode 2 propagate the fundamental and second-order modes.

To understand the meaning of these curves, it is important to understand the origin of the Δ' and Δ'' values. The real part of the dielectric step is related to the effective lateral index step; it is positive for index guiding and negative for gain or index antiguiding. The imaginary part is proportional to the effective gain and losses of the active layer. The fact that the ordinate contains Δ'' implies that for a given S, the gain of the active region can be made large enough to make *any mode* propagate. Mode selection is solely due to the cavity Q; those modes requiring the smallest gain from the active region are excited.

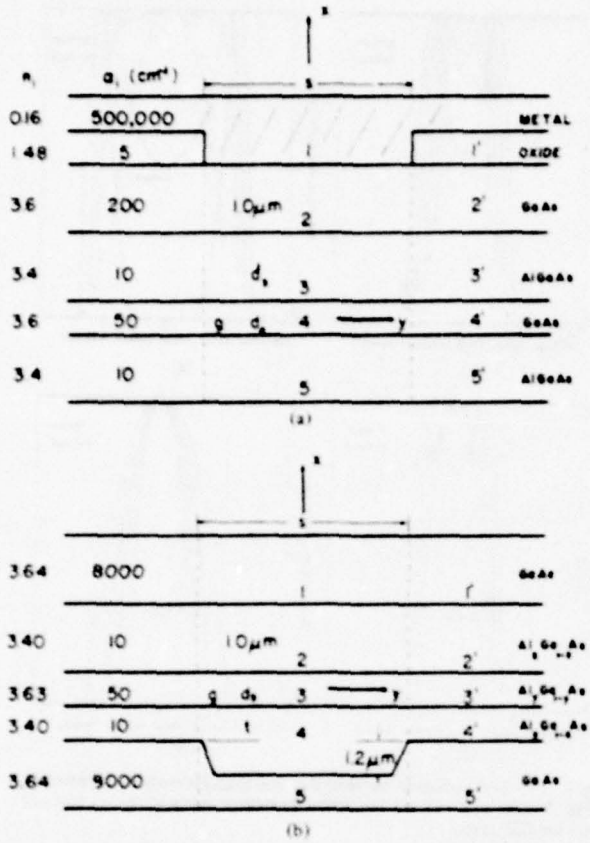


Fig. 4. Cross section and representative material constants used in calculations for the (a) stripe geometry and (b) CSP lasers.

Numerical Results

In this section we discuss some specific waveguide geometries and calculate lateral mode shapes and their radiation patterns. The lateral mode properties are determined from the effective dielectric step at the 4–4′ boundary; the value of the imaginary part of the dielectric step is dependent upon the gain/loss of regions 4 and 4′ as well as the overall laser geometry. The effective dielectric step for a given laser structure is used in (5) and (6) to obtain the lateral eigenvalues h_{y_e} and h_{y_o} for a given stripe width s and threshold gain g_{th}. This active region gain was adjusted to given a mode which travels with $G = 30$ cm^{-1} to account for radiation cavity-end losses.

Two structures examined here are the stripe geometry in Fig. 4(a) and the channel (CSP) in Fig. 4(b). Representative material parameters are included in the figures. Of particular interest is the ratio Δ'/Δ'' which is a measure of the strength of index (or index anti-) guiding in a laser and is a coordinate value for the cut-off curves. Δ'/Δ'' for the stripe geometry is plotted in Fig. 5(a) versus d_3, the p-wall thickness. As the p-wall shrinks (less than 1 μm) the defocusing nature of the contact becomes apparent in larger *negative* values of Δ'/Δ''. In this model no lateral index variation in the active layer is assumed (gain guiding only), so that negative Δ'/Δ'' ratios are solely the result of geometry and proximity of the active region to the contact. The ratio Δ'/Δ'' for the channel structure of Fig. 4(b) is plotted in Fig. 5(b) versus t, the confining n-wall thickness. The channel depth is 1.2 μm. All parameters are chosen to closely resemble those of Aiki *et al.* [10]. The ratio Δ'/Δ'' is positive when the guiding nature of the channel is enhanced for $t < 0.5$ μm. The channel model of Fig. 4(b) does not include the influence of the contact.

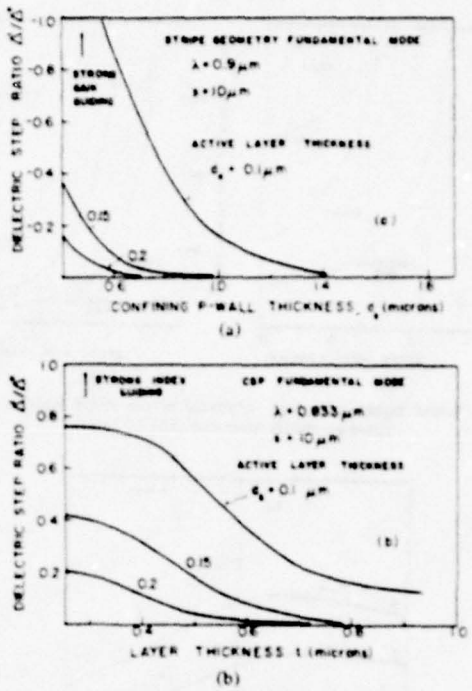


Fig. 5. Functional dependence of the dielectric step ratio Δ'/Δ'' on geometry of injection lasers. (a) Δ'/Δ'' versus the confining p-wall thickness for a stripe geometry laser; and (b) Δ'/Δ'' versus the confining n-wall thickness for a CSP laser.

Active region gain g_{th} is plotted as a function of stripe width s for the stripe geometry and CSP models in Figs. 6(a) and (b), respectively. In Fig. 6(a), for $d_3 = 2.0$ μm, the gain of the fundamental mode increases rapidly for $s < 5$ μm whereas the gain for the second mode increases for $s < 10$ μm. This implies an optimum s value lies between 5 and 10 μm. When $d_3 = 0.5$ μm, g_{th} values are higher because light leaks into the p-GaAs cap. In Fig. 6(b), g_{th} for the fundamental mode of the CSP laser has a soft dependence on t between 0.3 and 0.8 μm. However, for the second mode, g_{th} rises rapidly for $s < 10$ μm and $t = 0.8$ μm. For favorable single mode operation we conclude that for $t = 0.3$ μm, $s < 7$ μm while for $t = 0.8$ μm, $s < 8$ μm.

For all structures the gain curves show that fundamental mode operation always occurs because its threshold gain is smallest. However, actual devices with large s values operate in high-order modes. This occurs because gain profile deformations cause switchings of mode preference. These instabilities are frequently observed in stripe lasers and to a lesser degree in CSP devices. The prominent reason for instabilities is the fact that stripe geometry lasers have gain guided modes influenced by gain profile deformations. These index antiguided modes have negative Δ'/Δ'' values. Even though the actual refractive

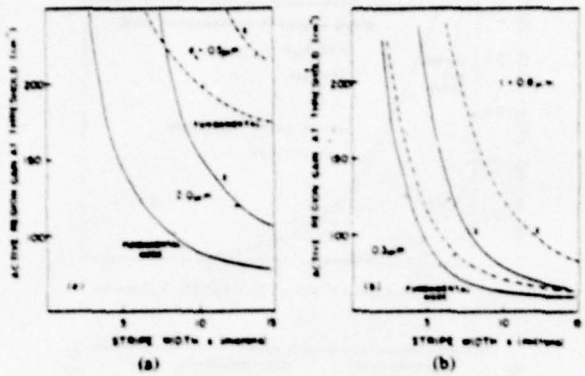


Fig. 6. Active region gain g at threshold versus stripe width s for (a) stripe geometry laser and (b) CSP laser.

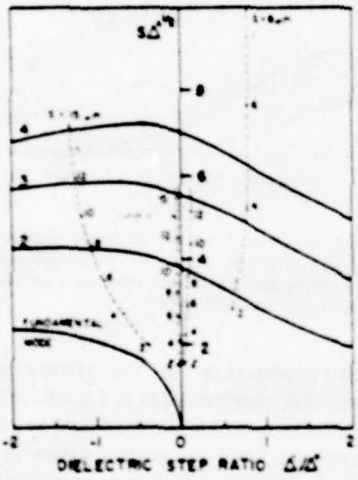


Fig. 7. Fundamental mode contour curves for various geometries plotted on the generalized cutoff curves. The dashed curves labeled a and b are for stripe geometries with active layers $d_a = 0.1$ μm. Curve a has $d_3 = 2.0$ μm while curve b has $d_3 = 0.5$ μm. Curves c and d correspond to CSP lasers with active layers $d_3 = 0.1$ μm. For curve c, $t = 0.8$ μm while for curve d, $t = 0.3$ μm. For all curves $G = 30$ cm^{-1}.

index of the active layer is assumed constant; the *effective* index step is negative because of mode interactions with the metallic and oxide contacts.

For a given stripe width s, the values of $S\Delta''^{1/2}$ and Δ'/Δ'' are calculated. Contours representing the different structures are computed for the fundamental mode gain. In Fig. 7 we plot the locus of points on the cutoff curves. High-order mode contours would follow those of the fundamental at large ordinant values but as $s \to 0$ the contours approach different limiting points; for example, the second mode terminates on $S\Delta''^{1/2} = 3.75$ and $\Delta'/\Delta'' = 0$. Note that for the stripe geometry device with $d_3 = 0.5$ μm (curve b), the fundamental mode contour crosses the second-order mode cutoff at $s \simeq 8$ μm; below this s value, the second mode does not exist at fundamental mode threshold gains. On the other hand, the CSP with $t = 0.3$ μm (curve d) crosses the second mode cutoff at $s \simeq 2.5$ μm.

The Δ'/Δ'' figure of merit for various structures is demonstrable in far-field calculations in the lateral plane, where the

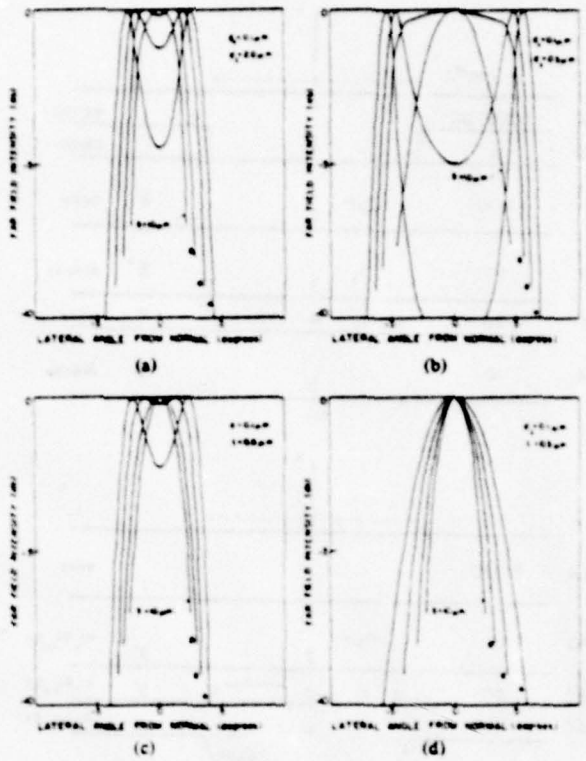


Fig. 8. Far-field radiation patterns for the four geometries depicted in Fig. 7. (a) and (b) are for stripe geometry lasers while (c) and (d) are for CSP lasers.

TE field intensity is

$$I(\theta) = \cos^2\theta \left| \int_{-\infty}^{\infty} E(y) \exp(ik_0 \sin\theta)\, dy \right|^2.$$

Fig. 8(a)-(d) is the fundamental mode far-field pattern for the four contours of Fig. 7. For the stripe geometry laser of Fig. 8(a), $d_3 = 2$ μm. Twin peaks start to develop for $s = 8$ μm and become more enhanced for smaller values of s. In Fig. 8(b), where $d_3 = 0.5$ μm, the twin peaks are more widely spaced. The larger negative Δ'/Δ'' value for $d_3 = 0.5$ μm has a defocusing effect on the far-field pattern. The twin peaks in these patterns are similar to patterns calculated by Asbeck *et al.* [7] for narrow stripes using an Eckart potential model.

Far-field patterns for a CSP laser are shown in Fig. 8(c) and (d). In the limit as the n-confining wall thickness t gets large, $\Delta'/\Delta'' \to 0$. Hence, the patterns of Fig. 8(c) are similar to those of Fig. 8(a) where Δ'/Δ'' is small. In Fig. 8(d), $t = 0.3$ μm and the twin peaks are absent; the light is closely confined to the center of the stripe where the defocusing effects of the light propagating in the primed regions are absent. The focusing nature of the channel is reflected in a large positive Δ'/Δ'' ratio.

Discussion

The theoretical analysis presented in this paper shows the powerful effect on the lateral mode content of lasers due to the radiation extending substantially beyond the recombina-

tion region either toward the device surface or substrate. Earlier work [4] showed the effect on the threshold current density from absorption in the external regions of double-heterojunction lasers. The present analysis indicates the strong effect on lateral mode propagation by suitable control of the perpendicular device profile of heterojunction structures.

The oxide-defined stripe geometry laser is theoretically shown to be sensitive to the fraction of the radiation reaching the surface regions of the device with regard to the propagation constants of the various lateral modes. The effect on the dielectric constant is such that antiguiding of the fundamental mode occurs. Because of the sensitivity of the propagation constants to the extent of radiation spread toward the surface of the device (and lack of stabilization of the fundamental mode) changes in laser current will produce perturbations in the dielectric profile. Owing to the free carrier density distribution, associated gain profile, and local heating, the cutoff conditions for various order lateral modes will change with drive. As described by Kirkby *et al.* [4], lateral mode shifts with current are indeed commonly seen in planar stripe lasers. Variations among lasers may be partially explained by differences in the degree of radiation confinement in the direction perpendicular to the junction plane.

The radiation fields calculated show the influence of geometry on the pattern shapes. In the stripe geometry structure, pattern distortion occurs for narrow stripes; this distortion reflects the amount of wave energy outside the active region. In the strong index guided CSP lasers, pattern distortion is absent. It should be noted that these calculations were made with a constant real refractive index in the active layer and that index antiguiding results from the effective dielectric profile. Inclusion of a real negative index step accentuates the distortion and spreads the pattern.

The dielectric ratio Δ'/Δ'' is positive for CSP lasers while it is negative for stripe geometry devices. CSP waveguides produce lateral confinement in the absence of gain/losses. For a reactive CSP waveguide, the complex propagation constant is imaginary. In our model this results in $\text{Imaginary}(\zeta) > \text{Imaginary}(\zeta')$ with the difference being the product of the free space wavenumber and the effective index step. If the channel were inverted, $\text{Imaginary}(\zeta) < \text{Imaginary}(\zeta')$ and the effective index step would be negative; there would be no lateral mode confinement. A stripe geometry waveguide with a perfect conducting stripe would behave similarly to an inverted channel waveguide in the sense that lateral mode confinement would not exist.

Finally, the step profile approximation loses accuracy as the stripe width narrows. Consequently, Figs. 6, 7, and 8 should be interpreted on a broad qualitative basis for small s values.

References

[1] H. Kressel and J. K. Butler, *Semiconductor Lasers and Heterojunction LED's*. New York: Academic, 1977.

[2] D. D. Cook and F. R. Nash, "Gain-induced guiding and astigmatic output beam of GaAs laser," *J. Appl. Phys.*, vol. 46, pp. 1660–1672, Apr. 1975.

[3] B. W. Hakki, "Striped GaAs lasers: Mode size and efficiency," *J. Appl. Phys.*, vol. 46, pp. 2723–2730, June 1975.

[4] P. A. Kirby, A. R. Goodwin, A. H. B. Thompson, and P. R. Selway, "Observations of self-focusing in stripe geometry semiconductor lasers and the development of a comprehensive model of their operation," *IEEE J. Quantum Electron.*, vol. QE-13, pp. 705–719, Aug. 1977.

[5] F. R. Nash, "Mode guidance parallel to the junction plane of double-heterostructure GaAs lasers," *J. Appl. Phys.*, vol. 44, pp. 4696–4707, Oct. 1973.

[6] T. L. Paoli, "Waveguiding in a stripe-geometry junction laser," *IEEE J. Quantum Electron.*, vol. QE-13, pp. 662–668, Aug. 1977.

[7] P. M. Asbeck, D. A. Cammack, and J. J. Daniele, "Non-Gaussian fundamental mode patterns in narrow-stripe-geometry lasers," *Appl. Phys. Lett.*, vol. 33, pp. 504–506, Sept. 1978.

[8] W. Streifer, D. R. Scifres, and R. D. Burnham, "Analysis of gain-induced waveguiding in stripe geometry diode lasers," *IEEE J. Quantum Electron.*, vol. QE-14, pp. 418–427, June 1978.

[9] K. Aiki, M. Nakamura, T. Kuroda, and J. Umeda, "Channeled-substrate planar structure (AlGa)As injection lasers," *Appl. Phys. Lett.*, vol. 30, pp. 649–651, June 1977.

[10] K. Aiki, M. Nakamura, T. Kuroda, J. Umeda, R. Ito, N. Chinone, and M. Maeda, "Transverse mode stabilized $Al_xGa_{1-x}As$ injection lasers with channeled-substrate-planar structure," *IEEE J. Quantum Electron.*, vol. QE-14, pp. 89–94, Feb. 1978.

[11] H. Kawaguchi and T. Kawakami, "Transverse-mode control in an injection laser by a strip-loaded waveguide," *IEEE J. Quantum Electron.*, vol. QE-13, pp. 556–560, Aug. 1977.

[12] E. A. J. Marcatili, "Dielectric rectangular waveguide and directional coupler for integrated optics," *Bell Syst. Tech. J.*, vol. 45, pp. 2071–2102, Sept. 1969.

[13] W. P. Dumke, "Current threshold in stripe-contact injection lasers," *Solid-State Electron.*, vol. 16, pp. 1279–1281, Nov. 1973.

[14] B. W. Hakki, "GaAs double heterostructure lasing behavior along the junction plane," *J. Appl. Phys.*, vol. 46, pp. 292–303, Jan. 1975.

[15] H. S. Sommers, Jr. and D. O. North, "Experimental and theoretical study of the spatial variation of junction voltage and current distribution in narrow stripe injection lasers," *J. Appl. Phys.*, vol. 48, pp. 4460–4467, Nov. 1977.

[16] I. Ladany, "The influence of stripe width on the threshold current of DH lasers," *J. Appl. Phys.*, vol. 48, pp. 1935–1940, May 1977.

[17] H. S. Sommers, Jr., "Experimental properties of injection lasers, V. Strong polarization," *J. Appl. Phys.*, vol. 45, pp. 237–242, Jan. 1974.

[18] J. K. Butler, C. S. Wang, and J. C. Campbell, "Modal characteristics of optical stripline waveguides," *J. Appl. Phys.*, vol. 47, pp. 4033–4043, Sept. 1976.

To Be Published in IEEE Trans. Microwave Theory and Techniques

RADIATION FIELDS OF OPTICAL STRIPLINE WAVEGUIDES*

by

M. W. Scott and J. K. Butler
Southern Methodist University
Dallas, Texas 75275

ABSTRACT

Dispersion characteristics and radiation fields of an optical stripline waveguide radiating into free space are calculated. The waveguides are fabricated as multiple layers of differing dielectric materials. A top layer is etched to form a "cap" with an effective waveguide in a layer below the cap. Confinement of the fields to the waveguide is obtained in the vertical direction by dielectric discontinuties, while lateral confinement occurs because of spatial interference of a continuum of plane waves. The radiation field of the fundamental mode in a plane perpendicular to the waveguide layers is characterized by the layer widths and index discontinuities. Beamwidths of the fundamental mode in the plane parallel to the dielectric layers are developed in terms of the waveguide parameters. Values of these parameters which yield the best optical confinement under the stripe can be obtained.

* Supported in part by the U.S. Army Research Office

I. Introduction

The optical stripline waveguide has potential applications as a low loss channel waveguide in integrated optical circuits [1]. The interest in this waveguide is due to the fact that it is relatively simple to fabricate compared to buried waveguide structures having built-in dielectric steps in both transverse directions. The basic structure of the optical stripline is shown in Fig. 1. A similar structure, with region 4 replaced by a conducting plane and $d_2=0$, has been proposed for use at millimeter and submillimeter wavelengths [2]. Current research is aimed at producing circuit elements and system applications using these waveguides.

An overview of dielectric waveguides for microwave integrated circuits has been given by Knox [3]. Among the most recent applications are scannable antennas and tunable filters. Structures have been fabricated for use as electronic phase shifters at millimeter [4] and submillimeter wavelenghts [5]. Itoh and Hebert [6] have simulated an electronically scannable antenna structure with a mechanical scan. A review of work in integrated optics has been given by Kogelnik [7]; many of the devices demonstrated use the optical stripline waveguide as a transmission element. An example is the directional coupler [8], which consists of several striplines spaced closely together to allow coupling between guides which has been analyzed using coupled mode theories [9].

The effective index method [1] is a mathematically simple way of predicting some of the properties of optical striplines. This method explains light confinement under the stripe by assuming an effective index of refraction step in the lateral direction in region 3 of Fig. 1. This effective index step is found by first obtaining the propagation constants for the structure shown in Fig. 1 with $w = \infty$ and then with $w = 0$. The difference between the two propagation constants divided by the free space wavenumber gives the effective index step.

The far field radiation pattern of a cleaved stripline radiating into free space is a useful way to characterize the structure. For example, the pattern can be measured experimentally and compared with these computed results to obtain values of the various waveguide parameters such as the refractive indices n_1,n_2, n_3 and n_4, or the dimensions d_2, d_3 and w. Another potential application of the stripline structure is in optical arrays where the waveguide is used as a member of the array. The pattern of the array of striplines is the product of the pattern of a single element and the array pattern.

In this paper we develop a series of rigorous calculations showing how the far-field radiation pattern behaves as a function of various waveguide parameters. In particular, we calculate the halfpower beamwidth in the lateral direction of a waveguide mode radiating into free space. The value of the beamwidth is closely related to the effective lateral index step and consequently, determines the degree with which the waveguide mode is confined to the region below the stripe. For example, broad patterns are due to strongly confined modes. (These modes should be less vulnerable to losses introduced by lateral waveguide bends).

A rigorous mathematical model of the optical stripline [10] does not require use of an effective lateral index step. An extention of this model has been developed for the structure in Fig. 1. The height is assumed to be infinite. Numerical results are given to show how the pattern depends on the parameters d_2,d_3,w, and the index discontinuity.

Since the effective index approximation involves considerably less computation, a method for obtaining information on the radiation pattern in the lateral direction using this approximation would be useful. One possible approach is to compute the effective index step in the lateral direction and then compute the radiation pattern of a symmetric three layer waveguide with this index step and a thickness equal to the stripe width. We have used this approximate technique

to compute the half power beamwidth of the fundamental mode in the lateral direction. A comparison is given with the results obtained by using the more exact model presented in this paper.

II. Theory

The analysis of the waveguide structure will parallel that given in Ref. [10]. We will assume, following Marcatilli [11], that there are two sets of modes, one polarized along the x direction and one along the y direction. For simplicity, we will deal with the modes polarized along the x direction. We will further restrict this discussion to include only the even modes. The general solutions to the wave equation in the various regions can be written:

$$\psi_1(x,y) = \sum_{n=1}^{\infty} A_n \cos p_n' x \exp\left(-p_n''(y - d_2)\right) \tag{1a}$$

$$\psi_2(x,y) = \int_0^{\infty} \cos qx \left[E(q) \exp(s''(y-d_2)) + F(q) \exp(-s''(y-d_2))\right] dq \tag{1b}$$

$$\psi_3(x,y) = \int_0^{\infty} \cos qx \left[B(q) \sin q''y + C(q) \cos q''y\right] dq \tag{1c}$$

$$\psi_4(x,y) = \int_0^{\infty} \cos qx \left[D(q) \exp r'' (d_3 + y))\right] dq \tag{1d}$$

where

ψ_i = solution of the wave equation in the i^{th} region

k_o = free space wavenumber

n_i = index of refraction in the i^{th} region

$$k_i = k_o n_i \tag{2}$$

$$p_n' = \frac{n\pi}{2w} \tag{3}$$

β = propagation constant

$$p_n'^2 - p_n''^2 = k_1^2 - \beta^2 \tag{4a}$$

$$q^2 - s''^2 = k_2^2 - \beta^2 \tag{4b}$$

$$q^2 + q''^2 = k_3^2 - \beta^2 \tag{4c}$$

$$q^2 - r''^2 = k_4^2 - \beta^2 \tag{4d}$$

Matching the fields and their derivatives at the boundaries yields a secular equation of the form:

$$\text{Det } (E - \Gamma) = 0 \tag{5}$$

where E is the unit matrix and Γ is a matrix whose elements depend on the unknown propagation constant β. Since the matrices in (5) are of infinite order the eigenvalue solutions are found by taking an increasing matrix order beginning with a first order matrix. This process forms a convergent sequence, converging to the true value of β. For the numerical results given in this paper, a fourth order matrix was used. This order is sufficient since the sequence converges rapidly.

The constants B,C,D,E, and F of Eq. (1) are found by matching the fields or derivatives at the boundaries. The field description can then be found by substituting these constants into Eq. (1), giving:

$$\psi_1(x,y) = \sum_{n=1}^{\infty} A_n \cos p_n' x \exp(-p_n'' (y-d_2)) \tag{6}$$

$$\psi_i(x,y) = \sum_{n=1}^{\infty} A_n I_i \qquad i = 2,3,4 \tag{7}$$

where I_i represents an integral expression.

The radiation pattern is related to the Fourier transform of the field at

the aperture [12]. Denote this transform by:

$$\bar{e}(k_x,k_y) = \int_{-\infty}^{\infty} \int_{-\infty}^{\infty} \bar{E}_f(x,y)\ e^{i(k_x x + k_y y)}\ dxdy \tag{8}$$

where $\bar{E}_f$ represents the transverse facet electric field, and

$$k_x = k_o \cos\phi \sin\theta \tag{9a}$$

$$k_y = k_o \sin\phi \sin\theta \tag{9b}$$

where θ denotes the angle from the z-axis and ϕ is the angle from the x-axis in the x-y plane. The far field pattern for the case of an aperture field polarized in the x direction can be written:

$$\bar{E}(\theta,\phi) = C[\hat{\theta}e_x \cos\phi - \hat{\phi}e_x \sin\phi \cos\theta] \tag{10}$$

where C is a constant and $\hat{\theta}$ and $\hat{\phi}$ are unit vectors. It is therefore necessary to obtain $e_x(k_x,k_y)$ which is the Fourier transform of the field distribution given previously. The result can be written:

$$e_x(k_x,k_y) = \sum_{i=1}^{4} F(\psi_i) \tag{11}$$

where $F(\psi_i)$ denotes the Fourier transform of ψ_i.

III. Numerical Results

The propagation constant for the structure in Fig. (1) with $d_2 = 0$ has been previously calculated [10]. The effect of region 2 on the propagation constant is shown in Fig. 2. We have used normalized values of the parameters so that the plot will be applicable to a wide class of structures. The normalized parameters are:

$$D_2 = d_2 k_0 (n_3^2 - n_4^2)^{1/2} \tag{12a}$$

$$D_3 = d_3 k_0 (n_3^2 - n_4^2)^{1/2} \tag{12b}$$

$$W = w\, k_0 (n_3^2 - n_4^2)^{1/2} \tag{12c}$$

$$B^2 = \frac{\beta^2}{k_0^2 (n_3^2 - n_4^2)} - \frac{n_4^2}{n_3^2 - n_4^2} \tag{12d}$$

$$\eta = \frac{n_3^2 - n_1^2}{n_3^2 - n_4^2} \tag{12e}$$

$$\eta' = \frac{n_3^2 - n_2^2}{n_3^2 - n_4^2} \tag{12f}$$

Fig. 3 shows the normalized propagation constant as a function of 2W, the normalized stripe width, for various values of D_2. The propagation constant approaches that of a three layer waveguide for sufficiently large values of the stripe width. For smaller values of the normalized stripe width, which are more typical of the values used in integrated optics, the propagation constant is a strong function of D_2. For large enough values of D_2, we would simply obtain a three layer waveguide, and the effect of the stripe would be inconsequential.

We now turn our attention to the radiation fields. The pattern of a waveguide radiating into free space depends on the actual values of the various waveguide parameters and thus cannot be expressed in terms of normalized parameters. Consequently, we chose values of the various parameters typical of those used in integrated optics. Consider a GaAs - AlGaAs waveguide with

$$n_1 = n_2 = n_4 = 3.55$$

$$n_3 = 3.6$$

$$d_3 = 1.0\ \mu m$$

We have chosen a wavelength of 1.15 μm corresponding to one of the transitions in a HeNe laser. At $\lambda = 1.15\ \mu m$ absorption in GaAs is low.

The halfpower beamwidth of the fundamental mode in the lateral direction is plotted as a function of the stripe width in Fig. 3. A scan in the lateral direction was chosen because the far field beamwidth will indicate how well the fields are confined laterally. This is significant because confinement of the fields in the lateral direction does not occur because of an index discontinuity, and so it is important to understand the waveguide parameters which yield the greatest lateral optical confinement. The degree of optical confinement is important in considerations of scattering at waveguide bends.

From Fig. 3, it is apparent that the beamwidth decreases as d_2 increases. For small values of the stripe width, the beamwidth is a strong function of d_2. Each plot exhibits a maximum in the beamwidth, which would correspond to an optimum value of w. Input coupling to the waveguide, which depends on the numerical aperture, would be maximized for this value of w. For $d_2 = 0$, for example, this optimum value would be a stripe width of approximately 3μ.

In obtaining Fig. 4, a structure was used with $n_1 = n_2 = n_4$, $n_3 = 3.6$, $d = 1\mu$, $\lambda = 1.15\mu$, $w = 3\mu$, and the difference $n_3 - n_1$ was denoted Δn. This plot shows that the dependence of the lateral beamwidth on the transverse Δn is enhanced by the presence of region 4. Since a large Δn is desired for confinement in the vertical direction, this is the region of the plot which is of interest. Note that when $\Delta n \cong 0.1$, the effect of the thickness of region 4 increasing from 0 to 0.2μ is to decrease the halfpower beamwidth by about 35%.

Figure 5 shows the dependence of the lateral beamwidth on the thickness of the waveguide region 2. The structure has $n_1 = n_2 = n_4 = 3.55$, $n_3 = 3.6$, $\lambda = 1.15$, and $w = 3\mu$.

It is of interest to note that the effective index step approximation discussed earlier yields good results for the lateral half power beamwidth. Figure 6 shows plots of half power beamwidth versus d_3 with $d_2 = 0$ computed using the theory above (curve 1) and using the effective index approximation (curve 2). It is apparent that the approximation predicts the correct shape of the curve. The error which can be made using the approximation is less than 26%. If the pattern is needed only in the lateral direction, the use of the approximation may be justified by the savings in computation time.

IV. CONCLUSION

The propagation constant β of the fundamental mode in the optical stripline waveguide has been calculated. For small stripe widths the value of β is strongly dependent on the presence of a region between the stripe and the waveguiding region. As the thickness of the isolating layer increases, the effect of the strip width on β decreases.

The halfpower beamwidth of the fundamental mode of the optical stripline waveguide in a plane parallel to the waveguide layers has been obtained; this is a useful indicator of the degree of optical confinement in the lateral direction. As the stripe widens the beamwidth decreases; indicating that the fields are spreading in the waveguide. As the stripe width is decreased beyond a critical point, the beamwidth begins to decrease; this indicates that the optical fileds are no longer confined uder the stripe. The effect of increasing the thickness of region 2 is always to reduce the halfpower beamwidth.

The lateral beamwidth also depends on the thickness of the waveguiding region, d_3. As d_3 is decreased the beamwidth increases, up to the point where d_3 becomes so small that the fields begin to spread outside the waveguiding region. Then the beamwidth drops sharply. This behavior is also predicted by using the effective index approximation to determine an index discontinuity, and then calculating the far field beamwidth of a three layer waveguide with this index step and a thickness of 2w.

REFERENCES

[1] H. Furuta, H. Noda, and A. Ihaya, "Novel optical waveguide for integrated optics," Applied Optics, vol. 13, no. 2, pp. 322-326, February 1974.

[2] W. McLevige, T. Itoh, and R. Mittra, "New waveguide structures for millimeter wave and optical integrated circuits," IEEE Trans. Microwave Theory Tech., vol. MTT-23, no. 10, October 1975.

[3] R.M. Knox, "Dielectric waveguide microwave integrated circuits - an overview," IEEE Trans. Microwave Theory Tech., vol. MTT-24, no. 11, pp. 806-814, November, 1976.

[4] H. Jacobs and M.M. Chrepta, "Electronic phase shifter for millimeter-wave semiconductor dielectric integrated circuits," IEEE Trans. Microwave Theory Tech., vol. MTT-22, pp. 411-417, April 1974.

[5] A.B. Buckman, "Theory of an efficient electronic phase shifter employing a multilayer dielectric - waveguide stucture," IEEE Trans. Microwave Theory Tech., vol. MTT-25, no. 6, pp. 480-483, June 1977.

[6] T. Itoh and A.S. Hebert, "Simulation study of electronically scannable antennas and tunable filters integrated in a quasi-planar dielectric waveguide," IEEE Trans. Microwave Theory Tech., vol. MTT-26, no. 12, pp. 987-991, December 1978.

[7] H. Kogelnik, "An introduction to integrated optics," IEEE Trans. Microwave Theory Tech., vol. MTT-23, no. 1, pp. 2-16, January 1975.

[8] S. Somekh, E. Garmire, A. Yariv, H.L. Garvin, and R.G. Hunsperger, "Channel optical waveguide directional couplers," Appl. Phys. Lett., vol. 22, no. 2, pp. 46-47, January 15, 1973.

[9] A. Yariv, Quantum Electronics, 2nd edition, New York: Wiley, 1975, pp. 508-523.

[10] J.K. Butler, C.S. Wang, and J.C. Campbell, "Modal characteristics of optical stripline waveguides," Journal of Applied Physics, vol. 47, no. 9, pp. 4033-4043, September 1976.

[11] E.A.J. Marcatilli, "Dielectric rectangular waveguide and directional coupler for integrated optics," Bell Syst. Tech. J., vol. 48, no. 7, pp. 2071-2102, September 1969.

[12] H. Kressel and J.K. Butler, Semiconductor Lasers and Heterojunction LEDS, New York: Academic Press, 1977, pp. 191-194.

FIGURES

Fig. 1. Cross section of the optical stripline waveguide

Fig. 2. Normalized propagation constant of the fundamental mode as a function of normalized stripe width

Fig. 3. Lateral halfpower beamwidth of the fundamental mode as a function of stripe width

Fig. 4. Lateral halfpower beamwidth of the fundamental mode as a function of the index discontinuity

Fig. 5. Lateral halfpower beamwidth of the fundamental mode versus the thickness of region 3, the region where light is confined.

Fig. 6. Comparison of the method given in this paper for calculating the lateral halfpower beamwidth (curve 1) with the effective index method (curve 2)

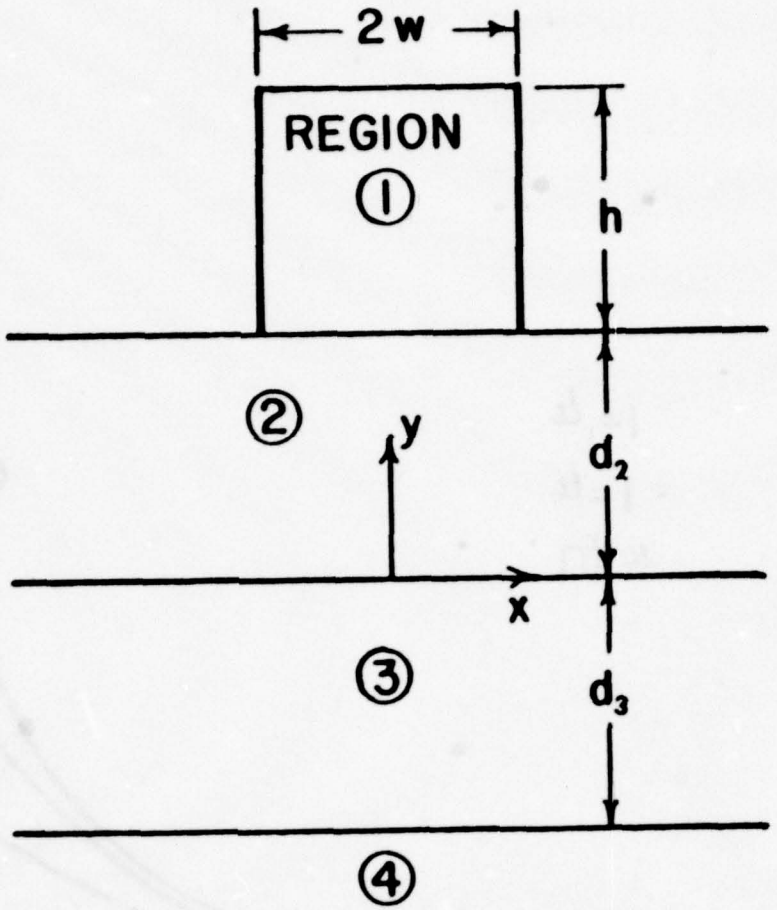


Fig. 1

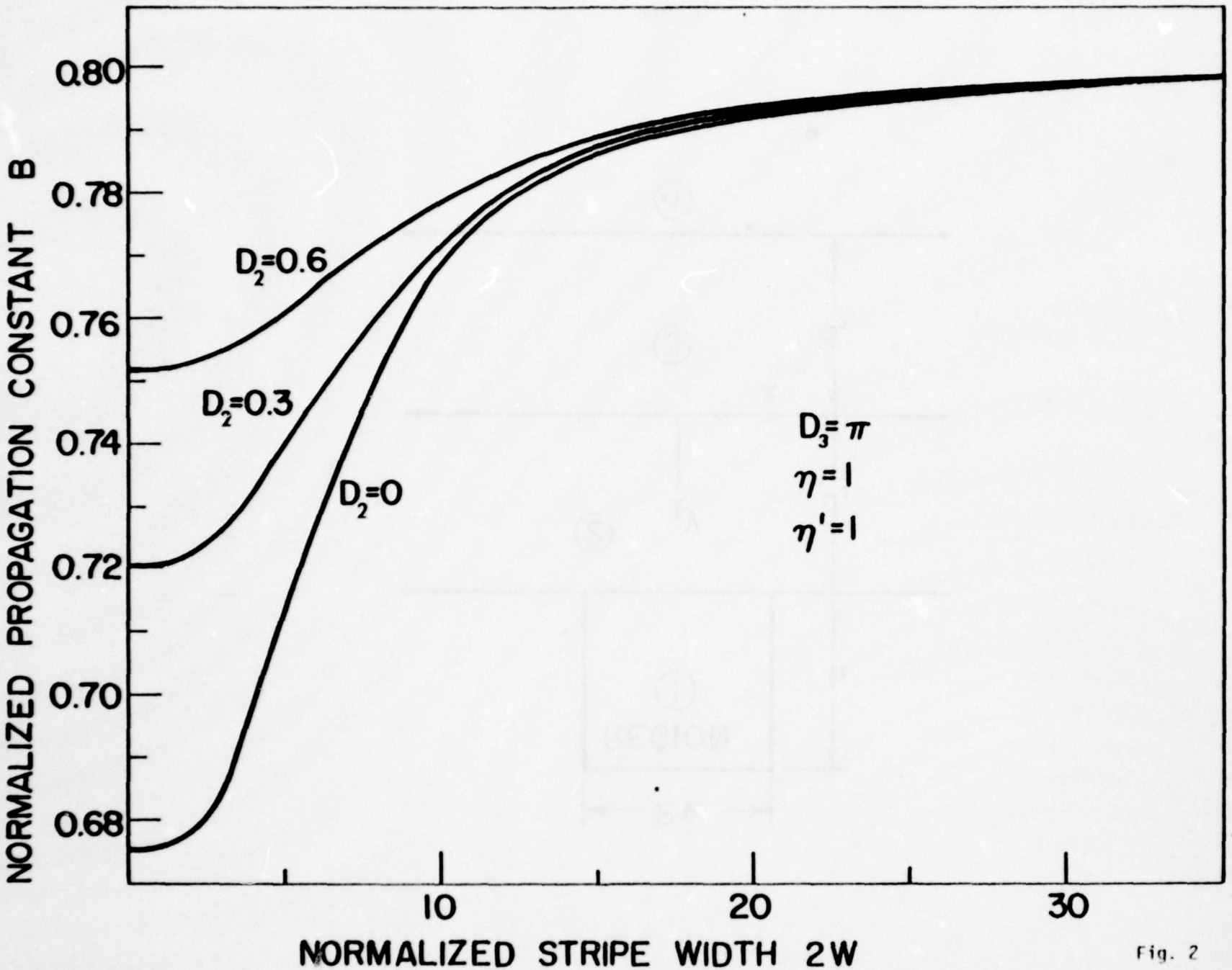

NORMALIZED PROPAGATION CONSTANT B
0.80
0.78
0.76
0.74
0.72
0.70
0.68
D2=0.6
D2=0.3
D2=0
D3= π
η=1
η'=1
10
20
30
NORMALIZED STRIPE WIDTH 2W

Fig. 2

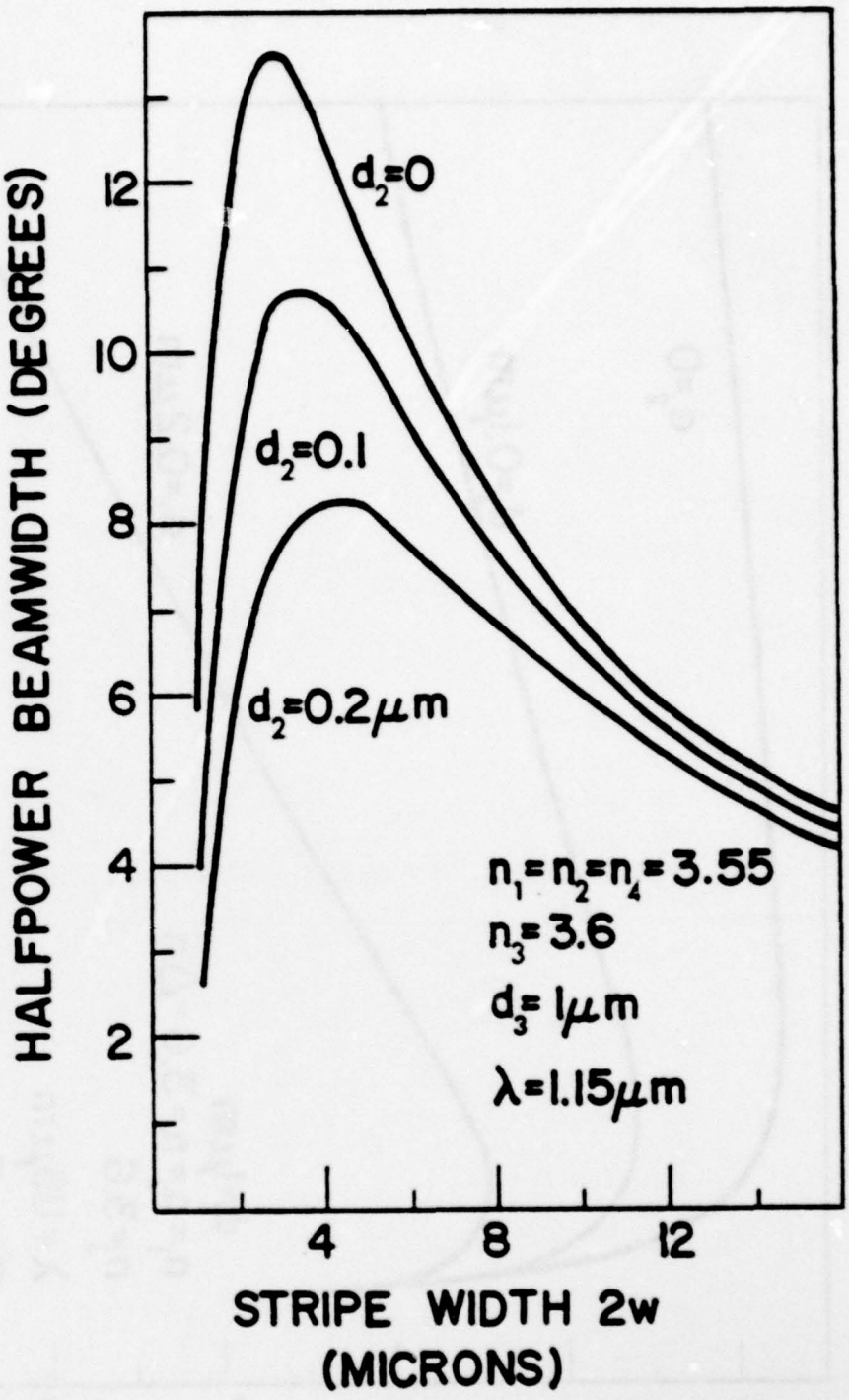

HALFPOWER BEAMWIDTH (DEGREES)
12
10
8
6
4
2
d_2=0
d_2=0.1
d_2=0.2μm
n_1=n_2=n_4=3.55
n_3=3.6
d_3=1μm
λ=1.15μm
4
8
12
STRIPE WIDTH 2w
(MICRONS)

Fig. 3

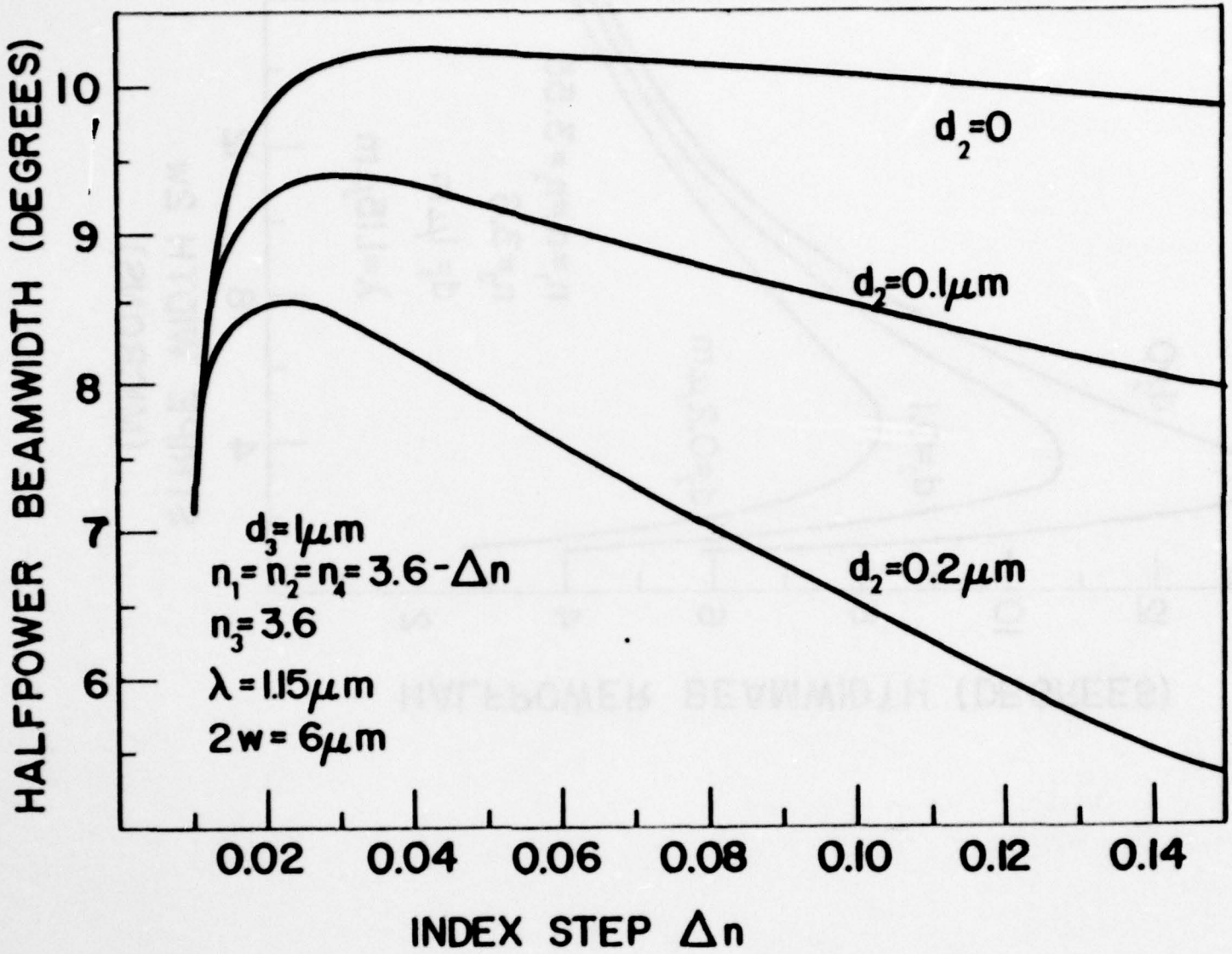

HALFPOWER BEAMWIDTH (DEGREES)
10
9
8
7
6
d_2=0
d_2=0.1μm
d_2=0.2μm
d_3=1μm
n_1= n_2= n_4= 3.6 - Δn
n_3= 3.6
λ = 1.15μm
2w = 6μm
0.02
0.04
0.06
0.08
0.10
0.12
0.14
INDEX STEP Δn

Fig. 4

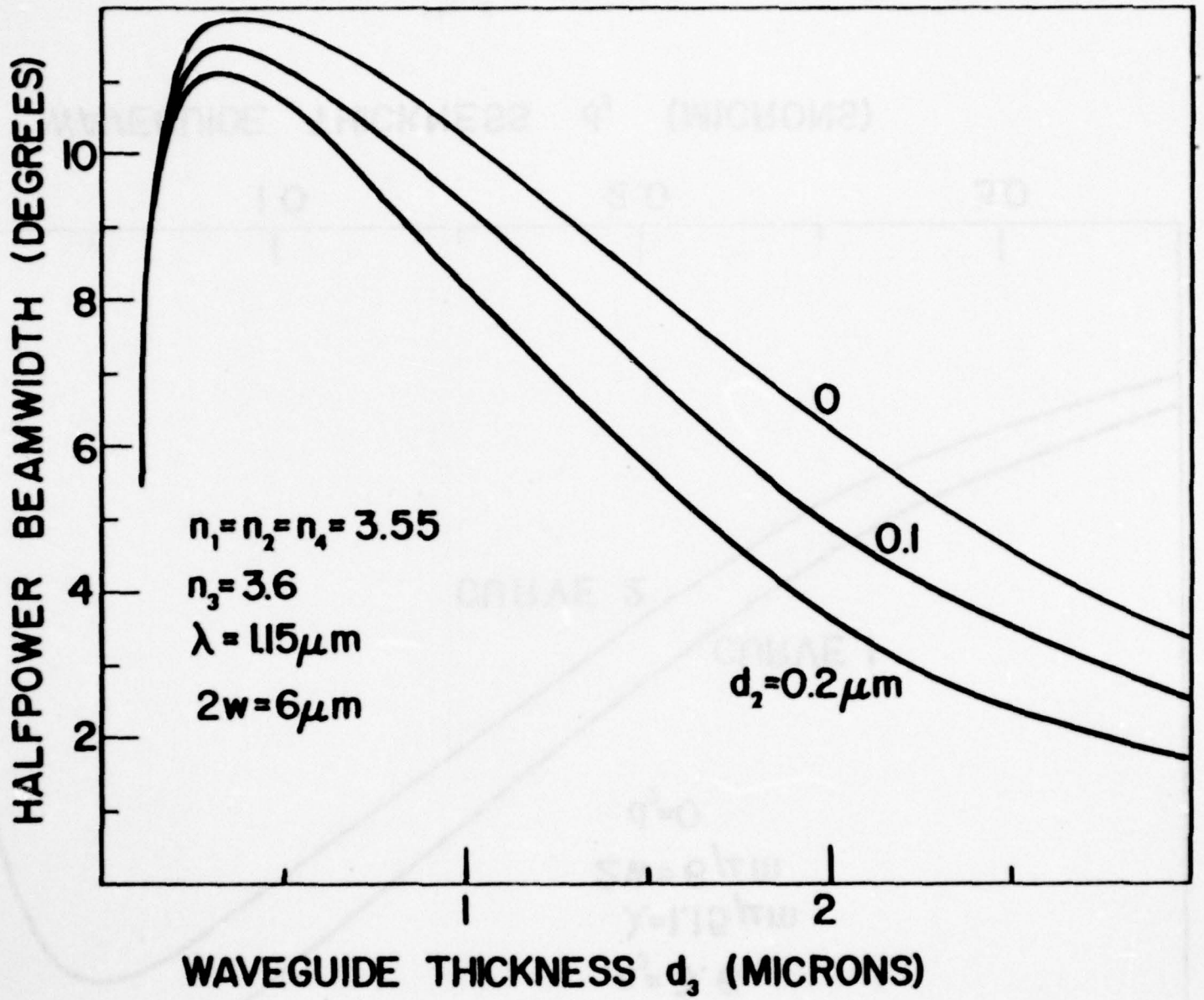

HALFPOWER BEAMWIDTH (DEGREES)
10
8
6
4
2
0
0.1
$n_1 = n_2 = n_4 = 3.55$
$n_3 = 3.6$
$\lambda = 1.15\mu m$
$2w = 6\mu m$
$d_2 = 0.2\mu m$
1
2
WAVEGUIDE THICKNESS d_3 (MICRONS)

Fig. 5

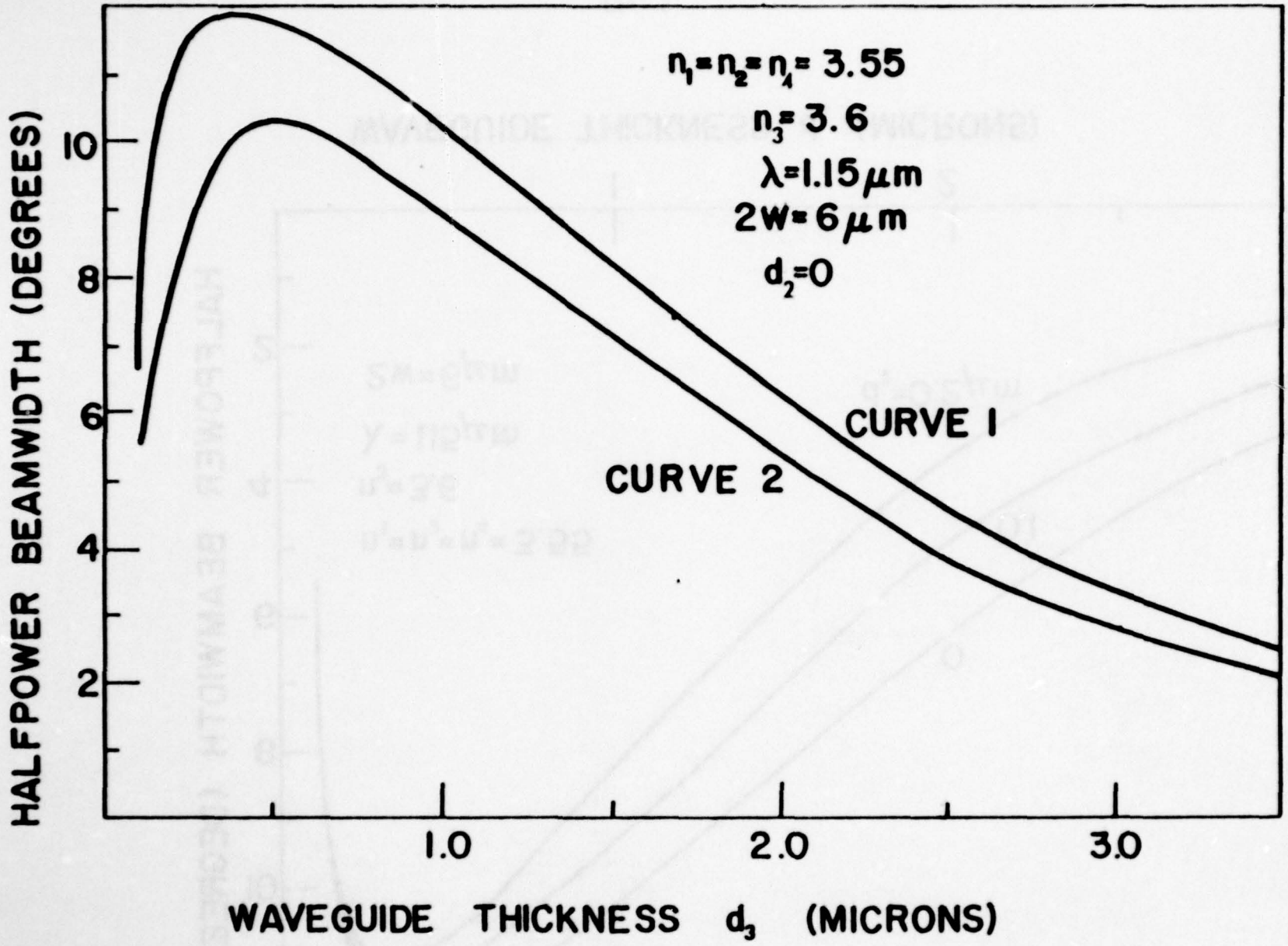

$n_1 = n_2 = n_4 = 3.55$
$n_3 = 3.6$
$\lambda = 1.15\mu m$
$2W = 6\mu m$
$d_2 = 0$
CURVE 1
CURVE 2
HALFPOWER BEAMWIDTH (DEGREES)
10
8
6
4
2
1.0
2.0
3.0
WAVEGUIDE THICKNESS d_3 (MICRONS)

Fig. 6

To be published: IEEE Journal of Quantum Electronics

Evaluation of Dielectric Optical Waveguides From Their Far Field Radiation Patterns*

by M. W. Scott and J. K. Butler

Southern Methodist University

Dallas, Texas 75205

ABSTRACT

An experimental technique for determining the characteristics of dielectric optical waveguides is presented. The far field pattern of a passive waveguide excited by an external source is measured and compared with a theoretical pattern. The presence of spurious light in the far field complicates the measurement, but this difficulty can be minimized for many structures. Application to semiconductor laser structures is discussed. Determining the waveguiding properties of laser structures prior to processing can result in the early detection of faults for increased yield.

*Supported by U. S. Army Research Office

Evaluation of Dielectric Optical Waveguides From Their Far Field Radiation Patterns

Dielectric optical waveguides are the basic building blocks used to construct integrated optical circuits [1,2]. Semiconductor lasers consist essentially of dielectric optical waveguides with optical "gain" in the active region to furnish light amplification [3-7]. The properties of dielectric waveguides depend on the geometry of the structure and the index of refraction discontinuities between the region where light is confined and the surrounding regions. Device geometrical dimensions can be studied using the scanning electron microscope (SEM) and the index of refraction profile can be estimated from published data [8], [9].

In this paper we present an experimental technique for determining the properties of certain optical waveguide structures. This technique can be applied to semiconductor laser wafers before they are cleaved to form individual deivces. The waveguiding properties of the structure can be determined prior to actually making the device. The detection of any faults in the wafer at this point would result in an increased yield.

The experimental apparatus used to excite a propagating mode in the waveguide has been used previously [10-14]. Light from a 1.15 um HeNe laser is focused into the waveguide by a microscope objective. A second microscope objective is focused on the output side of the waveguide. A camera with an infrared vidicon is then used to observe the near field of the waveguide.

After a propagating mode has been excited, a germanium detector with a small active area is scanned across the far field. An example of a far field pattern measured experimentally is shown with solid lines in Fig. 1. This pattern was obtained from a multi-layer structure. An n-type layer of AlGaAs doped with tellurium is grown on a GaAs substrate. This layer has about 1% aluminum; the next layer is GaAs lightly doped with silicon. The final layer is p-type AlGaAs

doped with germanium with about 20% aluminum. The thicknesses of the various regions are known quite accurately from measurements with the SEM.

The middle layer, which is lightly doped GaAs, will confine most of the light since it is the region with the highest index of refraction. The refractive index of this region can be extrapolated from data published previously [8]. If this value is not accurate, it makes very little difference since the waveguiding properties of the structure are determined by the index steps between this region and the other layers.

One other observation can further simplify the problem of obtaining a theoretical pattern to match the one recorded experimentally. Since there is a large index step between the active region and the layer with 20% aluminum, there will be very little light confined to this 20% aluminum layer. We can therefore estimate the step between the active region and the 20% aluminum layer to be 0.1 using the references cited earlier [8,9].

The index of refraction profile resulting from the estimates given above is shown in Fig. 2. The thicknesses of the various regions are also shown. The index step between regions 2 and 3 and regions 1 and 3 will have a significant effect on the far field pattern. These index steps are labeled Δn_2 and Δn_1, respectively, in Fig. 2.

For given values of Δn_1 and Δn_2, the far field pattern of a multi-layer waveguide with the index profile shown in Fig. 2 can be calculated [15]. Fig. 3 shows how the halfpower beamwidth of the fundamental mode of the structure in Fig. 2 varies as a function of Δn_2 for certain values of Δn_1.

The experimental pattern discussed earlier is obviously the pattern of a fundamental mode, since it has only one peak. The halfpower beamwidth of the experimental pattern is 17°. From Fig. 3 we note that there are an infinite number of combinations of Δn_1 and Δn_2 which would produce the same halfpower beamwidth.

Fortunately, all of these parameter values do not produce the same radiation pattern. For example, two radiation patterns with the same halfpower beamwidth but different shapes are shown superimposed on the experimental pattern in Fig. 1. One of these patterns agrees with the experimental result only at the halfpower points, with no agreement at other points. The second pattern more closely matches the experimental pattern. The values of Δn_1 and Δn_2 resulting in this pattern were found by requiring the theory to match experiment at the halfpower and 70% power points. Since small perturbations in the parameters Δn_1 and Δn_2 result in significant changes in the pattern, the parameters Δn_1 and Δn_2 have been determined quite accurately by this procedure.

The procedure outlined above does have certain limitations. It works best on structures designed for single mode operation, i.e., small active regions and small index steps, Δn_2. Although the method can be applied to multimoded structures, obtaining a theoretical match to the experimental pattern is often complicated by the presence of several modes adding together to form the aperture field. The fields of each of these modes must be multiplied by complex weighting coefficients to account for phase differences between the modes. This introduces several more unknowns into the problem, and makes the "trial and error" approach to pattern matching very tedious.

One other potential problem is the presence of scattered light in the far field. This problem is minimized by using an input microscope objective with a spot size smaller than the thickness of the active region of the waveguide. This ensures that most of the light will be focused into the waveguide. For waveguides with very small active regions, this poses a serious limitation.

Despite these limitations, there is a wide range of device parameters for which the technique is very useful. In addition to the layered waveguide discussed here, the technique can also be applied to optical stripline waveguides and stripe geometry lasers.

List of Illustrations

Fig. 1. Experimental and theoretical far field patterns for a multi-layer laser structure.

Fig. 2. Index of refraction profile of the multi-layer structure used in computing the theoretical far field patterns in Fig. 3. Thicknesses of layers are also shown.

Fig. 3. Halfpower beamwidth of fundamental mode of the structure in Fig. 4 as a function of Δn_2 for certain values of Δn_1.

REFERENCES

[1] S.E. Miller, "Integrated optics: an introduction," Bell Syst. Tech. J., vol. 48, pp 2059-2069, Sept. 1969.

[2] S.E. Miller, "A survey of integrated optics," I.E.E.E. J. Quantum Electronics, vol. QE-8, part 2, pp 199-205, Feb. 1972.

[3] A.L. McWhorter, "Electromagnetic theory of the semiconductor junction laser," Solid State Electron, vol. 6, pp 417-423, Sept.-Oct. 1963.

[4] A.L. McWhorter, H.J. Zeiger, and B. Lax, "Theory of semiconductor maser of GaAs," J. Appl. Phys., vol. 34, pp 235-236, Jan. 1963.

[5] A. Yariv and R.C.C. Leite, "Dielectric-waveguide mode of light propagation in p-n junctions," Appl. Phys. Lett., vol. 2, pp 55-57, 1 Feb. 1963.

[6] D.D. Cook and F.R. Nash, "Gain-induced guiding and astigmatic output beam of GaAs lasers," J. Appl. Phys., vol. 46, April 1975.

[7] W.O. Schlosser, "Gain-induced modes in planar structures," Bell Syst. Tech. J., vol. 52, pp 887-905, July-Aug. 1973.

[8] D.D. Sell, H.C. Casey Jr., and K.W. Wecht, "Concentration dependence of the refractive index for n- and p-type GaAs between 1.2 and 1.8 eV," J. Appl. Phys., vol. 45, pp 2650-2657, June 1974.

[9] H.C. Casey Jr., D.D. Sell, and M.B. Panish, "Refractive index of $Al_xGa_{1-x}As$ between 1.2 and 1.8 eV," Appl. Phys. Lett., vol. 24, pp 63-65, 15 Jan. 1974.

[10] J.C. Tracy, W. Wiegman, R.A. Logan, and F.K. Reinhart, "Three-dimensional light guides in single-crystal GaAs - $Al_xGa_{1-x}As$," Appl. Phys. Lett., vol. 22, pp 511-512, 15 May 1973.

[11] E. Garmire, H. Stoll, A. Yariv, and R.G. Hunsperger, "Optical waveguiding in proton-implanted GaAs," Appl. Phys. Lett., vol. 21, pp 87-88, 1 Aug. 1972.

[12] H.F. Taylor, W.E. Martin, D.B. Hall, and V.N. Smiley, "Fabrication of single-crystal semiconductor optical waveguides by solid-state diffusion," Appl. Phys. Lett., vol. 21, pp 95-98, 1 August 1972.

[13] F.A. Blum, D.W. Shaw, and W.C. Holton, "Optical striplines for integrated optical circuits in epitaxial GaAs," Appl. Phys. Lett., vol. 25, pp 116-118, 15 July 1974.

[14] D.B. Hall, A. Yariv, and E. Garmire, "Observation of propagation cutoff and its control in thin optical waveguides," Appl. Phys. Lett., vol. 17, pp 127-129, 1 Aug. 1970.

[15] H. Kressel and J.K. Butler, Semiconductor Lasers and Heterojunction LED's, New York: Academic Press, 1977.

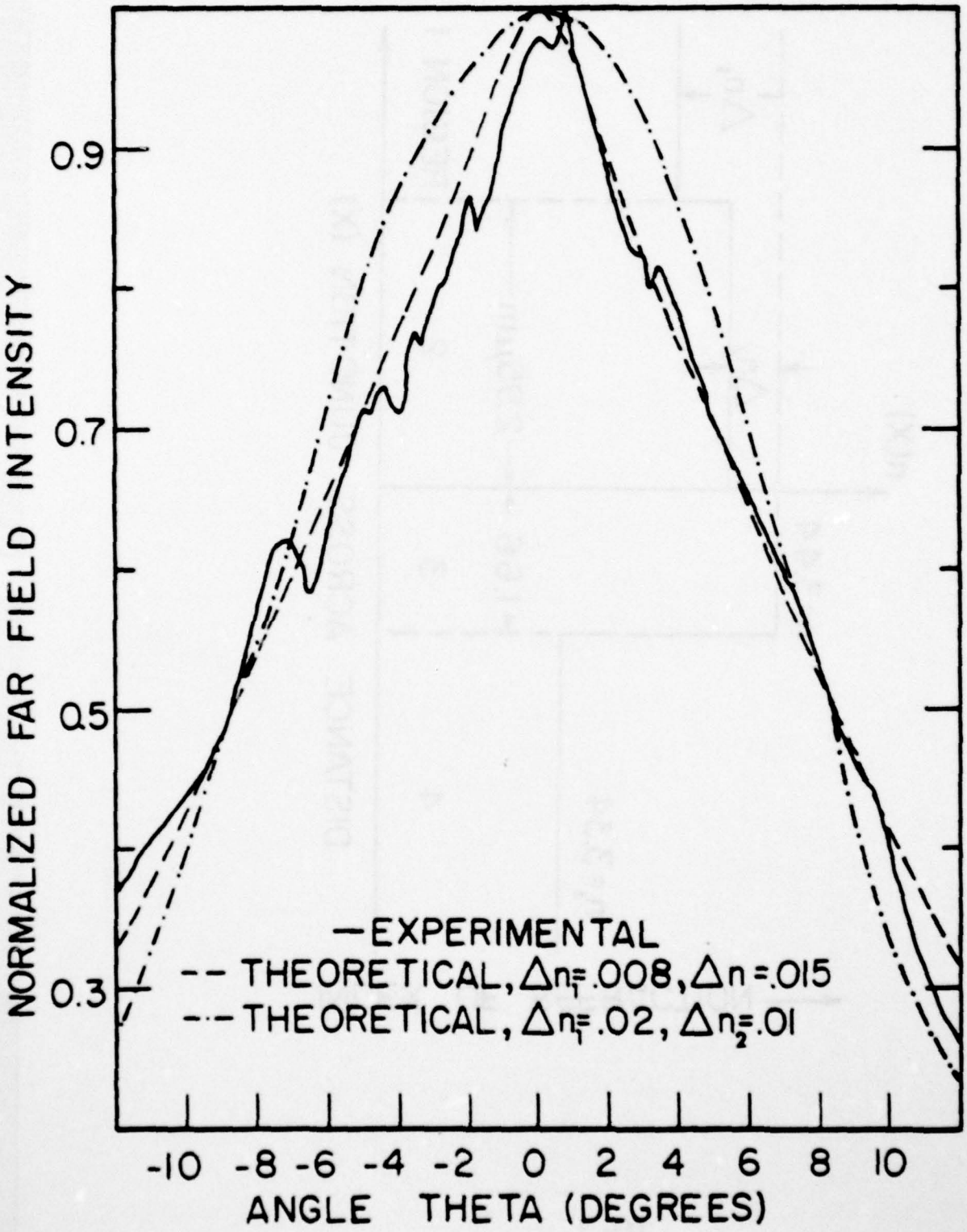

NORMALIZED FAR FIELD INTENSITY
0.9
0.7
0.5
0.3
—EXPERIMENTAL
-- THEORETICAL, Δn₁=.008, Δn=.015
-·- THEORETICAL, Δn₁=.02, Δn₂=.01
-10 -8 -6 -4 -2 0 2 4 6 8 10
ANGLE THETA (DEGREES)

Fig. 1

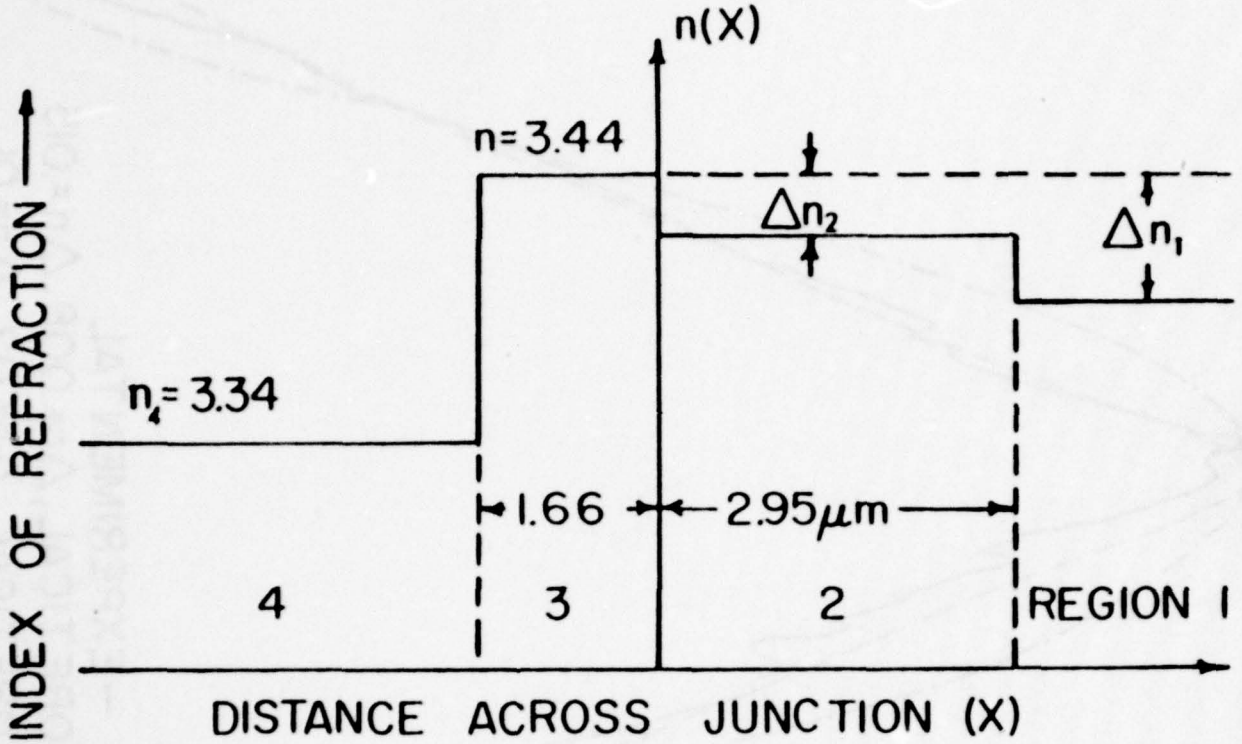

n(X)
n=3.44
Δn_2
Δn_1
n_4= 3.34
1.66
2.95μm
4
3
2
REGION 1
INDEX OF REFRACTION
DISTANCE ACROSS JUNCTION (X)

Fig. 2

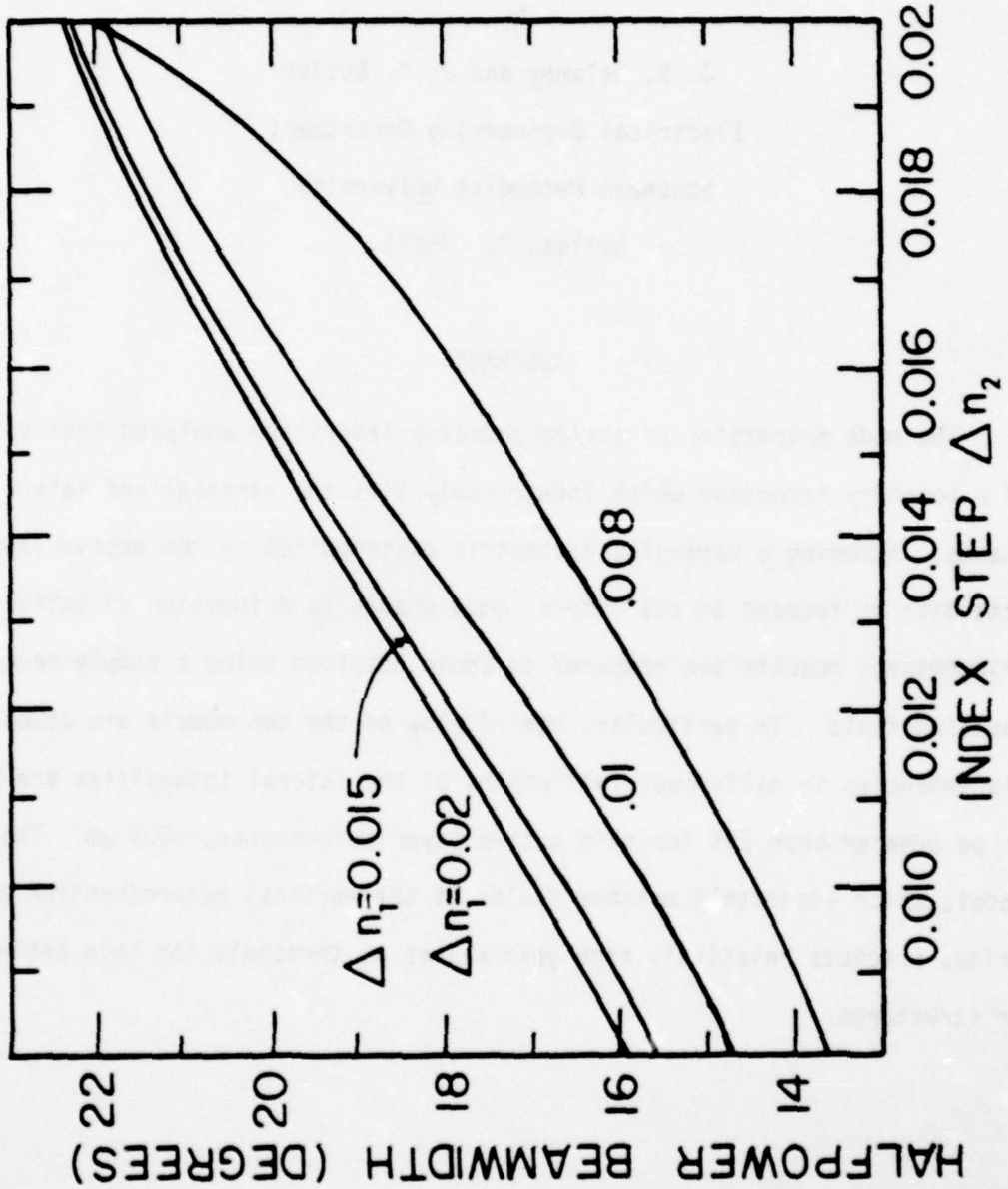

HALFPOWER BEAMWIDTH (DEGREES)
22
20
18
16
14
0.010
0.012
0.014
0.016
0.018
0.02
INDEX STEP Δn_2
.008
.01
Δn_1=0.02
Δn_1=0.015

Fig. 3

Field Solutions for the Lateral Modes of Stripe Geometry Injection Lasers*

by

J. B. Delaney and J. K. Butler

Electrical Engineering Department

Southern Methodist University

Dallas, TX 75275

ABSTRACT

The mode properties of stripe geometry lasers are analyzed from solutions of a boundary technique which inextricably ties the vertical and lateral mode shapes. Assuming a parabolic dielectric distribution in the active layer, attention is focused on the lateral mode shapes as a function of active layer thicknesses; results are compared to those obtained using a simple Hermite-Gaussian field. In particular, near-fields of the two models are compared and discrepancies in half-power full widths of the lateral intensities are found to be greater than 25% for thin active layer thicknesses, ~0.1 μm. The new model, which accurately matches fields at the vertical heterojunction boundaries, predicts relatively high gain values at threshold for thin active layer structures.

* Supported by U. S. Army Research Office

AD-A078 519 SOUTHERN METHODIST UNIV DALLAS TEX F/G 20/9
DESIGN OF INJECTION LASERS FOR IMPROVED RADIATION PERFORMANCE.(U)
NOV 79 J K BUTLER DAAG29-76-G-0146

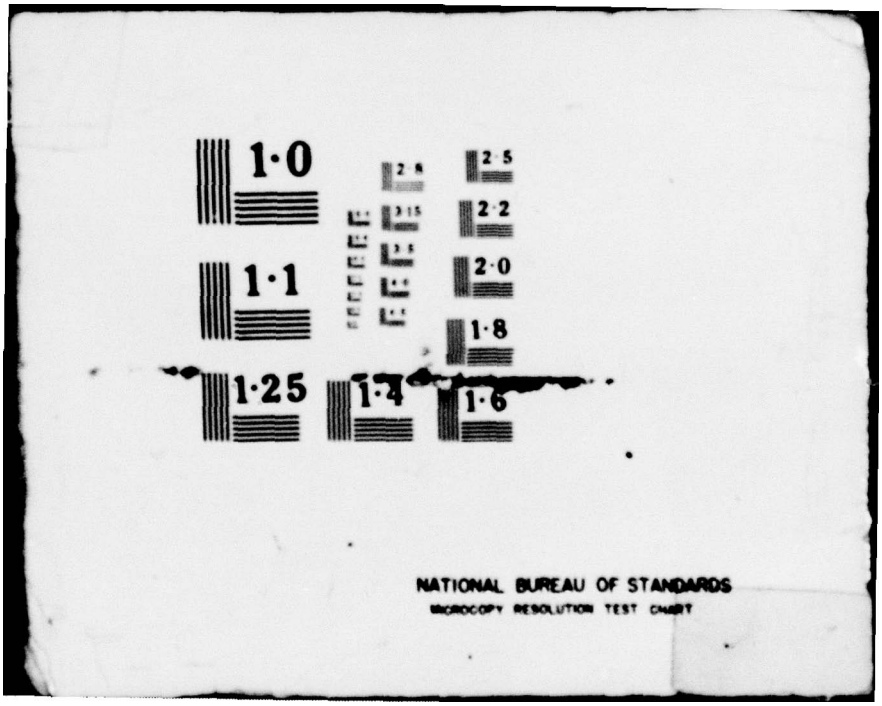
UNCLASSIFIED ARO-13568.9-EL NL

2 OF 2
AD
A078519





END
DATE
FILMED
1-80
DDC


1·0
1·1
1·25
1·4
1·6
2·5
2·2
2·0
1·8
NATIONAL BUREAU OF STANDARDS
MICROCOPY RESOLUTION TEST CHART

Stripe geometry $Al_xGa_{1-x}As$ lasers have been modeled with a complex dielectric constant in the active layer of the form[1-4]

$$\kappa(x) = \kappa_0^2 - k_0^2 a^2 x^2 \tag{1}$$

where κ_0 is the complex dielectric constant at x=0 and k_0 is the free space wave number. With this dielectric distribution, modes can be described by simple Hermite-Gaussian functions.[5-7] Such quantities as peak active region gain and lateral index changes can be estimated from measurements of near/far field half-power widths and a virtual waist position. However, if the fields are matched at the heterojunctions ($x=\frac{\pm d}{2}$ of Fig. 1) it is necessary to use a summation of Hermite-Gaussian functions to describe a mode, with the consequence that the near and far radiation fields are altered.[8] We briefly compare the major discrepancies which arise between using a single term and a summation to describe the lateral field.

Referring to the geometry of Fig. 1, a summary of the field representation for a symmetric TE mode of the form $\exp(i\omega t-\gamma z)$, where $\gamma = -\frac{G}{2} + i\beta$, is

$$E_x(x,y) = \sum_{\ell=0}^{\infty} A_\ell \cos(q_\ell y) H_\ell(\sqrt{a}\, k_0 x) \exp(-\tfrac{1}{2} a k_0^2 x^2) \qquad |x|<\tfrac{d}{2} \tag{2}$$

$$E_x(x,y) = \int_0^{\infty} B(\chi)\cos(\chi x)\exp\{(\tfrac{d}{2} - y)(\chi^2 - k_0^2\kappa_a - \gamma^2)^{\frac{1}{2}}\}d\chi \qquad |x|>\tfrac{d}{2} \tag{3}$$

where $\ell=0,2,4,\ldots$ for even modes, H_ℓ is the Hermite polynomial and κ_a is the dielectric constant for the sandwiching layers. The vertical eigenvalue, q_ℓ, satisfies

$$k_0^2\kappa_0 + \gamma^2 = q_\ell^2 + k_0^2 a(2\ell+1) \tag{4}$$

The far field intensity in the lateral plane is[9]

$$I = I_0 \cos^2\theta \, |e_x(0, k_0 \sin\theta)|^2 \tag{5}$$

where e_x is the two dimensional Fourier transform of $E_x(x,y)$.

Comparison of the radiation field for matched fields to the single term case is accomplished with the parameter "a" in equation (1) defined as[8]

$$a = \frac{(n_0 g_0)^{\frac{1}{2}}}{k_0 x_0} (2R + i10^{-4}/k_0)^{\frac{1}{2}} \tag{6}$$

$$R = \delta n / \delta g \qquad \text{cm}$$

where $x=x_0$ is defined as the point at which the gain has fallen to zero, i.e., $\delta g = g_0$. δn is the refractive index change at $x=x_0$.

Numerical solutions illustrating the differences between the two models are presented in Figs. 2 and 3. In Figs. 2(c) and (d) the fundamental mode half-power full width B of the lateral near-field is plotted against the full gain width $2x_0$ for various active region thicknesses d. The small dashed lines are for the single term case; the solid lines are for the summation case arising from matching fields at the heterojunctions; and the large dashed curve corresponds to the asymptotic case as d→large (e.g., 1.0 μm). It should be noted at the outset that the two models coincide for large active regions and display contrasting trends as d gets small with less energy confined to the active layer. The beamwidth is a soft function of d for the summation case, with B <u>increasing</u> as more energy is confined to the active region. In contrast, beamwidths for the single term case change more rapidly with B <u>decreasing</u> as the active layer progresses to a large thickness. These trends are graphically exhibited in Fig. 3 (b), where B is plotted directly against d. The

fact that the two models coincide in the asymptotic case d→large is illustrated in the expansion coefficients, A_ℓ, used in equation (2). As d→large and all the light is confined to the active layer, we find that $|A_0|=1$, $|A_\ell|\to 0$ for $\ell\neq 0$, and the lateral field expression for the summation case is Gaussian. As Fig. 3(b) indicates, the difference in the two models is negligible for d>0.5μm.

The far-field half power full widths, $\theta_{\|}$, are calculated for completeness and presented in Figs. 2 (a) and (b) and Fig. 3 (a). Again, the two models overlay for d>0.5μm. A value of $R=-10^{-6}$ includes a small refractive index rise at $x=x_0$ over the value at x=0. For instance, with $2x_0=12\mu m$, d=0.2μm, Δn=0.2, the peak gain numerically calculated for the summation case is $g_0=135\ cm^{-1}$. This is the gain required to propagate a mode with a modal gain $G=50cm^{-1}$ to satisfy radiation end losses. Thus $\delta n = \delta g R = -0.000135$.

Typical peak gains are plotted against the active region thickness in Fig.4 for the case $R=0, 2x_0=12\mu m$. The solid lines are for the summation and the dashed lines are for the single term. The differences in peak gain values are quite notable for d<0.2μm. The peak gain follows similar trends for other values of the parameter R. The more rapid rise of the gain as d drops in the solid curves implies higher currents at threshold.

A worst case example of the difference in the two models is $R=-10^{-6}$, $2x_0=12\mu m$, d=0.1μm, Δn=0.2. The single term near-field spot width is 29% larger than that for the summation model. The single term far-field width is 27% smaller than its summation counterpart.

In conclusion, a simple Hermite Gaussian mode description of the lateral field has the inherent attractiveness of analytic simplicity, with the concomitant ease of matching experimental evidence of the laser. However, the approximation loses accuracy for very thin active layers. Properly matched fields yield an expression for the lateral field intensity which can significantly

differ from a single term description as the active layer narrows. Resorting to the more complicated summation expression has the disadvantage in that a computer has to be used to manage an infinite series. When the active layer is thicker than 0.25μm, it is likely that the error in using one term for the lateral field is not more crucial than the error unavoidable in laboratory experiment.

REFERENCES

1. T. H. Zachos and J. E. Ripper, IEEE J. Quantum Electron. QE-5,29(1969).

2. T. L. Paoli, J. E. Ripper, and T. H. Zachos, IEEE J. Quantum Electron. QE-5,271(1969).

3. F. R. Nash, J. Appl. Phys., Vol. 44, 4696 (1973).

4. B. W. Hakki, J. Appl. Phys., Vol. 44, 5021 (1973).

5. D. D. Cook and F. R. Nash, J. Appl. Phys., Vol. 56, 1660 (1975).

6. P. A. Kirkby, A. R. Goodwin, C. H. B. Thompson, and P. R. Selway, IEEE J. Quantum Electron. QE-13, 705 (1977).

7. T. L. Paoli, IEEE J. Quantum Electron. QE-13, 662 (1977).

8. J. K. Butler and J. B. Delaney, IEEE J. Quantum Electron. QE-14, 507 (1978).

9. H. Kressel and J. K. Butler, Semiconductor Lasers and Heterojunction LEDs. New York: Academic, 1977, p. 185.

FIGURE CAPTIONS

Figure 1. Cross-section of the active region of a stripe geometry laser. The complex dielectric constant of the active layer is parabolic in x.

Figure 2. B is the fundamental mode half-power full width of the lateral near-field intensity. $\theta_{\parallel}$ is the fundamental mode half-power full width of the lateral far field intensity. $2x_0$ is the full gain width of the active layer under the stripe. Small dashed lines correspond to a single term representation of the lateral field; solid lines are for the lateral field represented by a summation of Hermite-Gaussian functions; and the large dashed lines are for the asymptotic case d→large (1.0 μm).

Figure 3. B and $\theta_{\parallel}$ are plotted against the active region thickness d in microns. The dashed lines are for the case where the lateral field is a single term. The solid lines are for a summation of Hermite-Gaussian functions. $2x_0$=12μm. All curves are for the fundamental mode.

Figure 4. Peak gain g_0 is plotted against the active region thickness d in microns for the fundamental and second mode. The solid curves are for a summation while the dashed curves are for a single term representation of lateral mode.

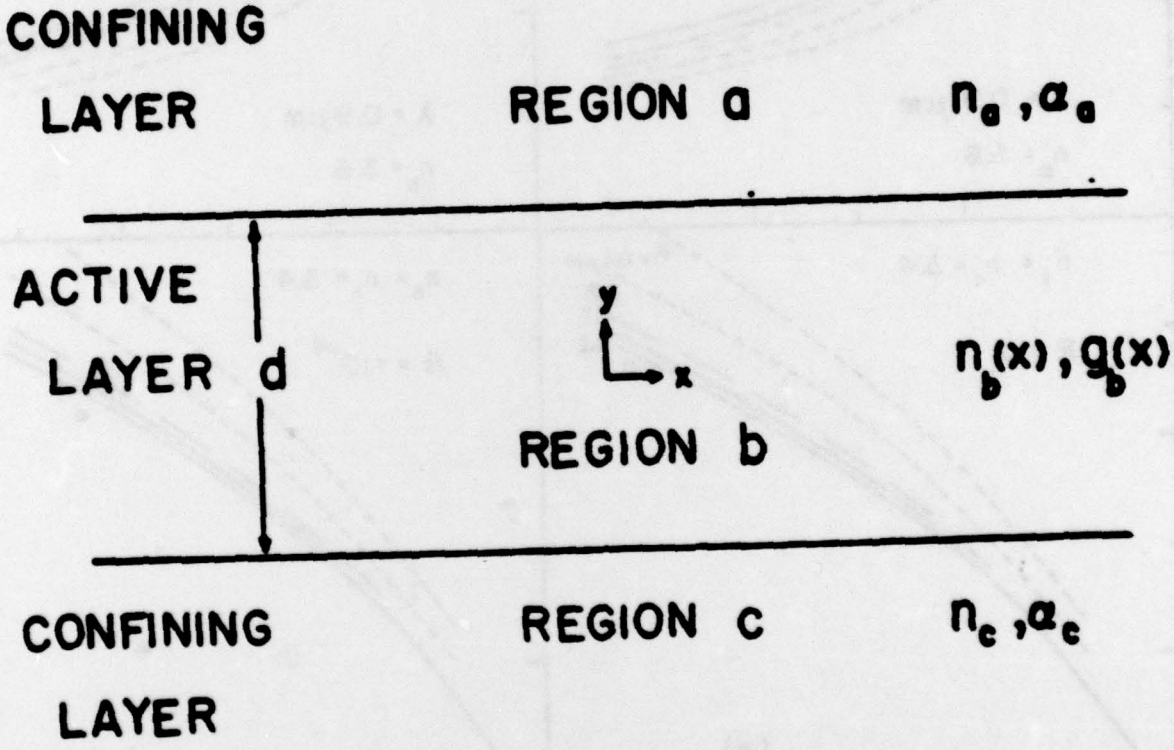

CONFINING
LAYER
REGION a
n_a , α_a
ACTIVE
LAYER
d
y
x
$n_b(x)$, $\alpha_b(x)$
REGION b
CONFINING
LAYER
REGION c
n_c , α_c

Fig. 1

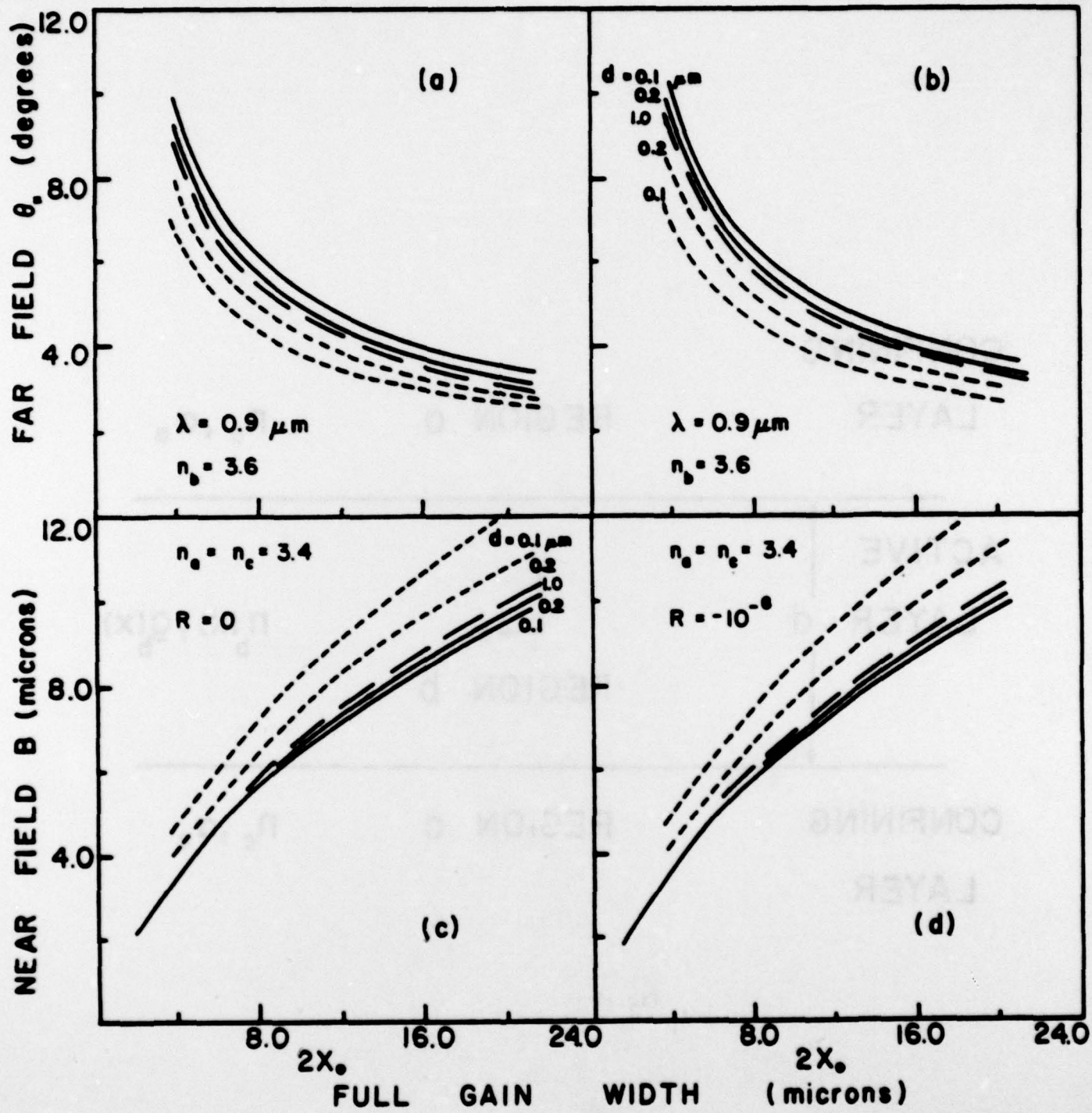

FAR FIELD θ_o (degrees)
12.0
8.0
4.0
(a)
λ = 0.9 μm
n_b = 3.6
(b)
d = 0.1 μm
0.2
1.0
0.2
0.1
λ = 0.9 μm
n_b = 3.6
NEAR FIELD B (microns)
12.0
8.0
4.0
n_a = n_c = 3.4
R = 0
d = 0.1 μm
0.2
1.0
0.2
0.1
(c)
n_a = n_c = 3.4
R = -10^{-8}
(d)
8.0
16.0
24.0
$2X_o$
FULL GAIN WIDTH (microns)

Fig. 2

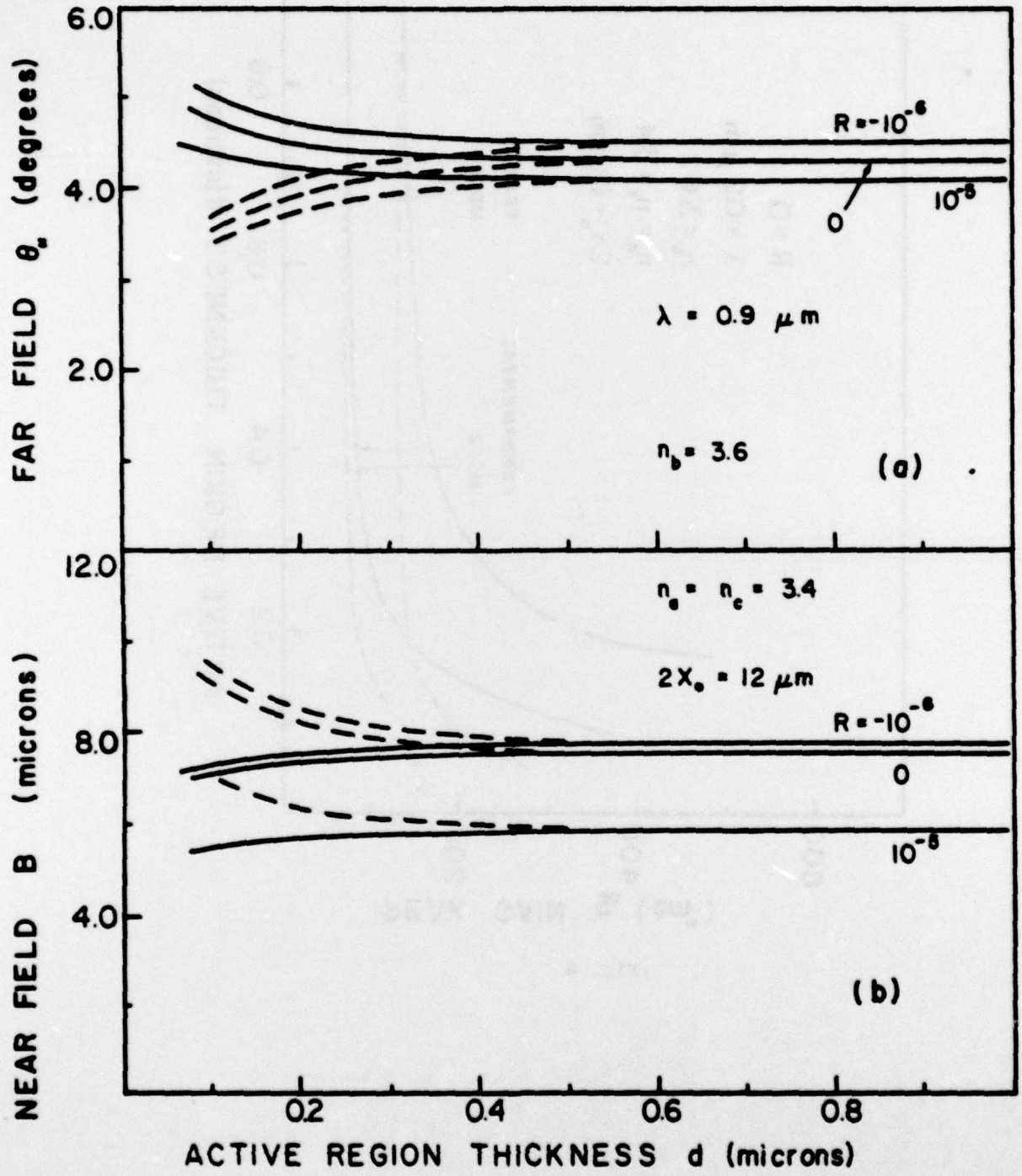

6.0
4.0
2.0
FAR FIELD θ_a (degrees)
$R = -10^{-6}$
0
10^{-6}
$\lambda = 0.9\ \mu m$
$n_b = 3.6$
(a)
12.0
8.0
4.0
NEAR FIELD B (microns)
$n_a = n_c = 3.4$
$2X_o = 12\ \mu m$
$R = -10^{-6}$
0
10^{-6}
(b)
0.2
0.4
0.6
0.8
ACTIVE REGION THICKNESS d (microns)

Fig. 3

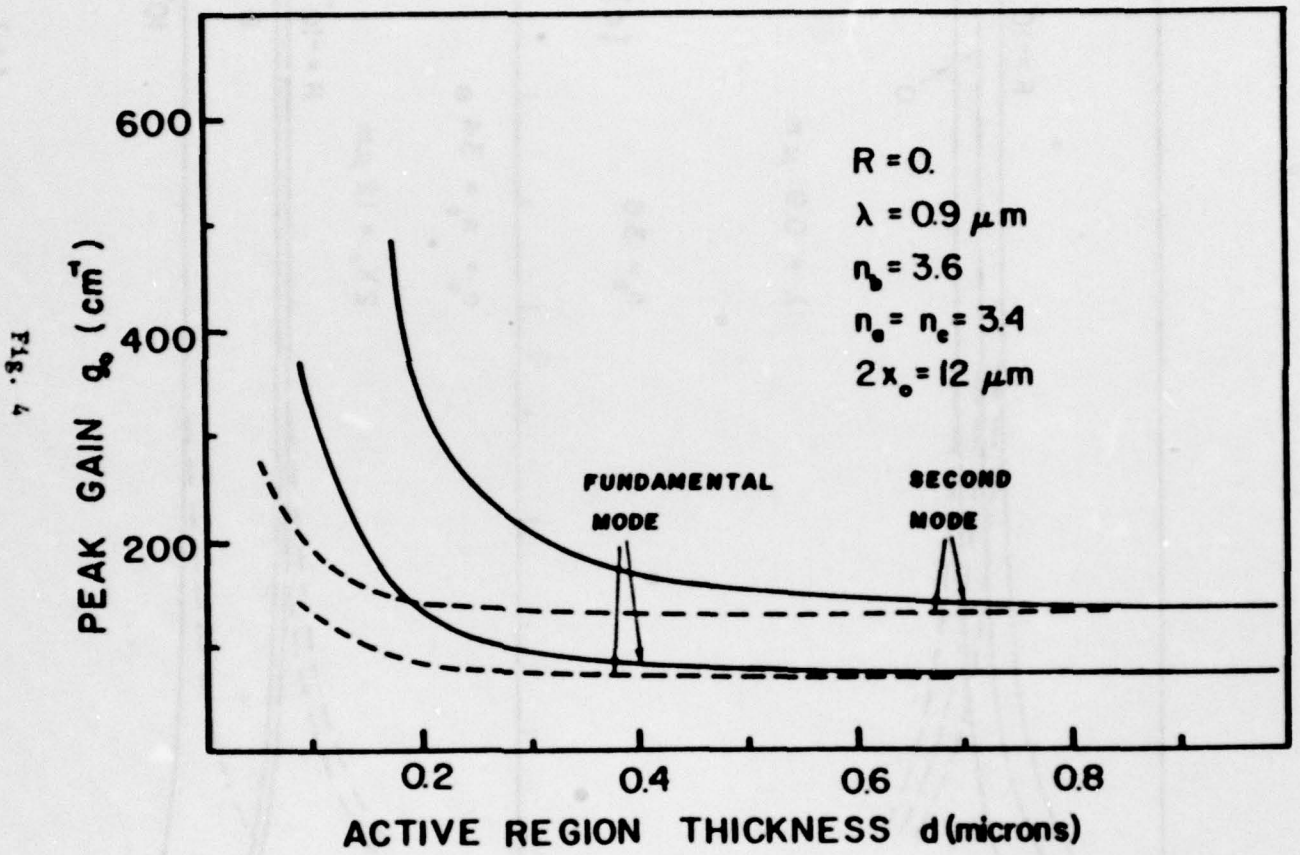

600
400
200
PEAK GAIN g_0 (cm^{-1})
R = 0.
λ = 0.9 μm
n_b = 3.6
n_a = n_c = 3.4
$2x_o$ = 12 μm
FUNDAMENTAL MODE
SECOND MODE
0.2
0.4
0.6
0.8
ACTIVE REGION THICKNESS d (microns)

FIG. 4

APPENDIX C

DISSERTATION ABSTRACTS

Wang, Chung-Shu

B.S. Electrophysics, National Chiao-Tung University, June 1970
M.S.E.E., The University of New Mexico, December 1972

ELECTROMAGNETIC MODES OF HETEROJUNCTION INJECTION LASERS

Advisor, Professor Jerome K. Butler

Doctor of Philosophy degree conferred: May 1977

Dissertation completed: January 21, 1977

School of Engineering and Applied Science, Southern Methodist University

This research is concerned with the theoretical modeling of heterojunction injection lasers. Studies have been made on two dimensional radiation patterns, mode reflectivities due to cleved facets, transverse mode selection, and the relationships between the threshold gain and aluminum concentration of various grown layers in the GaAs-AlGaAs device structure.

Two dimensional mode confinement is discussed for several laser structures including stripe geometry devices. Radiation patterns and mode reflectivities were calculated using the two dimensional model.

Transverse mode selection due to a thin film coating on the laser facet is discussed.

The threshold behavior for CW operation is investigated. The aluminum mole fraction in the active region determining the lasing wavelength, affects the active region gain at threshold. Lasers with a given active region width and index step have the smallest threshold gain when aluminum fraction of the active region is the largest; the peak fractional value of aluminum cannot exceed 0.37.

Jerome K. Butler

Scott, Marion Wayne

B.S.E.E., Southern Methodist University, May 1975
M.S.E.E., Southern Methodist University, December 1976

RADIATION FIELDS OF DIELECTRIC OPTICAL WAVEGUIDES

Advisor, Professor Jerome K. Butler

Doctor of Philosophy degree conferred: August 6, 1979

Dissertation completed: July 3, 1979

School of Engineering and Applied Science, Southern Methodist University

An experimental method of measuring the far field radiation pattern of dielectric optical waveguides is presented. The patterns of three-layer and five-layer structures, obtained using this technique, are given. Matching the experimental results with patterns calculated using the theory of layered waveguides determines the geometry and index of refraction profile of the waveguide.

Dispersion characteristics and radiation fields of an optical stripline waveguide radiating into free space are calculated. The halfpower beamwidth of the fundamental mode in a plane parallel to the dielectric layers is used as an indication of the degree of optical confinement under the stripe. Plots of the beamwidth versus the various waveguide parameters indicate the parameter values which give the best optical confinement. An approximate, and computationally simpler, method of calculating this beamwidth is also discussed.

Jerome K. Butler

Unclassified

SECURITY CLASSIFICATION OF THIS PAGE (When Data Entered)

REPORT DOCUMENTATION PAGE

READ INSTRUCTIONS BEFORE COMPLETING FORM

1. REPORT NUMBER: FINAL
2. GOVT ACCESSION NO.
3. RECIPIENT'S CATALOG NUMBER

4. TITLE (and Subtitle): DESIGN OF INJECTION LASERS FOR IMPROVED RADIATION PERFORMANCE.

5. TYPE OF REPORT & PERIOD COVERED: FINAL rept. 23 Feb 76 — 22 Feb 79

6. PERFORMING ORG. REPORT NUMBER

7. AUTHOR(s): JEROME K. BUTLER

8. CONTRACT OR GRANT NUMBER(s): DAAG29-76-G-0146

9. PERFORMING ORGANIZATION NAME AND ADDRESS: Southern Methodist University, Dallas, Texas 75275

10. PROGRAM ELEMENT, PROJECT, TASK AREA & WORK UNIT NUMBERS: 1T161102BH57-03, Communications Eng. & Elec.

11. CONTROLLING OFFICE NAME AND ADDRESS: U. S. Army Research Office, P. O. Box 12211, Research Triangle Park, NC 27709

12. REPORT DATE: November 1979

13. NUMBER OF PAGES: 7 plus appendices

14. MONITORING AGENCY NAME & ADDRESS (if different from Controlling Office)

15. SECURITY CLASS. (of this report): Unclassified

15a. DECLASSIFICATION/DOWNGRADING SCHEDULE

16. DISTRIBUTION STATEMENT (of this Report)

Approved for public release; distribution unlimited.

17. DISTRIBUTION STATEMENT (of the abstract entered in Block 20, if different from Report)

18. SUPPLEMENTARY NOTES

The view, opinions, and/or findings contained in this report are those of the author(s) and should not be construed as an official Department of the Army position, policy, or decision, unless so designated by other documentation.

19. KEY WORDS (Continue on reverse side if necessary and identify by block number)

Injection Laser
Radiation Patterns
Waveguide Modes
Mode Stability

20. ABSTRACT (Continue on reverse side if necessary and identify by block number)

This research was concerned with (1) the electromagnetic modes and (2) the radiation pattern characteristics of contemporary injection laser structures. The objective was to investigate laser structures which can produce stable-beam radiation patterns. The control of lateral fields in lasers has been accomplished with many novel devices such as the channeled-substrate-planar, buried heterostructure and strip-loaded waveguide. The drawback to the stripe

(over)

DD FORM 1 JAN 73 1473 EDITION OF 1 NOV 65 IS OBSOLETE

Unclassified

SECURITY CLASSIFICATION OF THIS PAGE (When Data Entered)

327950

laser is that it is laterally unstable. Much of our work has been aimed at rigorously modeling the electromagnetic modes of stripe lasers. We have also applied our analysis to other lasers such as the channeled-substrate-planar device.